# EXHIBIT 1

# Two Novel IL-1 Family Members, IL-1δ and IL-1ε, Function as an Antagonist and Agonist of NF-κB Activation Through the Orphan IL-1 Receptor-Related Protein 2[1]

**Reno Debets, Jackie C. Timans, Bernhard Homey, Sandra Zurawski, Theodore R. Sana, Sylvia Lo, Janet Wagner, Gina Edwards, Teresa Clifford, Satish Menon, J. Fernando Bazan, and Robert A. Kastelein[2]**

IL-1 is of utmost importance in the host response to immunological challenges. We identified and functionally characterized two novel IL-1 ligands termed IL-1δ and IL-1ε. Northern blot analyses show that these IL-1s are highly abundant in embryonic tissue and tissues containing epithelial cells (i.e., skin, lung, and stomach). In extension, quantitative real-time PCR revealed that of human skin-derived cells, only keratinocytes but not fibroblasts, endothelial cells, or melanocytes express IL-1δ and ε. Levels of keratinocyte IL-1δ are ~10-fold higher than those of IL-1ε. In vitro stimulation of keratinocytes with IL-1β/TNF-α significantly up-regulates the expression of IL-1ε mRNA, and to a lesser extent of IL-1δ mRNA. In NF-κB-luciferase reporter assays, we demonstrated that IL-1δ and ε proteins do not initiate a functional response via classical IL-1R pairs, which confer responsiveness to IL-1α and β or IL-18. However, IL-1ε activates NF-κB through the orphan IL-1R-related protein 2 (IL-1Rrp2), whereas IL-1δ, which shows striking homology to IL-1 receptor antagonist, specifically and potently inhibits this IL-1ε response. In lesional psoriasis skin, characterized by chronic cutaneous inflammation, the mRNA expression of both IL-1 ligands as well as IL-1Rrp2 are increased relative to normal healthy skin. In total, IL-1δ and ε and IL-1Rrp2 may constitute an independent signaling system, analogous to IL-1αβ/receptor agonist and IL-1R1, that is present in epithelial barriers of our body and takes part in local inflammatory responses. *The Journal of Immunology*, 2001, 167: 1440–1446.

I nterleukin 1 family members are known to alter the host response to an inflammatory, infectious, or immunological challenge (1). The biological activity of IL-1 is tightly controlled under physiological conditions. The classical IL-1 family comprises several ligands (i.e., IL-1α, IL-1β, and IL-1 receptor antagonist (IL-1ra)[3] (2–4), and surface and soluble IL-1 receptors (IL-1RI, IL-1RII, and IL-1R accessory protein (5–7), termed IL-1R1, IL-1R2, and IL-1R3 in this paper, respectively, in keeping with our previously proposed numbering system (8). IL-1 signaling is initiated by high-affinity binding of IL-1α and β to IL-1R1, which gets subsequently bound by IL-1R3 (5, 7). This results in an intracellular signaling cascade quite similar to stress-induced signal transduction (9), with the end effect being activation of NF-κB (10). IL-1ra and IL-1R2 antagonize the response to IL-1α and β at the ligand and (co)receptor levels (2, 3, 11, 12). Numerous studies have shown that perturbation of such control contributes to the pathogenesis of inflammatory and immunological diseases (i.e., leukemia, rheumatoid arthritis, and psoriasis; Refs. 13 and 14).

Recently, new members of the IL-1 family were identified based on both sequence homology and the presence of key structural patterns. For example, IL-18 (15, 16) is predicted to fold as a β-rich trefoil, typical for IL-1 ligands (17). Moreover, with respect to processing, receptor usage, and signaling, IL-18 can be classified as an IL-1 family member (i.e., IL-1γ; Refs. 18–23). In addition, new IL-1 ligands have been identified that show strong structural similarities to IL-1ra (24–29). To date, the expression and especially the receptor usage and function of these IL-1ra-like IL-1 ligands have only been characterized to a limited extent. At the IL-1 receptor level, there also exist additional IL-1R-like molecules. Many of these molecules are currently orphan receptors, such as T1/ST2 (termed IL-1R4; Refs. 30 and 31), IL-1R-related proteins 1 (IL-1R5; Ref. 32) and 2 (IL-1R6; Ref. 33), IL-1R accessory protein ligand (IL-1R7; Ref. 18), single Ig domain IL-1R-related protein (IL-1R8; Ref. 34), IL-1R accessory protein-like (IL-1R9) (35), and IL-1R10 (36), all harboring extracellular Ig-folds and an intracellular domain homologous to the cytosolic part of the *Drosophila* Toll protein. It is interesting to note that the majority of the IL-1 ligands (i.e., IL-1αβ/ra and some IL-1ra-like IL-1 ligands) and IL-1Rs (i.e., IL-1R1, IL-1R2, IL-1R4, IL-1R5, IL-1R6, and IL-1R7) are clustered and localized to chromosome 2 (18, 25, 28, 37–40).

The presence of several orphan IL-1Rs suggests the existence of additional corresponding IL-1 ligands. In line with recent reports (24–28), we have independently identified two novel IL-1 ligands based on sequence homology with IL-1ra, which we termed IL-1δ and IL-1ε. IL-1δ corresponds to the reported sequences of IL1Hy1 (24), FIL1δ (25), murine IL1H3 (26), IL-1RP3 (27) and IL-1L (28), whereas IL-1ε corresponds to IL1H1 (26) and IL-1RP2 (27). These novel IL-1s are strongly expressed in embryonic tissue and epithelial cells, such as skin keratinocytes. The expression of IL-1ε, and to a lesser extent of IL-1δ, is significantly up-regulated in IL-1β/TNF-α-stimulated human keratinocytes. Human IL-1δ and IL-1ε proteins do not activate NF-κB through the classical IL-1Rs,

i.e., the IL-1Rs used by IL-1α and β (IL-1R1 and IL-1R3) or IL-18 (IL-1R5/IL-1R7). Instead, IL-1ε activates this transcription factor via IL-1R6, and this response is potently and specifically antagonized by IL-1δ. Lesional psoriasis skin shows a substantially increased expression of both the IL-1 ligands as well as their IL-1R. IL-1δ and ε and IL-1R6 probably constitute an independent signaling system, present in epithelial barriers of our body, which may take part in local inflammatory responses.

## Materials and Methods

### Biological reagents and cell culture

Recombinant human IL-1α, IL-1β, IL-4, IFN-γ, and TNF-α were provided by R&D Systems (Minneapolis, MN). Recombinant human IL-18 and IL-1ra were produced at DNAX Research Institute of Molecular and Cellular Biology (Palo Alto, CA). The Q293 and 293-T cell lines were maintained in DMEM supplemented with 5% FBS, 0.3 mg/ml L-glutamine, 100 U/ml penicillin G, and 100 μg/ml streptomycin (Life Technologies, Paisley, U.K.). Human primary epidermal keratinocytes, dermal fibroblasts, dermal microvascular endothelial cells, and melanocytes (Clonetics, San Diego, CA) were cultured in specialized growth medium according to the suppliers recommendations. The Jurkat E6.1 cell line was maintained in RPMI 1640 medium supplemented with 10% FBS, glutamine, and antibiotics.

### Cloning of human and mouse IL-1δ and IL-1ε

BLAST searches in the public mouse expressed sequence tag (EST) database with the common portion of murine IL-1ra revealed EST mb49b11.r1 (GenBank accession no. W08205). The insert contained the full-length sequence of a novel IL-1-like molecule, designated IL-1δ. With this mouse sequence as a query, a human EST (5120028H1), derived from RNA from bronchial smooth muscle cells, was found in our proprietary Incyte database (Palo Alto, CA) that contained the full-length open reading frame of the human ortholog of mouse IL-1δ. The same query sequence revealed an additional EST mi08c10.r1 in the public mouse database (GenBank accession no. AA030324), which contained partial sequence of a second novel IL-1-like molecule, designated IL-1ε. The full-length sequence of murine IL-1ε was obtained by extending the 5' sequence by PCR on murine 17-day-old embryo Marathon-Ready library cDNA (Clontech, Palo Alto, CA). Separately, a Hidden Markov Model HMMer search (http://hmmer.wustl.edu/) with a PFAM alignment of IL-1α, IL-1β, and IL-1ra (http://pfam.wustl.edu/) revealed an EST (HAICR08) derived from RNA from epithelial cells in the Human Genome Sciences database (Rockville, MD) that contained the full-length open reading frame of human IL-1ε.

A multiple alignment of these novel IL-1 sequences and published IL-1 sequences was created using CLUSTALW (41), guided by tertiary structures and predicted secondary structures (with a consensus derived from several algorithms at http://circinus.ebi.ac.uk:8081/submit.html), and refined by eye. Conserved alignment patterns were drawn by Consensus (http://www.bork.embl-heidelberg.de/Alignment/consensus.html). Evolutionary tree analysis was performed with a neighbor-joining algorithm and viewed with TreeView 1.5 (http://taxonomy.zoology.gla.ac.uk/rod/treeview.html).

### Protein expression and purification of human IL-1δ and IL-1ε

Adenoviral vectors containing full-length human IL-1δ and IL-1ε sequences were constructed by PCR and used to transfect Q293 packaging cells. Viruses were subsequently purified, with all procedures according to the manufacturer's protocols (Invitrogen, Carlsbad, CA). Q293 cells (5 × 10⁸) were infected (adenoviruses used at 10 multiplicity of infection) and incubated for 5 days in a cell factory in a total volume of 1 L of serum-free CMF-1 medium (Life Technologies). Culture medium was dialyzed (Spectra/Por membrane tubing; molecular mass cut-off, 6–8 kDa; Spectrum Laboratories, Rancho Dominguez, CA) against 50 mM Tris-HCl, pH 8.0, and 1 mM EDTA, and subsequently passed through hitrap Q Sepharose and heparin columns. The flow-through, containing the IL-1 proteins, was sterile-filtered and concentrated ~70 times with an Amicon 8400 ultrafiltration cell with a 10-kDa molecular mass cut-off membrane (Millipore, Bedford, MA). The samples were dialyzed against PBS, and the protein content was quantified by PAGE and Coomassie blue staining with lysozyme as a standard. Protein identities were confirmed by N-terminal sequencing. Identically treated culture medium of Q293 cells infected with adenovirus encoding green fluorescent protein served as a negative control. Endotoxin levels were determined by using the Limulus amebocyte lysate assay (Bio-Whittaker, Walkersville, MD) and were <1.5 EU/100 μg protein. Protein samples were stored at 4°C.

### Expression plasmids

Plasmids encoding full-length human R1, mouse R3, mouse R4, human R5, and human R7 sequences were constructed by inserting PCR-generated cDNA fragments into pME18S (42). Human IL-1R6 cDNA, a generous gift of Dr. R.A. Maki (Neurocrine Biosciences, San Diego, CA), was subcloned directly into pME18S. The reporter gene plasmid pNF-κB-Luc (Stratagene, La Jolla, CA) contains five NF-κB sites and a basic promoter element to drive luciferase expression, and pRSV-βGal results in constitutive expression of β-galactosidase.

### Northern blots

Mouse Northern blots containing ~2 μg of poly(A)⁺RNA per lane, derived from either total embryo at different days postgestation (Clontech) or from various adult tissues (Origene Technologies, Rockville, MD), were hybridized to the mouse IL-1δ and IL-1ε cDNA probes containing the complete open reading frames. Probes were labeled with ³²P by using the Redivue labeling kit (Amersham Pharmacia Biotech, Uppsala, Sweden). Prehybridization, hybridization, stringency washes, and stripping were conducted according to the manufacturer's protocols. Membranes were exposed to a phosphorimager.

### Quantitative real-time PCR

A panel of various human skin-derived cells, i.e., primary epidermal keratinocytes, dermal fibroblasts, dermal microvascular endothelial cells, and melanocytes, as well as skin biopsies and PBMC were used for TaqMan-PCR analyses. Skin-derived cells were left untreated or were treated with IL-4 (50 ng/ml), IFN-γ (20 ng/ml), or a combination of IL-1β (5 ng/ml) and TNF-α (10 ng/ml) for 18 h before RNA isolation. Biopsies from lesional psoriasis skin and normal healthy skin were kindly donated by Dr. T. Ruzicka (Department of Dermatology, University of Dusseldorf, Germany) and homogenized before RNA isolation. PBMC from a healthy donor, prepared by standard protocols, stimulated with and without PHA served as controls. RNA isolation, cDNA synthesis, and PCR were performed as described elsewhere (43). The amplicons for human IL-1δ (nt 17–90, with numbers starting at first methionine codon), human IL-1ε (nt 337–409), and human IL-1R6 (nt 1378–1448) were analyzed with 6-carboxy-fluorescein-labeled probes. 18S RNA quantities were measured with a VIC-labeled probe and served as internal controls to normalize for the total amount of cDNA. Values are expressed as fg/5 ng total cDNA.

### Reporter assay

Jurkat E6.1 cells (4 × 10⁶) were transiently transfected with pNF-κB-Luc reporter gene plasmid, pRSV-βGal plasmid, and IL-1R-encoding cDNA plasmid(s) as described previously (43). Twenty hours after transfection, cells were stimulated with 20 ng/ml of human IL-1α, IL-1β, IL-18, or IL-1ra, or 50 ng/ml human IL-1δ or IL-1ε for 6 h. Cells were lysed with reporter lysis buffer (Promega, Madison, WI), and luciferase and β-galactosidase activities were assessed with luciferase assay reagent (Promega) and Galacto-Light Kit (Tropix, Bedford, MA), respectively. Luciferase activities (in RLU) were normalized on the basis of β-galactosidase activities. For inhibition studies of IL-1R1-mediated activation of NF-κB, IL-1α was used at 50 pg/ml in the presence of IL-1ra and IL-1δ at concentrations ranging from 10 pg/ml to 10 μg/ml. Inhibition of the IL-1R6-mediated response was analyzed with IL-1ε used at 50 ng/ml and IL-1δ or IL-1ra at concentrations ranging from 64 pg/ml to 10 μg/ml.

## Results

### IL-1δ and ε were identified computationally

Computational analyses led to the discovery of two novel IL-1 ligands: IL-1δ and IL-1ε. In short, the strategies used both homology-based and probabilistic-based (HMMer) searches (see Materials and Methods for details). The sequences, and a comparison with the previously known IL-1 family members, are given in Fig. 1A. Fig. 1B, the corresponding dendrogram, shows evolutionary relationships.

### IL-1δ and IL-1ε messenger RNA are highly expressed in embryonic tissue and in epithelial cells

Northern blot analyses show that IL-1δ and IL-1ε are expressed in embryonic tissue and tissues containing epithelial cells (i.e., stomach and skin; Fig. 2). Quantitative PCR analyses on a large panel of mouse and human tissue cDNAs (including various lymphoid

**A**



**B**
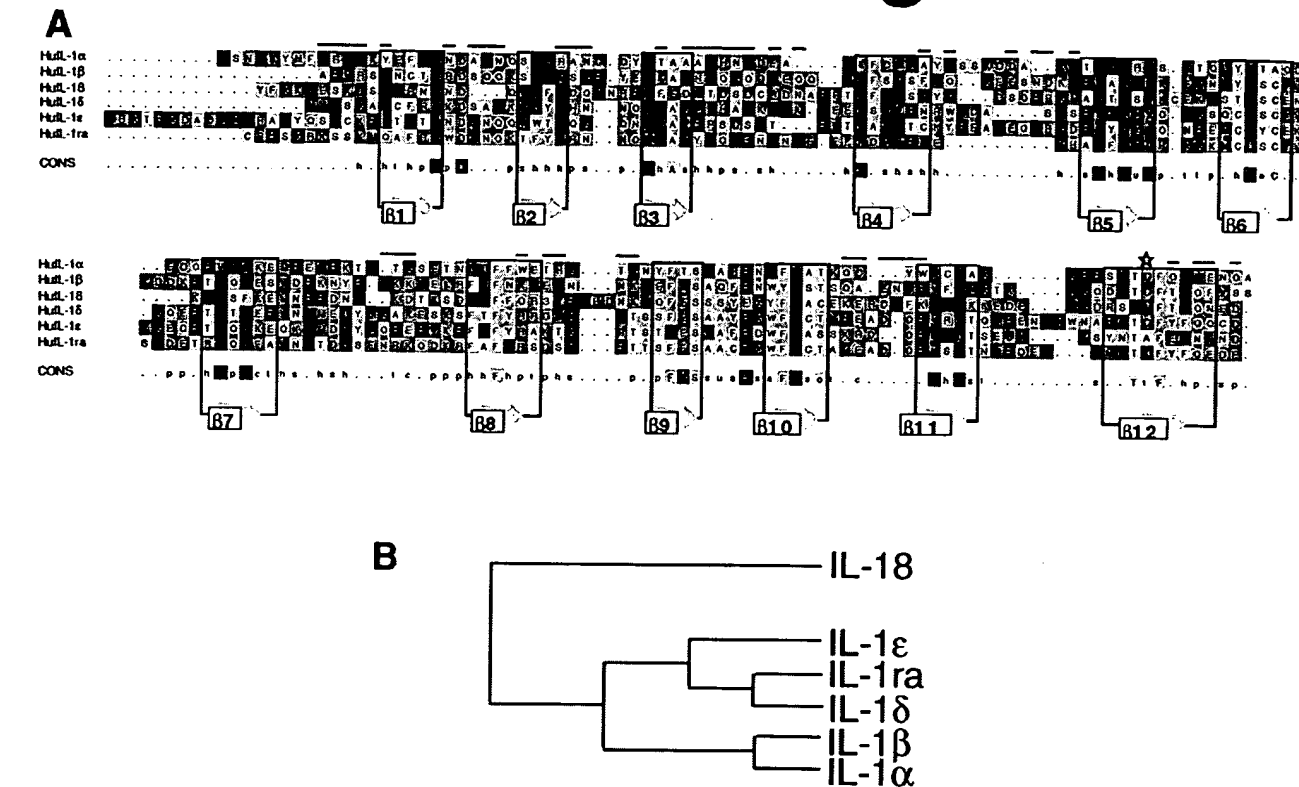


**FIGURE 1.** Typical IL-1-like structural patterns are conserved in IL-1δ and IL-1ε. *A*, Sequence alignment of mature IL-1 sequences: human IL-1α starts at L119 (GenBank accession no. AAA59134), human IL-1β starts at A117 (AAA59135), human IL-18 starts at Y37 (BAA08706), and human IL-1ra starts at C25 in the common region (CAA36262). Human IL-1δ and IL-1ε both start at their first M. The 12 β-strands, typical for IL-1 ligands, are depicted by arrows numbered from β1 to β12. The β-strands are boxed according to known (i.e., human IL-1β and IL-1ra; Refs. 50 and 51) and predicted secondary structures. Lines above the alignment indicate residues of human IL-1β that interact with IL-1R1 (sites A and B as in (51), in black and red, respectively). The asterisk indicates a residue, which together with the loop region between β4 and β5, is crucial in determining antagonist activity in IL-1ra (49, 52). The amino acid coloring scheme depicts chemically similar residues: green (hydrophobic); red (acidic); blue (basic); yellow (C); orange (aromatic); black (structure breaking); and gray (tiny). Diagnostic sequence patterns for IL-1s were derived by CONSENSUS at a stringency of 70%. Symbols for amino acid subsets are as follows: o, alcoholic; l, aliphatic; dot, any amino acid; a, aromatic; c, charged; h, hydrophobic; −, negative; p, polar; +, positive; s, small; u, tiny; and t, turnlike. *B*, Evolutionary dendrogram of IL-1s. Sequence data for human and mouse IL-1δ are available from GenBank under accession nos. AF230377 and AF230378, respectively; sequence data for human and mouse IL-1ε are available under AF206696 and AF206697, respectively.



**Embryonic tissues**          **Adult tissues**
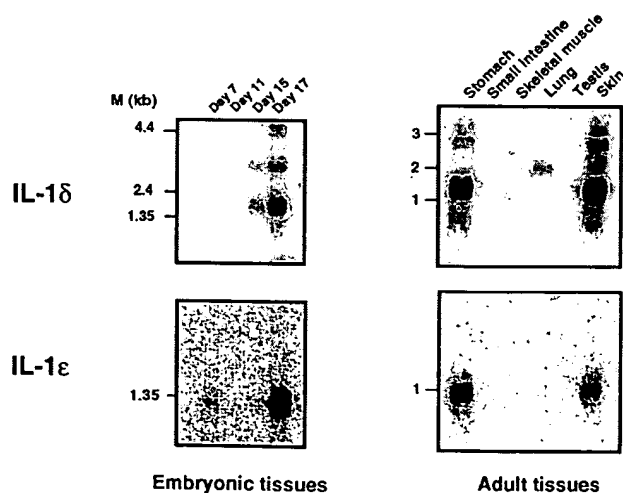
**FIGURE 2.** IL-1δ and IL-1ε messenger RNA are highly expressed in embryonic tissue and in tissues containing epithelial cells. Northern blot analyses of mouse IL-1δ and IL-1ε messenger RNA expression in embryonic tissues at different days postgestation and in different adult tissues. Multiple tissue blots containing ~2 μg poly(A)+ RNA per lane were hybridized to the IL-1δ and IL-1ε cDNA probes. Molecular weight RNA sizes in kilobases are indicated. See *Materials and Methods* for details.

organs, kidney, heart, lung, brain, liver, organs of the digestive tract, reproductive organs, and skin) confirmed these findings. Messenger RNA expression in lung tissue appears to be unique to IL-1δ (Fig. 2). It should also be noted that IL-1δ mRNA analysis shows the presence of multiple variants. More in-depth studies, based on quantitative PCR, revealed that in skin, keratinocytes but not fibroblasts, endothelial cells, or melanocytes are the main producers of IL-1δ and IL-1ε (Fig. 3). In vitro-cultured keratinocytes contained ~10-fold more IL-1δ mRNA relative to IL-1ε mRNA. Stimulation with IL-4 or IFN-γ hardly affected the expression levels of IL-1δ and ε mRNA, whereas stimulation with a combination of IL-1β and TNF-α resulted in an enormous increase in the expression of IL-1ε mRNA and to a lesser extent of IL-1δ mRNA (Fig. 3).

*IL-1δ and IL-1ε do not activate NF-κB through classical IL-1Rs*

The ability of the novel IL-1s to initiate IL-1R-mediated signaling was studied via an NF-κB-dependent reporter assay with ligand-stimulated Jurkat T cells transiently transfected with different pairs of IL-1Rs. The R1/R3 combination, conferring responsiveness to IL-1α and IL-1β (5, 44), did not generate a response to IL-1δ or IL-1ε. Also, the R5/R7 combination, required to mediate a response to IL-18 (18, 43), did not result in signaling on addition of the novel IL-1 ligands (Fig. 4A). The next step was to test the
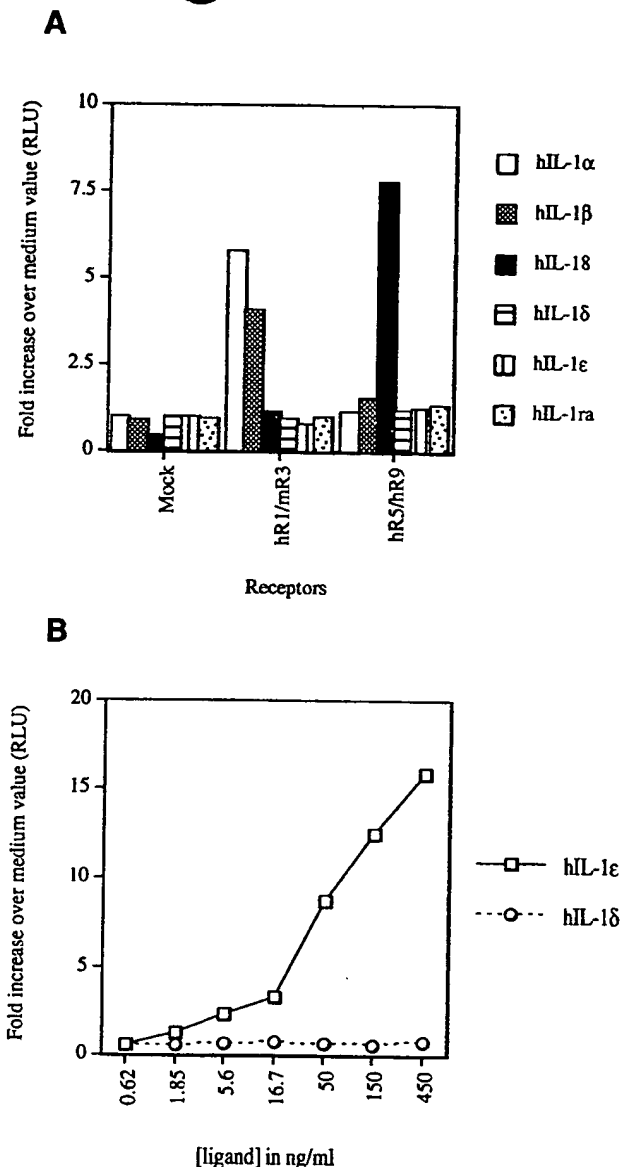
**fg/5 ng total cDNA**
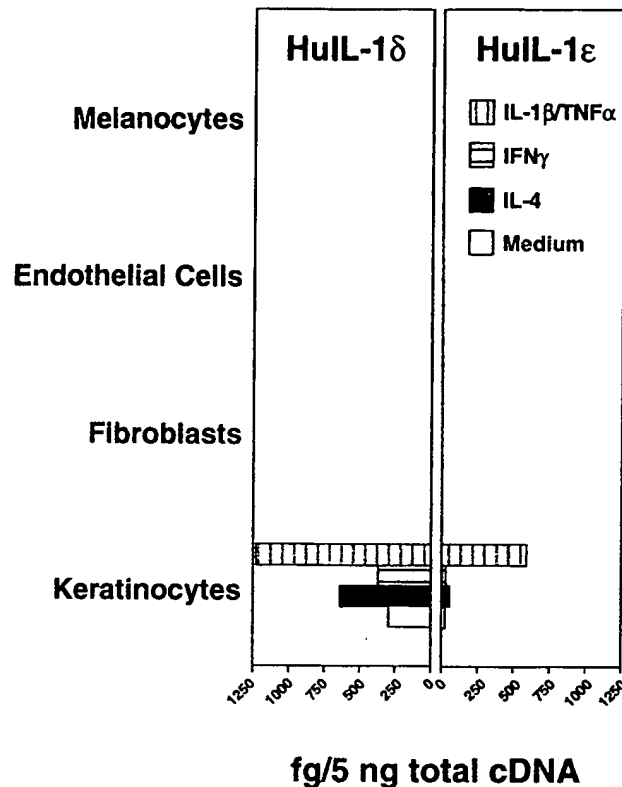
**FIGURE 3.** Keratinocytes are the main source for IL-1δ and IL-1ε messenger RNA in skin tissue. A panel of human cDNAs from various skin-derived cells were analyzed for expression levels of human IL-1δ and IL-1ε by the Flurogenic 5'-nuclease PCR assay. The novel IL-1s were analyzed by FAM-labeled probes. Expression levels were normalized to reverse-transcribed 18S RNA quantities and expressed as fg/5 ng total cDNA. Cells were left untreated or treated with different cytokines for 18 h as indicated before RNA was isolated. See *Materials and Methods* for details.



[ligand] in ng/ml

**FIGURE 4.** *A*, IL-1δ and IL-1ε do not activate NF-κB through classical IL-1Rs. Jurkat cells (4 × 10⁶) were transfected with 2 μg of pNF-κB-Luc reporter gene plasmid, 0.5 μg of pRSV-βGal plasmid, and 4 μg of each IL-1R plasmid (in pME18S, all human, except mouse IL-1R3 plasmid) as indicated. Twenty hours after transfection, cells were left untreated or were stimulated for 6 h with human IL-1 ligands (20 ng/ml final, except IL-1δ or IL-1ε, which is used at 50 ng/ml final). Luciferase activities were determined and normalized on the basis of β-galactosidase activities. Single receptors did not give any luciferase response. Data shown are from one of two independent experiments with similar results. *B*, IL-1ε, but not IL-1δ, activates NF-κB through IL-1R6. See *A* for details. Jurkat cells were transfected with 0.5 μg of human IL-1R6 plasmid (in pME18S). Twenty hours after transfection, cells were left untreated or were stimulated for 6 h with human IL-1δ or IL-1ε at different concentrations. Mock protein control for human IL-1δ and IL-1ε gave a luciferase response similar to medium only. Data shown are from one of three independent experiments with similar results.

orphan IL-1R-like molecules IL-1R4 and IL-1R6 (classified as potential ligand-binding receptors based on their homology to IL-1R1; Ref. 36) paired with various other IL-1R-like molecules, i.e., IL-1R3, IL-1R7, IL-1R9, and IL-1R10 (classified as potential signaling receptors based on their homology to IL-1R3; Ref. (36) for their capacity to confer responsiveness to IL-1δ and IL-1ε. Data consistently showed an IL-1R6-mediated activation of NF-κB upon stimulation with IL-1ε, but not IL-1δ or the mock control (Fig. 4*B*).

*IL-1δ specifically and very potently antagonizes the IL-1R6 response to IL-1ε*

In line with the striking similarity between IL-1δ and IL-1ra, we tested the possibility of IL-1δ being an antagonist of IL-1 responses rather than being an IL-1 agonist. With the same reporter assay with IL-1R-transfected Jurkat T cells, we showed that IL-1ra, but not IL-1δ, is able to antagonize the IL-1R1-mediated activation of NF-κB on stimulation with IL-1α (Fig. 5*A*). Vice versa, IL-1δ, but not IL-1ra, is able to antagonize the IL-1R6-mediated activation of NF-κB on stimulation with IL-1ε (Fig. 5*B*). Importantly, IL-1ra shows a 50% inhibition of the IL-1R1-mediated response to IL-1α at about a 1000-fold excess over IL-1α, whereas IL-1δ results in a similar inhibition of the IL-1R6-mediated response to IL-1ε at concentrations similar to or even less than IL-1ε.
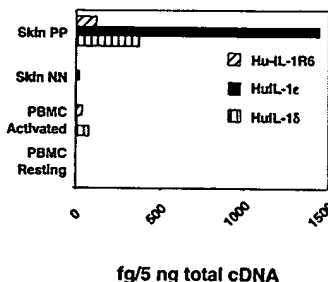
*IL-1δ and ε and IL-1R6 levels are substantially up-regulated in lesional psoriasis skin*

In lesional psoriasis skin, characterized by chronic cutaneous inflammation, the expression of the novel IL-1 ligands, IL-1δ and IL-1ε, and IL-1R6 are all significantly increased relative to skin

## A



Fold XS over hIL-1α (50 pg/ml)

## B



Fold XS over hIL-1ε (50 ng/ml)
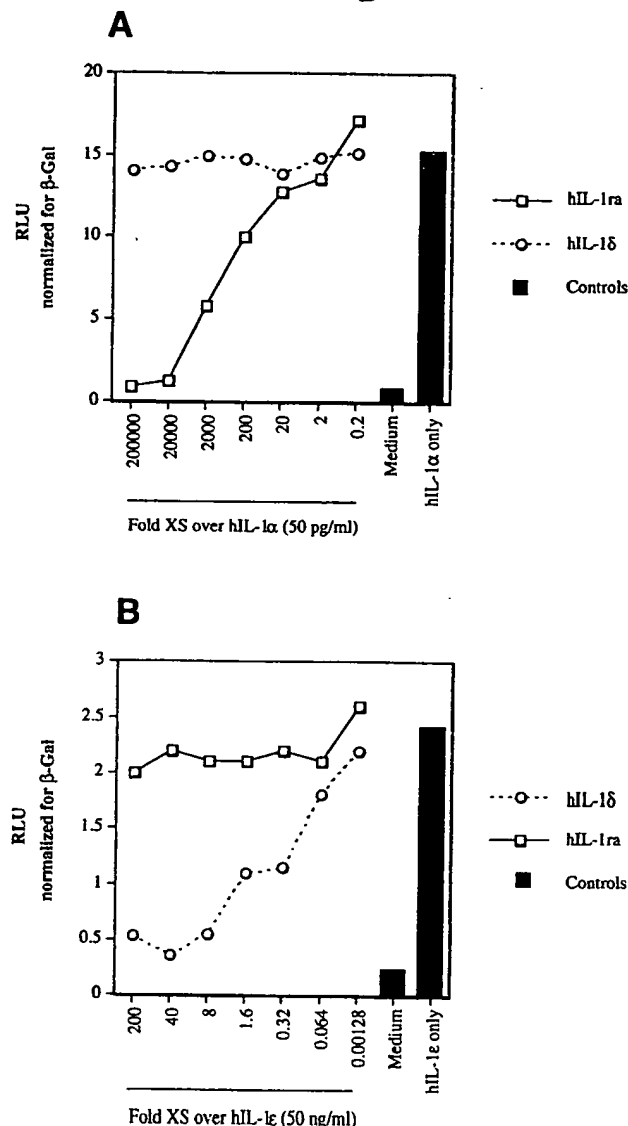
**FIGURE 5.** IL-1δ specifically antagonizes the IL-1R6-mediated response to IL-1ε. A, IL-1ra, but not IL-1δ, antagonizes the IL-1R1-mediated response to IL-1α. See legend to Fig. 4A for details. Jurkat cells were transfected with 0.5 μg of human IL-1R1 plasmid. Twenty hours after transfection, cells were left untreated or were stimulated for 6 h with human IL-1α at 50 pg/ml final concentration with or without human IL-1ra or IL-1δ at final concentrations ranging from 10 pg/ml to 10 μg/ml. Antagonist only (i.e., IL-1ra or IL-1δ) and mock protein controls, even at high concentrations, did not give any luciferase response. Data shown are from one of two independent experiments with similar results. B, IL-1δ, but not IL-1ra, antagonizes the IL-1R6-mediated response to IL-1ε. Jurkat cells were transfected with 0.5 μg of human IL-1R6 plasmid. Twenty hours after transfection, cells were left untreated or were stimulated for 6 h with human IL-1ε at 50 ng/ml final with or without human IL-1δ or IL-1ra at final concentrations ranging from 64 pg/ml to 10 μg/ml. Antagonist only and mock protein controls, even at high concentrations, did not give any luciferase response. Data shown are from one of three independent experiments with similar results.



fg/5 ng total cDNA

**FIGURE 6.** Expression of both IL-1δ and IL-1ε and IL-1R6 are increased in lesional psoriasis skin. Biopsies from lesional psoriasis skin (PP) and normal healthy skin (NN) and PBMC from a healthy donor stimulated with and without PHA were analyzed for expression levels of human IL-1δε and IL-1R6 by the Flurogenic 5'-nuclease PCR assay. See Fig. 3 for details.

## Discussion

This paper describes the discovery of two novel members of the IL-1 family, termed IL-1δ and IL-1ε. Several recent studies have reported on the cloning and molecular characterization of IL-1δ and IL-1ε (24–28). However, the present study is the first to report on the expression in human skin-derived cell types, receptor usage, and initial functional characterization of IL-1δ and IL-1ε.

The structurally aided alignment of both the novel and classical IL-1s in Fig. 1A shows the conservation of the core 12 β-strands, making up the β-trefoil structure. The presented sequence of human IL-1δ protein is identical with the reported sequences of IL1Hy1 (24), FIL1δ (25), IL-1RP3 (27), and IL-1L (28). At the amino acid level, human IL-1δ and IL-1ra show a high degree of similarity, which is confirmed by the evolutionary tree analysis (Fig. 1B). With respect to IL-1ε, the presented sequence is identical with the sequences of IL1H1 (26) and IL-1RP2 (27). It is interesting to note that several public mouse ESTs exist, mostly derived from tongue epithelium, with only slight variations relative to the IL-1ε sequence. In addition, FIL1ε (25) also shows a very high similarity to the human IL-1ε sequence presented in this paper (i.e., 51%). How these IL-1ε variants are generated and their biological significance remain unclear.

IL-1δ and IL-1ε are strongly expressed in embryonic development and in tissues such as stomach, lung, and skin (Fig. 2 and PCR analyses on a panel of various tissue cDNAs not shown). Lung tissue only showed expression of IL-1δ messenger RNA (at the Northern blot level), although at the PCR level, expression of both IL-1δ and IL-1ε can be detected in lung-derived cDNAs. Sizes of the predominant messages for IL-1δ are 1.4 and 2.7 kb for stomach and skin tissues, respectively, and 2.0 kb for lung tissue. Interestingly, IL-1δ messenger RNA in lung tissue is reported to lack the second exon relative to other tissues (25). In analogy to IL-1ra, the different IL-1δ messages might reflect different (tissue-specific) splice variants (2, 45–47). In fact, both IL-1δ and IL-1ra mRNA sequences diverge at the 5' ends because of usage of alternative first exons (27). A detailed analysis of human skin was performed with quantitative PCR analysis on a panel of first-strand cDNAs derived from various skin-specific cell types. Keratinocytes, but not fibroblasts, endothelial cells, or melanocytes were identified as the major source for IL-1δ and IL-1ε, with levels of IL-1δ being ~10-fold higher than those of IL-1ε (Fig. 3). In addition, Langerhans cells but not skin-homing T cells, freshly isolated from skin biopsies, showed some expression of IL-1δ and ε (data not shown). In vitro stimulation of keratinocytes with proinflammatory cytokines (i.e., IL-1β/TNF-α) but not with IL-4 or IFN-γ significantly up-regulated the expression of IL-1ε, and to a

from a healthy individual (Fig. 6). The increase is most prominent for IL-1ε, in line with in vitro-cultured keratinocytes stimulated with the pro-inflammatory cytokines IL-1β/TNF-α (Fig. 3). Activation of PBMC also leads to increased levels of both IL-1 ligands and their receptor, albeit to a lesser extent than observed in lesional psoriasis skin.

lesser extent of IL-1δ (Fig. 3). Our observations are in line with reports on the constitutive and induced expression of keratinocyte IL-1δ and IL-1ε mRNA (26, 27). Preliminary in situ hybridization data using mouse tissue sections confirmed that cells of epithelial origin, such as the parietal and chief cells in stomach, and basal keratinocytes in skin are the predominant cellular sources of these IL-1s (not shown). In addition, esophageal squamous epithelium is also reported to express IL-1ε (27). The presence of IL-1δε in epithelial barriers of our body (i.e., skin, digestive, and respiratory tracts), suggests that these novel IL-1s fulfill similar roles as their known family members (i.e., IL-1α and IL-1β) to promote a response to injury or infection (1, 48). In fact, Kumar and colleagues have shown that the epidermal expression of murine IL-1ε is up-regulated in vivo in response to contact hypersensitivity or a viral infection (26).

It is important to note that IL-1δ and IL-1ε neither possess a classical leader sequence (as does secreted IL-1ra; Ref. 2) nor do they possess a distinct pro-form (as do IL-1αβ and IL-18; Refs. 4, 15, and 16). However, monitoring the presence of C-terminally tagged versions of IL-1δ and IL-1ε in the supernatants and lysates of transfected 293-T cells (human epithelial cells) revealed that these molecules are secreted as 20-kDa proteins (data not shown). This is in agreement with the finding that the human trophoblastic tumor cell line JEG-3 is able to secrete IL-1δ (28), and argues that an alternative mechanism exists to secrete these novel IL-1s. To functionally characterize the novel IL-1s, we expressed and purified adenovirally derived human IL-1δ and IL-1ε and tested these proteins for their capacity to initiate IL-1 signaling, with NF-κB activation as a read-out. The observation that IL-1R1/3 and IL-1R5/7 do not respond to these new protein preparations (Fig. 4A) might be explained by the fact that receptor-ligand combinations within the IL-1 system are very specific (43). Therefore, we subsequently tested the orphan receptors IL-1R4 and IL- 1R6 paired with various other IL-1R-like molecules. These studies consistently showed that IL-1R6 responded to IL-1ε but not IL-1δ in activating NF-κB in Jurkat cells (Fig. 4B). Even IL-1R6 single transfectants showed this response. The IL-1 system, as we know it today, typically requires two receptors, a ligand-binding subunit and a signaling subunit, to get an IL-1 response (5, 18). Because IL-1R6 is very homologous to IL-1R1 (33), a ligand-binding type of receptor, we believe that Jurkat cells endogenously express a second signaling type of receptor that can pair with IL-1R6 in the presence of IL-1ε. We know that the following IL-1R-like molecules are expressed by nontransfected Jurkat cells: IL-1R3, IL-1R4, IL-1R8, IL-1R9, and IL-1R10 (PCR data, not shown). Co-transfection of IL-1R6 with either IL-1R3, IL-1R9, or IL-1R10 does not potentiate the response to IL-1ε relative to IL-1R6 single transfectants (not shown). In addition, studies by others with IL-1R1 chimeras and IL-1α-mediated activation of NF-κB as a read-out do not support a combination of IL-1R6 and IL-1R8 to mediate an IL-1 response (34). The search for the additional IL-1ε receptor(s) is currently ongoing.

IL-1δ is most closely related to IL-1ra, and, like IL-1ra, lacks the loop between the fourth and fifth β-strands (see Fig. 1A), which is typical for IL-1 agonists: IL-1α, IL-1β, IL-18 and IL-1ε. In fact, insertion of the loop amino acids QGEESN of IL-1β confers agonist activity to IL-1ra (49). Therefore, we hypothesized that IL-1δ acts as an antagonist. Indeed, IL-1δ is a very potent antagonist of the IL-1R6-mediated response to IL-1ε at a ratio of IL-1δ:IL-1ε <1 (Fig. 5). Note that the potency of IL-1ra to antagonize the IL-1R1-mediated response to IL-1α is ~3 orders of magnitude less. The observation by others (25) that their FIL1δ and FIL1ε proteins do not bind to IL-1R6 is in our opinion not contradictory to our findings. Binding studies with partially purified IL-1δ and

IL-1ε proteins from conditioned medium of transfected cells and an Fc fusion of IL-1R6 might not be sensitive enough to show binding to these new IL-1s. Moreover, the second receptor might actually be needed for affinity conversion and for binding to become detectable (5, 43).

IL-1δ is a highly specific antagonist of the IL-1R6-mediated response to IL-1ε. For instance, IL-1δ does not respond through IL-1R1, either as an agonist or antagonist (see Figs. 4 and 5), which confirms the reported lack of IL-1δ to induce the production of IL-6 or inhibit the IL-1αβ-induced production of IL-6 by cultured fibroblasts or endothelial cells (28). Moreover, IL-1δ does not respond through IL-1R5 because IL-1δ does not induce the production of IFN-γ or inhibit the IL-18-induced production of IFN-γ by KG-1 cells (28). In fact, a recently cloned IL-1ra homologue, termed IL-1H (with various isoforms: FIL1ζ (25), IL1H4 (26), and IL-1RP1 (27)) was shown to bind to IL-1R5 but not IL-1R1 (29), and may act as a specific IL-18 antagonist.

Expression of human IL-1R6 is restricted to lung epithelium and brain vasculature (33). In extension to these findings, we observed expression of IL-1R6 mRNA in monocytes and in skin-derived keratinocytes, fibroblasts and to a lesser extent endothelial cells. With respect to skin cells, IL-1R6 may in fact mediate proliferation and production of matrix metalloproteinases in response to IL-1ε (preliminary data, not shown). Activated monocytes also show an up-regulated expression of IL-1δ and IL-1ε mRNA that probably explains the presence of these IL-1s in activated PBMC (Fig. 6). The expression of IL-1δ and IL-1ε, as well as IL-1R6, mRNA are all, but most notably IL-1ε mRNA, highly increased in lesional psoriasis skin samples relative to normal control skin samples (Fig. 6). These data are momentarily followed up, but already confirm the involvement of these novel IL-1s in response to skin inflammation (26) and extend the notion that IL-1 ligands and receptors contribute to the pathogenesis of psoriasis (13).

Taken together, IL-1δ and ε and IL-1R6 may constitute an independent signaling system analogous to IL-1αβ/ra and IL-1R1. The IL-1R6 system, present in epithelial barriers of our body, as a result from the coexpression of IL-1δ and IL-1ε, may be in a default off-state. However, perturbation of homeostasis can shift this balance to an IL-1ε-mediated inflammatory or proliferative response, as seen in lesional psoriatic skin.

## Acknowledgments

## References

1. Dinarello, C. A. 1994. The biological properties of interleukin-1. *Eur. Cytokine Netw.* 5:517.

2. Eisenberg, S. P., R. J. Evans, W. P. Arend, E. Verderber, M. T. Brewer, C. H. Hannum, and R. C. Thompson. 1990. Primary structure and functional expression from complementary DNA of a human interleukin-1 receptor antagonist. *Nature* 343:341.

3. Hannum, C. H., C. J. Wilcox, W. P. Arend, F. G. Joslin, D. J. Dripps, P. L. Heimdal, L. G. Armes, A. Sommer, S. P. Eisenberg, and R. C. Thompson. 1990. Interleukin-1 receptor antagonist activity of a human interleukin-1 inhibitor. *Nature* 343:336.

4. March, C. J., B. Mosley, A. Larsen, D. P. Cerretti, G. Braedt, V. Price, S. Gillis, C. S. Henney, S. R. Kronheim, and K. Grabstein. 1985. Cloning, sequence and expression of two distinct human interleukin-1 complementary DNAs. *Nature* 315:641.

5. Greenfeder, S. A., P. Nunes, L. Kwee, M. Labow, R. A. Chizzonite, and G. Ju. 1995. Molecular cloning and characterization of a second subunit of the interleukin 1 receptor complex. *J. Biol. Chem.* 270:13757.

6. McMahan, C. J., J. L. Slack, B. Mosley, D. Cosman, S. D. Lupton, L. L. Brunton, C. E. Grubin, J. M. Wignall, N. A. Jenkins, and C. I. Brannan. 1991. A novel IL-1 receptor, cloned from B cells by mammalian expression, is expressed in many cell types. *EMBO J.* 10:2821.

7. Sims, J. E., C. J. March, D. Cosman, M. B. Widmer, H. R. MacDonald, C. J. McMahan, C. E. Grubin, J. M. Wignall, J. L. Jackson, and S. M. Call. 1988. cDNA expression cloning of the IL-1 receptor, a member of the immunoglobulin superfamily. *Science 241:585.*

8. Rock, F. L., G. Hardiman, J. C. Timans, R. A. Kastelein, and J. F. Bazan. 1998. A family of human receptors structurally related to *Drosophila* Toll. *Proc. Natl. Acad. Sci. USA 95:588.*

9. Freshney, N. W., L. Rawlinson, F. Guesdon, E. Jones, S. Cowley, J. Hsuan, and J. Saklatvala. 1994. Interleukin-1 activates a novel protein kinase cascade that results in the phosphorylation of Hsp27. *Cell 78:1039.*

10. O'Neill, L. A., and C. Greene. 1998. Signal transduction pathways activated by the IL-1 receptor family: ancient signaling machinery in mammals, insects, and plants. *J. Leukocyte Biol. 63:650.*

11. Colotta, F., S. K. Dower, J. E. Sims, and A. Mantovani. 1994. The type II "decoy" receptor: a novel regulatory pathway for interleukin 1. *Immunol. Today 15:562.*

12. Lang, D., J. Knop, H. Wesche, U. Raffetseder, R. Kurrle, D. Boraschi, and M. U. Martin. 1998. The type II IL-1 receptor interacts with the IL-1 receptor accessory protein: a novel mechanism of regulation of IL-1 responsiveness. *J. Immunol. 161:6871.*

13. Debets, R., J. P. Hegmans, P. Croughs, R. J. Troost, J. B. Prins, R. Benner, and E. P. Prens. 1997. The IL-1 system in psoriatic skin: IL-1 antagonist sphere of influence in lesional psoriatic epidermis. *J. Immunol. 158:2955.*

14. Dinarello, C. A. 1996. Biologic basis for interleukin-1 in disease. *Blood 87:2095.*

15. Okamura, H., H. Tsutsi, T. Komatsu, M. Yutsudo, A. Hakura, T. Tanimoto, K. Torigoe, T. Okura, Y. Nukada, and K. Hattori. 1995. Cloning of a new cytokine that induces IFN-γ production by T cells. *Nature 378:88.*

16. Ushio, S., M. Namba, T. Okura, K. Hattori, Y. Nukada, K. Akita, F. Tanabe, K. Konishi, M. Micallef, M. Fujii, et al. 1996. Cloning of the cDNA for human IFN-γ-inducing factor, expression in *Escherichia coli,* and studies on the biologic activities of the protein. *J. Immunol. 156:4274.*

17. Bazan, J. F., J. C. Timans, and R. A. Kastelein. 1996. A newly defined interleukin-1? *Nature 379:591.*

18. Born, T. L., E. Thomassen, T. A. Bird, and J. E. Sims. 1998. Cloning of a novel receptor subunit, AcPL, required for interleukin-18 signaling. *J. Biol. Chem. 273: 29445.*

19. Ghayur, T., S. Banerjee, M. Hugunin, D. Butler, L. Herzog, A. Carter, L. Quintal, L. Sekut, R. Talanian, M. Paskind, et al. 1997. Caspase-1 processes IFN-γ-inducing factor and regulates LPS-induced IFN-γ production. *Nature 386:619.*

20. Gu, Y., K. Kuida, H. Tsutsui, G. Ku, K. Hsiao, M. A. Fleming, N. Hayashi, K. Higashino, H. Okamura, K. Nakanishi, et al. 1997. Activation of interferon-γ inducing factor mediated by interleukin-1β converting enzyme. *Science 275:206.*

21. Kojima, H., M. Takeuchi, T. Ohta, Y. Nishida, N. Arai, M. Ikeda, H. Ikegami, and M. Kurimoto. 1998. Interleukin-18 activates the IRAK-TRAF6 pathway in mouse EL-4 cells. *Biochem. Biophys. Res. Commun. 244:183.*

22. Robinson, D., K. Shibuya, A. Mui, F. Zonin, E. Murphy, T. Sana, S. B. Hartley, S. Menon, R. Kastelein, F. Bazan, and A. O'Garra. 1997. IGIF does not drive Th1 development but synergizes with IL-12 for interferon-γ production and activates IRAK and NFκB. *Immunity 7:571.*

23. Torigoe, K., S. Ushio, T. Okura, S. Kobayashi, M. Taniai, T. Kunikata, T. Murakami, O. Sanou, H. Kojima, M. Fujii, et al. 1997. Purification and characterization of the human interleukin-18 receptor. *J. Biol. Chem. 272:25737.*

24. Mulero, J. J., A. M. Pace, S. T. Nelken, D. B. Loeb, T. R. Correa, R. Drmanac, and J. E. Ford. 1999. IL1HY1: a novel interleukin-1 receptor antagonist gene. *Biochem. Biophys. Res. Commun. 263:702.*

25. Smith, D. E., B. R. Renshaw, R. R. Ketchem, M. Kubin, K. E. Garka, and J. E. Sims. 2000. Four new members expand the interleukin-1 superfamily. *J. Biol. Chem. 275:1169.*

26. Kumar, S., P. C. McDonnell, R. Lehr, L. Tierney, M. N. Tzimas, D. E. Griswold, E. A. Capper, R. Tal-Singer, G. I. Wells, M. L. Doyle, and P. R. Young. 2000. Identification and initial characterization of four novel members of the interleukin-1 family. *J. Biol. Chem. 275:10308.*

27. Busfield, S. J., C. A. Comrack, G. Yu, T. W. Chickering, J. S. Smutko, H. Zhou, K. R. Leiby, L. M. Holmgren, D. P. Gearing, and Y. Pan. 2000. Identification and gene organization of three novel members of the IL-1 family on human chromosome 2. *Genomics 66:213.*

28. Barton, J. L., R. Herbst, D. Bosisio, L. Higgins, and M. J. Nicklin. 2000. A tissue specific IL-1 receptor antagonist homolog from the IL-1 cluster lacks IL-1, IL-1ra, IL-18 and IL-18 antagonist activities. *Eur. J. Immunol. 30:3299.*

29. Pan, G., P. Risser, W. Mao, D. T. Baldwin, A. W. Zhong, E. Filvaroff, D. Yansura, L. Lewis, C. Eigenbrot, W. J. Henzel, and R. Vandlen. 2001. IL-1H, an interleukin 1-related protein that binds IL-18 receptor/IL-1Rrp. *Cytokine 13:1.*

30. Klemenz, R., S. Hoffmann, and A. K. Werenskiold. 1989. Serum- and oncoprotein-mediated induction of a gene with sequence similarity to the gene encoding carcinoembryonic antigen. *Proc. Natl. Acad. Sci. USA 86:5708.*

31. Tominaga, S. 1989. A putative protein of a growth specific cDNA from BALB/c-3T3 cells is highly similar to the extracellular portion of mouse interleukin 1 receptor. *FEBS Lett. 258:301.*

32. Parnet, P., K. E. Garka, T. P. Bonnert, S. K. Dower, and J. E. Sims. 1996. IL-1Rrp is a novel receptor-like molecule similar to the type I interleukin-1 receptor and its homologues T1/ST2 and IL-1R AcP. *J. Biol. Chem. 271:3967.*

33. Lovenberg, T. W., P. D. Crowe, C. Liu, D. T. Chalmers, X. J. Liu, C. Liaw, W. Clevenger, T. Oltersdorf, E. B. De Souza, and R. A. Maki. 1996. Cloning of a cDNA encoding a novel interleukin-1 receptor related protein (IL 1R-rp2). *J. Neuroimmunol. 70:113.*

34. Thomassen, E., B. R. Renshaw, and J. E. Sims. 1999. Identification and characterization of SIGIRR, a molecule representing a novel subtype of the IL-1R superfamily. *Cytokine 11:389.*

35. Carrie, A., L. Jun, T. Bienvenu, M. C. Vinet, N. McDonell, P. Couvert, R. Zemni, A. Cardona, G. Van Buggenhout, S. Frints, et al. 1999. A new member of the IL-1 receptor family highly expressed in hippocampus and involved in X-linked mental retardation. *Nat. Genet. 23:25.*

36. Sana, T. R., R. Debets, J. C. Timans, J. F. Bazan, and R. A. Kastelein. 2000. Computational identification, cloning, and characterization of IL-1R9, a novel interleukin-1 receptor-like gene encoded over an unusually large interval of human chromosome Xq22.2-q22.3. *Genomics 69:252.*

37. Dale, M., and M. J. Nicklin. 1999. Interleukin-1 receptor cluster: gene organization of IL1R2, IL1R1, IL1RL2 (IL-1Rrp2), IL1RL1 (T1/ST2), and IL18R1 (IL-1Rrp) on human chromosome 2q. *Genomics 57:177.*

38. Lafage, M., N. Maroc, P. Dubreuil, M. R. de Waal, M. J. Pebusque, Y. Carcassonne, and P. Mannoni. 1989. The human interleukin-1α gene is located on the long arm of chromosome 2 at band q13. *Blood 73:104.*

39. Patterson, D., C. Jones, I. Hart, J. Bleskan, R. Berger, D. Geyer, S. P. Eisenberg, M. F. Smith, Jr., and W. P. Arend. 1993. The human interleukin-1 receptor antagonist (IL1RN) gene is located in the chromosome 2q14 region. *Genomics 15:173.*

40. Sims, J. E., S. L. Painter, and I. R. Gow. 1995. Genomic organization of the type I and type II IL-1 receptors. *Cytokine 7:483.*

41. Thompson, J. D., D. G. Higgins, and T. J. Gibson. 1994. CLUSTAL W: improving the sensitivity of progressive multiple sequence alignment through sequence weighting, position-specific gap penalties and weight matrix choice. *Nucleic Acids Res. 22:4673.*

42. Kitamura, T., K. Hayashida, K. Sakamaki, T. Yokota, K. Arai, and A. Miyajima. 1991. Reconstitution of functional receptors for human granulocyte/macrophage colony-stimulating factor (GM-CSF): evidence that the protein encoded by the AIC2B cDNA is a subunit of the murine GM-CSF receptor. *Proc. Natl. Acad. Sci. USA 88:5082.*

43. Debets, R., J. C. Timans, T. Churakowa, S. Zurawski, M. R. de Waal, K. W. Moore, J. S. Abrams, A. O'Garra, J. F. Bazan, and R. A. Kastelein. 2000. IL-18 receptors, their role in ligand binding and function: anti-IL- 1RAcPL antibody, a potent antagonist of IL-18. *J. Immunol. 165:4950.*

44. Cullinan, E. B., L. Kwee, P. Nunes, D. J. Shuster, G. Ju, K. W. McIntyre, R. A. Chizzonite, and M. A. Labow. 1998. IL-1 receptor accessory protein is an essential component of the IL-1 receptor. *J. Immunol. 161:5614.*

45. Haskill, S., G. Martin, L. Van Le, J. Morris, A. Peace, C. F. Bigler, G. J. Jaffe, C. Hammerberg, S. A. Sporn, and S. Fong. 1991. cDNA cloning of an intracellular form of the human interleukin 1 receptor antagonist associated with epithelium. *Proc. Natl. Acad. Sci. USA 88:3681.*

46. Muzio, M., N. Polentarutti, M. Sironi, G. Poli, L. De Gioia, M. Introna, A. Mantovani, and F. Colotta. 1995. Cloning and characterization of a new isoform of the interleukin 1 receptor antagonist. *J. Exp. Med. 182:623.*

47. Weissbach, L., K. Tran, S. A. Colquhoun, M. F. Champliaud, and C. A. Towle. 1998. Detection of an interleukin-1 intracellular receptor antagonist mRNA variant. *Biochem. Biophys. Res. Commun. 244:91.*

48. Kupper, T. S. 1989. Mechanisms of cutaneous inflammation: interactions between epidermal cytokines, adhesion molecules, and leukocytes. [Published erratum appears in *1989 Arch. Dermatol. 125:1643.*] *Arch. Dermatol. 125:1406.*

49. Greenfeder, S. A., T. Varnell, G. Powers, K. Lombard-Gillooly, D. Shuster, K. W. McIntyre, D. E. Ryan, W. Levin, V. Madison, and G. Ju. 1995. Insertion of a structural domain of interleukin (IL)-1β confers agonist activity to the IL-1 receptor antagonist: implications for IL-1 bioactivity. *J. Biol. Chem. 270:22460.*

50. Schreuder, H., C. Tardif, S. Trump-Kallmeyer, A. Soffientini, E. Sarubbi, A. Akeson, T. Bowlin, S. Yanofsky, and R. W. Barrett. 1997. A new cytokine-receptor binding mode revealed by the crystal structure of the IL-1 receptor with an antagonist. *Nature 386:194.*

51. Vigers, G. P., L. J. Anderson, P. Caffes, and B. J. Brandhuber. 1997. Crystal structure of the type-I interleukin-1 receptor complexed with interleukin-1β. *Nature 386:190.*

52. Ju, G., E. Labriola-Tompkins, C. A. Campen, W. R. Benjamin, J. Karas, J. Plocinski, D. Biondi, K. L. Kaffka, P. L. Kilian, and S. P. Eisenberg. 1991. Conversion of the interleukin 1 receptor antagonist into an agonist by site-specific mutagenesis. *Proc. Natl. Acad. Sci. USA 88:2658.*

# EXHIBIT 2

# Four New Members Expand the Interleukin-1 Superfamily*

## Dirk E. Smith, Blair R. Renshaw, Randal R. Ketchem, Marek Kubin, Kirsten E. Garka, and John E. Sims‡

*From Immunex Corp., Seattle, Washington 98101*

We report here the cloning and characterization of four new members of the interleukin-1 (IL-1) family (FIL1δ, FIL1ε, FIL1ζ, and FIL1η, with FIL1 standing for "Family of IL-1"). The novel genes demonstrate significant sequence similarity to IL-1α, IL-1β, IL-1ra, and IL-18, and in addition maintain a conserved exon-intron arrangement that is shared with the previously known members of the family. Protein structure modeling also suggests that the *FIL1* genes are related to IL-1β and IL-1ra. The novel genes form a cluster with the IL-1s on the long arm of human chromosome 2.

The cytokine interleukin-1 (IL-1)[1] elicits a wide array of biological activities that initiate and promote the host response to injury or infection, including fever, sleep, loss of appetite, acute phase protein synthesis, chemokine production, adhesion molecule up-regulation, vasodilatation, the pro-coagulant state, increased hematopoiesis, and production and release of matrix metalloproteinases and growth factors (1). It does so by activating a set of transcription factors that includes NFκB and AP-1, which in turn promote production of effectors of the inflammatory response, such as the inducible forms of cyclooxygenase and nitric oxide synthase (2, 3). Interleukin 1 activity actually resides in each of two molecules, IL-1α and IL-1β, which act by binding to a common receptor composed of a ligand binding chain, the type I IL-1 receptor, and a required signaling component, the IL-1R accessory protein (AcP) (4–7). A third member of the family, the IL-1 receptor antagonist (IL-1ra), also binds to the type I IL-1 receptor but fails to bring about the subsequent interaction with AcP, thus not only not signaling itself but also, by blocking the receptor, preventing the action of the agonist IL-1s (8, 9). Additional regulation is provided by the type II, or decoy, IL-1 receptor, which binds and sequesters the agonist IL-1s (especially IL-1β) without inducing any signaling response of its own (10–13). The two agonist IL-1s (IL-1α and IL-1β) are synthesized as larger precursors which undergo proteolytic removal of their pro-domains to generate the mature cytokines (14). At least for IL-1β, this processing is coupled to secretion (15, 16). IL-1ra, in contrast, contains a signal peptide and is secreted by the more traditional route through the endoplasmic reticulum (9).

Recently, another cytokine, interleukin 18 (17, 18) was recognized to be related to the interleukin-1 family based on the similarity of its amino acid sequence and predicted tertiary structure (19). IL-18 induces the production of γ-interferon from T cells, especially in combination with IL-12, and stimulates the killing activity of cytotoxic T lymphocytes and NK cells by up-regulating Fas ligand (20). Like the agonist IL-1s, IL-18 contains a prodomain that is removed by the same protease, caspase-1, that processes IL-1β (21, 22). Consistent with its being related to the IL-1s, IL-18 binds a receptor which is homologous to the IL-1 receptor. The ligand-binding chain IL-1Rrp1 (or IL-18Rα) (23, 24) was cloned initially on the basis of its homology to the IL-1R (25). The signaling subunit (IL-18Rβ) was originally named AcPL (AcP-like) for its similarity to the IL-1R signaling subunit (26). The IL-18 receptor subunits are encoded in the same gene cluster on chromosome 2 as are the type I and II IL-1 receptors (25–27).

We have searched for novel members of the IL-1 family. We report here the sequences and some of the characteristics of four genes that appear to have descended from the same common ancestor as did IL-1α, IL-1β, IL-1ra, and IL-18. We propose that these novel molecules be designated FIL1δ, -ε, -ζ, and -η, with FIL1 being an acronym for Family of IL-1.

## EXPERIMENTAL PROCEDURES

### Cloning of Novel Human IL-1 Family Members

The following details supplement the general descriptions given under "Results" for the cloning of the individual IL-1 family members.

*FIL1δ*—A 469-base pair single-stranded ³²P-labeled PCR product spanning the entire mouse FIL1δ coding region (found in GenBank™ W08205) was used to probe a human placenta cDNA library (in λUni-ZAP XR; Stratagene number 937225) (hybridization in 40% formamide at 42 °C; wash in 0.3 M NaCl at 55 °C). Several clones were isolated, all of which appeared to lack the full open reading frame by comparison with mouse FIL1δ. Vector-anchored PCR on DNA from the same library was used to isolate the remaining coding sequence.

*FIL1ε*—A human genomic library (Stratagene catalog number 946205; in λFixII) was screened using a ³²P-labeled single-strand DNA probe corresponding to the entire IL-1-like coding sequence present in GenBank™ EST AA030324 (hybridization in 45% formamide at 42 °C; wash in 0.3 M NaCl at 63 °C). The insert from one positive plaque was mapped to locate the hybridizing region, sequencing of which then revealed the 3'-most exon of the human *FIL1ε* gene. 5.3 kilobases of human genomic DNA to the 5' side of this exon was isolated using the CLONTECH Human GenomeWalker kit (catalog number K1803-1). Sequencing of this DNA allowed identification of the remaining coding exons. The structure of the gene was confirmed by isolation of a PCR product in which the predicted exons were indeed spliced, using as template first-strand cDNA from the cell lines HL60 and THP1, and from human thymic tissue. Interestingly, while the original genomic DNA sequence coded for glutamine at amino acid 12, cDNA clones from all three sources contain arginine at amino acid 12.

*FIL1ζ*—The FIL1ζ open reading frame was identified in a cDNA library made from the pancreatic tumor cell line HPT-4.

*FIL1η*—A human genomic DNA sequenced to identify the *FIL1η* 3' exon was obtained using the CLONTECH Human GenomeWalker kit (catalog number K1803-1).

---

[1] The abbreviations used are: IL, interleukin; AcP, accessory protein; IL-1ra, interleukin 1 receptor antagonist; PCR, polymerase chain reaction; PDF, probability density function; LPS, lipopolysaccharide.

TABLE I

*PCR primer sequences used for analyzing expression of novel IL-1 family member mRNA*

On some occasions, a second PCR reaction using nested primers was performed for FIL1δ and FIL1ε. Cycle numbers and annealing temperatures are also given.

| Molecule | Primary or nested | Sense/anti | Sequence | No. cycles | Anneal °C |
|---|---|---|---|---|---|
| FIL1δ | Primary | Sense | GGGAGTCTACACCCTGTGGAGCTCAA | 30 | 58 |
| FIL1δ | Primary | Antisense | CTGCTGGAAGTAGAAGTCTGTGATGG | | |
| FIL1δ | Nested | Sense | GGAGCTCAAGATGGTCCTGAGTGGGGCGCT | 30 | 58 |
| FIL1δ | Nested | Antisense | GCATTCCAGCCACCATTCTCGGGAAGCT | | |
| FIL1ε | Primary | Sense | GACACACCTCAGCAGGGGAGCATTCAGG | 40 | 60 |
| FIL1ε | Primary | Antisense | AACAGCATAGTTAACCCAAAGTCAGTAG | | |
| FIL1ζ | Primary | Sense | TGAGATCCTATGTCAGGCTGTGATAGG | 40 | 60 |
| FIL1ζ | Primary | Antisense | TGCTATGAGATTCCCAGAGTCCAGGACC | | |
| FIL1η | Primary | Sense | ACATCATGAACCCACAACGGGAGGCAGCAC | 35 | 60 |
| FIL1η | Primary | Antisense | CTCTATCCTGGAACCAGCCACCCACAGC | | |
| FIL1η | Nested | Sense | CCAAATCCTATGCTATTCGTGATTCTCGAC | 35 | 58 |
| FIL1η | Nested | Antisense | GGATTTATTCCACAGAATCTAAGTAGAAG | | |

## Structure Modeling

Template sequences for structure modeling were extracted from the Protein Data Bank (28). A sequence alignment for the superfamily was generated based on that proposed by Bazan *et al.* (19) for the IL-1s and IL-18, which appeared valid by examination of both cysteine and real *versus* predicted sheet alignments. Preliminary analysis using the program Gene Fold (29) demonstrated that the experimentally determined structures for IL-1β (Protein Data Bank designations 1hib, 2i1b, 1iob, 1itb, and 2i1bi) and IL-1ra (Protein Data Bank designations 1ilr, 1ira, and 1irp) were valid templates for the new IL-1 family members FIL1δ, FIL1ε, and FIL1ζ. Although the sequence identity of the new IL-1-like cytokines is greater to IL-1ra, Gene Fold showed a stronger match to the structure of IL-1β. In addition, the various IL-1β structures appear better aligned structurally (as seen by superposition) than do the IL-1ra structures, so both templates were used for modeling. Modeler (30) was used to generate a family of 20 structures for each query sequence. All structures showed a well defined core β-trefoil, with higher variability in the outer loops; the per molecule probability density function (PDF) used by modeler varied from 1194 to 1984. The structure with the lowest overall PDF violation was visualized using a variable width ribbon based on the per residue PDF violation and showed that the highest violation was in the region of highest structural difference between IL-1ra and IL-1β. At this point the cysteine positions for the three models were revisited to ensure that no disulfide links were missed. A representative structure for each model was chosen by first ordering the models within a family by total PDF violation. After discarding structures with obvious problems, such as knots, the remaining members were then superimposed onto their mean. The structure with the lowest all atom root mean square deviation from the mean was chosen as the representative structure. Finally, the models were analyzed using Procheck (31) and it was shown that the structures are valid at 2.0-Å resolution with no major structural problems. The structure models for FIL1δ, FIL1ε, and FIL1ζ can be examined by contacting the authors.

## Intron/Exon Mapping

Intron placement was determined by direct cloning or amplification of genomic DNA from the various novel IL-1 loci. Primers were designed so that the PCR products overlapped one another to ensure that small introns were not overlooked. The sequence of the PCR products from genomic DNA was compared with the cDNA sequence in order to determine the exon/intron junctions.

## Chromosome Mapping

Chromosome mapping was performed using the Genebridge 4 radiation hybrid panel (32) (catalog number RH02.05 from Research Genetics) which consists of 93 human/hamster hybrid cell lines. Genomic DNA from the cell lines was amplified using PCR primers specific for the human version of each novel IL-1 family gene. Products were separated by agarose gel electrophoresis and visualized by ethidium bromide staining. Each hybrid was scored in the following manner: 0 was assigned if there was clearly no amplification; 1 was assigned where there clearly was amplification; a score of 2 was assigned where the data was ambiguous. Scores were then submitted to the Whitehead Institute/MIT for chromosomal assignment and placement relative to known framework markers on the radiation hybrid map. Scores for each gene are as follows: *FIL1δ*, 1000000100000000100012010010012-

00001101100001000000000101000010001120000000100010000100010100; *FIL1ε*, 10100001000010001000110112100110000110110100100-00001000101010021011110000001000010001100010100; *FIL1ζ*, 1010-0001000010001000120122100100000110110100100000100010101001-1021110000001000010001120010100; *FIL1η*, 1220002000100000100-0000100100100012000110020100000000010100000100022000000010-00010001100010100. Scores used for concomitant map placement of IL-1α, IL-1β, and IL-1ra were obtained from the NCBI (*IL-1α*, X02851; *IL-1β*, D20737 and AA150507; *IL-1ra*, H50548, R49297, and T72887).

## Expression Analysis

First-strand cDNAs present in CLONTECH (Palo Alto, CA) Human Multiple Tissue cDNA Panels I (catalog number K1420-1) and II (catalog number K1421-1) and the Human Immune Panel (catalog number K1426-1) were screened by PCR amplification using primers given in Table I. The primers were designed to span introns so that products arising from genomic DNA and cDNA could be distinguished. In some cases, nested primers were used in a second PCR reaction. The presence of an amplification product for each gene/tissue combination was determined by analysis on agarose gels stained with ethidium bromide.

Alternatively, individual cell types from human peripheral blood were isolated from multiple donors, and stimulations were performed as described (33, 34, 41). In brief, NK cells were incubated with IL-12 (R & D Biosystems; 1 ng/ml) for either 2 or 4 h. T cells were unstimulated or stimulated with anti-CD3 (OKT-3 antibody, immobilized on plastic at 5 μg/ml) or with the combination of anti-CD3 and anti-CD28 (the anti-CD28 antibody was CK248, used in soluble form as a 1:500 dilution of ascites fluid), for 4 h. Monocytes were unstimulated, or stimulated with LPS (Sigma, 1 μg/ml) for 2 or 3 h. B cells were unstimulated, or stimulated with a combination of 005% SAC + 500 ng/ml CD40L trimer (Immunex) + 5 ng/ml IL-4 (Immunex) for 3.5 or 4 h. Dendritic cells were stimulated with LPS as for monocytes for 2 or 4 h. After isolation of RNA and synthesis of first-strand cDNA, PCR amplifications and gel analysis were performed as described above.

## Expression of Novel IL-1 Family Proteins for Receptor Binding

Novel IL-1 family members, as well as control IL-1β and IL-18 molecules, were generated by transfection of expression vector constructs into COS cells using DEAE-dextran (35). Expression vectors used were pDC409 (36) for FIL1ε and FIL1ζ, or pDC412, a close relative, for FIL1δ and FIL1η. The unmodified open reading frames were used for FIL1δ, ε, and η. For FIL1ζ, the sequence beginning with Lys[27] (KNLN. . . . .) was fused downstream of the human immunoglobulin κ light chain signal peptide. IL-1β, with an ATG codon added to the N terminus of the mature form (beginning with Ala[117]), was expressed in pDC409. Human IL-18 was expressed as the mature form fused to the IL-7 signal peptide in the expression vector pDC206 (37). For radiolabeling, 48 h after transfection cells were starved of cysteine and methionine for 60 min, then labeled with 70 μCi/ml of a [35S]cysteine/methionine mixture (Amersham; >1000 Ci/mmol) for 4–6 h. It is perhaps of interest that FIL1δ, FIL1ε, and FIL1η appear to be secreted from the COS cells despite the absence of either signal peptide or prodomain. C-terminal FLAG-tagged FIL1δ and -ε were partially purified from the conditioned medium using the tags, and their N termini sequenced. The N-terminal amino acid of the secreted FIL1ε was methionine 1; it had been modified by N-terminal acetylation. The N-terminal amino acid of the secreted FIL1δ is valine 2. Thus, there does not appear to have been
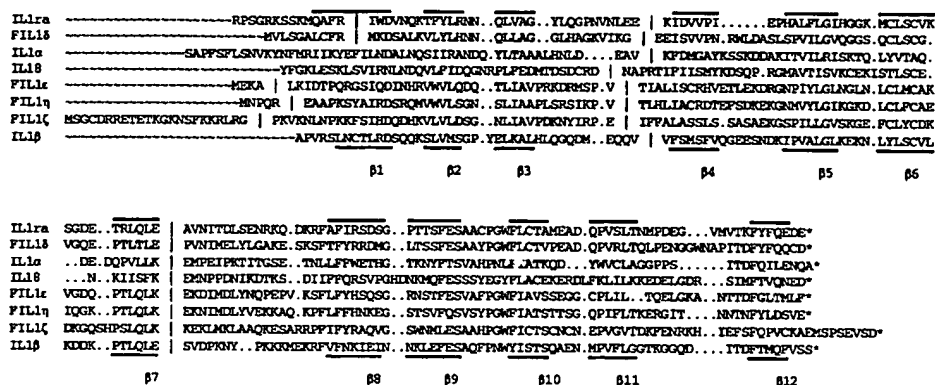
```
ILlra   ---------------RPSGRKSSKMQAFR | IWDVNQKTFYLRNN..QLVAG..YLQGPNVNLEE | KIDVVPI......EPHALFLGIHGGK.MCLSCVK
FIL1S   ---------------MVLSGALCFR | NKDSALKVLYLHNN..QLLAG..GLHAGKVIKG | EEISVVPN.RMLDASLSPVILGVQGGS.QCLSCG.
ILla    ------SAPFSFLSNVKYNFMRIIKYEFIIADALNQSIIRANDQ.YLFAAALHNLD....EAV | KFDMGAYKSSKIDAKITVILRISKTQ.LYVTAQ.
IL18    -------------YFGKLESKLSVIRNLNDQVLFIDQGNRPLFEDMTDSDCRD | NAPRTIPIISHYKDSQP.RGMAVTISVKCEKISTLSCE.
FIL1c   ------MEKA | LKIDTPQRGSIQODNHRVWVLQDQ..TLIAVPRKDRMSP.V | TIALISCRHVETLEKDRGNPIYLGLNGLN.LCLMCAK
FIL1n   ------MNPQR | EAAPKSYAIRDSRQMVWVLSGN..SLIAAPLSRSIKP.V | TLHLIACRDTEPSDREKGNMVYLGIKGRD.LCLPCAE
FIL1C   MSGCDRRETETKGKNSFKKRLRG | PKVKNLNPKKFSIHDQDHKVLVLDSG..NLIAVPDKNYIRP.E | IPFALASSLS.SASAEKGSPILLGVSKGE.PCLYCDK
IL1B    ------APVRSLNCTLRDSQQKSLVMSGP.YELKALHLQGQDM..EQQV | VFSMSFVQGEESNDKIPVALGLKEKN.LYLSCVL

                      B1       B2        B3              B4              B5        B6


ILlra   SGDE..TRLQLE | AVNITDLSENRKQ.DKRFAPIRSDSG..PTTSFESAACPGWFLCTAMEAD.QPVSLTNMPDEG...VNVTKFYFQEDE*
FIL1S   VGQE..PTLTLE | PVNIMELYLGARE.SKSPTFYRRDMG..LITSSFESAAYPGWFLCTVPEAD.QPVRLTQLPENGGWNAPITDFYFQQCD*
ILla    ..DE.DQPVLLK | EMPEIPKTITGSE..TNLLFPWETHG..TKNYPTSVAHRNLF.ATKQD...YWVCLAGGPPS......ITDFQILENQA*
IL18    ...N..KIISFK | EMNPPDNIKDTKS..DIIPFQRSVPGHDNKMQFESSSYEGYFLACEKERDLFKLILKKEDELGDR...SIMFTVQNED*
FIL1c   VGDQ..PTLQLK | EKDIMDLYNQPEPV.KSFLFYHSQSG..RNSTFESVAFPGWFIAVSSEGG.CPLIL..TQELGKA..NTTDFGLTHLF*
FIL1n   IQGK..PTLQLK | EKNIMDLYVEKKAQ.KPFLFFHNKEG..STSVFQSVSYPGWFIATSTTSG.QPIPLTKERGIT....NMTNFYLDSVE*
FIL1C   DKGQSHPSLQLK | KEKLMKLAAQKESARRPFIFYRAQVG..SWNMLESAAHPGWFICTSCNCN.EPVGVTDKFENRKH..IEFSFQPVCKAEMSPSEVSD*
IL1B    KDDK..PTLQLE | SVDPKNY..PKKMEKRFVFNKIEIN..NKLEFESAQFPNWYISTSQAEN.MPVFLGGTRGGQD....ITDFTMQPVSS*

            B7          B8          B9       B10        B11             B12
```

FIG. 1. **Alignment of amino acid sequences for human members of the IL-1 superfamily.** The full-length predicted translation products are shown for FIL1δ, -ε, -ζ, and -η, whereas the mature peptides, without prodomains or signal peptide, are given for IL-1α, IL-1β, IL-1ra, and IL-18. The alignment is based on that presented by Bazan *et al.* (19) with slight modifications. *Bars above* and *below* the sequence indicate regions of experimentally determined (IL-1β and IL-1ra) or proposed β-strand. The *vertical lines* within each sequence indicate intron positions. Some of these are taken from GenBank™ (*IL-1α*, accession number X03833; *IL-1β*, accesssion number X04500; *IL-1ra*, accession number X64532; *IL-18*, accession number E17138). The rest were determined for this paper. The sequences of FIL1δ, FIL1ε, FIL1ζ, and FIL1η have been deposited in GenBank™ (accession numbers AF201830, AF201831, AF201832, and AF201833).

cleavage of an unrecognized signal peptide or prodomain in either molecule. There are a number of proteins which, when transfected into COS cells, do not later appear in the medium, so this is not a general phenomenon attributable to leaky cells. However, the intracellular version of IL-1ra (icIL-1ra, a kind gift of William Arend, University of Colorado) also appears in the medium following transfection of COS cells. The significance of these findings is currently unknown.

### Receptor Binding Assays

The novel IL-1 family members, present as ^{35}S-labeled proteins in conditioned medium from transfected COS cells, were tested for binding to Fc fusion proteins of the IL-1 receptor superfamily members (see Footnote 2 for general methods)[2] IL-1R type I, IL-1R AcP, IL-1Rrp1, IL-1Rrp2, IL-1R AcPL, and T1/ST2 as follows: 0.5–1.0 ml of conditioned medium was pre-cleared for 2 h at 4 °C with 50 $\mu$l of protein G-Sepharose (Amersham Pharmacia Biotech; 50% solution in phosphate-buffered saline) containing 1% Triton X-100, 0.02% NaN$_3$, and protease inhibitors (Roche Molecular Biochemicals catalog number 1 836 145). After a brief spin (3 min, 1000 rpm), the supernatant was transferred to a fresh tube and incubated overnight at 4 °C with 1 $\mu$g of receptor/Fc fusion protein plus another 50 $\mu$l of protein G-Sepharose. The mixture was centrifuged briefly, and the supernatant mixed with 0.5 ml of phosphate-buffered saline containing 5% glucose and protease inhibitors and spun again. The pellet was washed four times with 1 ml of a solution containing 0.4 M NaCl, 0.05% SDS, 1% Nonidet P-40, and protease inhibitors, and resuspended in 25 $\mu$l of 2 × reducing sample buffer (Zaxis, catalog number 220-2110106). Samples were run on 4–20% Tris glycine gels (Novex) and autoradiographed.

### RESULTS

The four previously known members of the IL-1 family (IL-1α, IL-1β, IL-1ra, and IL-18), while possessing a low overall fractional amino acid identity, share certain common amino acid sequence motifs, the most obvious of which can be summarized as F($X_{10-12}$)FXS(AVS)$XX$(PE)$XX$(FY)(LI)(CAS)(TC) where $X$ is any amino acid, and parentheses indicate that one of the included amino acids is present at that position. There are similarities in intron placement within the family as well. Relying on the sequence similarity, we searched public EST data bases and found sequences corresponding to three novel IL-1 family members, described below as FIL1δ, FIL1ε, and FIL1ζ. A fourth novel family member, described below as FIL1η, was originally revealed in a published patent application. Examination of the sequence (called IL-1δ by the inventors) in the patent application suggested that it was derived from an aberrantly spliced mRNA. We searched for and found

an alternative form of mRNA that contains the conserved family sequence motif in the extreme 3' exon. A brief description of the cloning and characteristics of each of the family members is given below. The sequences, and a comparison with the previously known IL-1 superfamily members, are given in Fig. 1.

### FIL1δ

A search of GenBank™ revealed a murine EST, accession number W08205, that resembled the known IL-1s but was not identical to any. The IMAGE clone corresponding to the EST was sequenced and found to contain the entire open reading frame of an IL-1-like molecule. Unlike the known family members, this novel polypeptide (called FIL1δ) appeared to contain neither a signal peptide nor a prodomain at the N terminus. A human FIL1δ cDNA was then isolated from a human placenta cDNA library, using mouse FIL1δ as a probe. The human sequence predicted an open reading frame similar to that of mouse FIL1δ. Multiple FIL1δ cDNA clones from both species were subsequently isolated, and all had the same predicted open reading frame, with no evidence for isoforms containing either signal peptide or prodomain. Interestingly, among the cDNA clones from both species were found several different 5'-untranslated region sequences (data not shown). These different 5' sequences appear to derive from separate exons, in that they can be found (separately) in genomic sequence upstream of the *FIL1δ* coding region, and have potential splice donor sites at their 3' ends. Presumably the *FIL1δ* gene is transcribed from at least two promoters.

### FIL1ε

A later search of GenBank™ revealed a murine EST, accession number AA030324, that resembled a second novel IL-1 family member. Sequencing of the IMAGE clone corresponding to the EST showed an open reading frame that appeared to encode the C-terminal portion of an IL-1 molecule, but which could not be extended in the 5' direction. The mouse sequence was used to probe a human genomic library, and a positive clone was identified and the insert sequenced. The sequence revealed a 212-base pair region with homology to the 3'-most exon of mouse *FIL1ε*. There was a potential splice acceptor site at the 5' end of this region, and a stop codon at the 3' end of the 70-amino acid open reading frame. More human genomic DNA to the 5' side of this open reading frame was then isolated and sequenced, revealing three additional putative exons with sequence similarity to the mouse EST and to other IL-1 family members. On the assumption that the four putative exons were

---

spliced to form a single coding region, PCR primers were designed and used successfully to amplify the predicted product from several different human RNA sources. As for FIL1δ, the predicted FIL1ε reading frame contains neither a signal peptide nor a prodomain.

## FIL1ζ

A third EST, accession number AI014548, was found in Gen-Bank™ that appeared to encode an IL-1-like molecule. However, further sequencing revealed that the corresponding (human) IMAGE clone contained a stop codon upstream of the open reading frame but no initiating methionine. Screening of two other cDNA libraries resulted in isolation of a second, distinct aberrant clone, as well as a clone that contained an open reading-frame that did begin with a methionine and that extended for 192 amino acids. This last clone was named FIL1ζ. Sequence comparison with other family members suggests that FIL1ζ has a prodomain of some 15–30 amino acids.

Analysis of genomic DNA demonstrated that an intron lies between the nucleotides encoding the $23^{rd}$ and $24^{th}$ amino acids of the 192 amino acid open reading frame form (see Figs. 1 and 4). The stop codon-containing sequences found in the aberrant cDNA clones lie within this intron, and appear to be incorporated into mRNA by cryptic splicing events. Since we had found three different cDNA isoforms for FIL1ζ, only one of which appeared to contain a functional open reading frame, it was important to determine the relative levels of the different transcripts. This was done by designing PCR primers that would amplify and distinguish the three isoforms, and using them to examine expression in a panel of first-strand cDNAs. The (presumably functional) FIL1ζ transcript was found in lymph node, thymus, bone marrow stroma, lung, testis, and placenta (Table II). We could not detect the form of mRNA represented by the EST in any tissue, whereas that represented by the other form of "aberrant" mRNA was present in bone marrow stroma (from which we had originally isolated it), lung, and placenta but not in the other tissues (not shown). The mRNA encoding that form appeared to be much less abundant than the functional FIL1ζ mRNA.

## FIL1η

A cDNA clone containing part of the FIL1η sequence was originally identified in an osteoclastoma library (38). The DNA sequence presented in this document appeared to encode the N-terminal half of an IL-1 like molecule, which then diverged in the C-terminal portion. Since the C-terminal regions of the different IL-1 family members contain the greatest sequence conservation, including the motif described above, and since the point of divergence lay exactly at the position of a conserved intron in the IL-1 family (see below), we searched for an alternative transcript that might encode a more typical member of the family.

PCR with first strand cDNA templates from various tissue sources, using primers lying entirely within the 5′-half of the osteoclastoma coding sequence (38), gave products from tonsil, bone marrow, heart, placenta, lung, testis, and colon. Only very faint bands were obtained, and only in tonsil and testis, when a 5′ primer from the 5′-half and a 3′ primer from the 3′-half of the osteoclastoma coding sequence were used, consistent with our interpretation. Human genomic DNA containing the 5′-half of the osteoclastoma sequence and extending further downstream was then isolated and sequenced. A putative exon was found 823 base pairs downstream of the point of divergence of the osteoclastoma sequence from other family members; this putative exon contained the expected sequence motifs for the C-terminal portion of an IL-1 family member, as well as a

TABLE II
*Expression data for novel IL-1 family members*

The table summarizes all available expression data on the novel IL-1 family members. "−" indicates that the mRNA was looked for but not found; a blank space indicates that the analysis was not done for that particular gene/RNA combination. Positive results were derived as follows: "a", by PCR analysis from a panel of first strand cDNAs (Clontech); "b", by cDNA library screening; "c", by the existence of an EST; "d", by PCR analysis of an individual RNA. "e" indicates that expression of the gene was increased by LPS. In the source column for tissues, "pool" was a mixture of fetal lung, testis, and B cell. In the source column for human cell lines, MoT and HUT102 are T-cell lines; Raji is a B cell line; THP-1 and U937 are macrophage lines; IMTLH is an unpublished bone marrow stromal cell line, derived at Immunex; HL60 is an early hematopoietic precursor line; HPT-4 is a pancreatic tumor line; T84 is a colon tumor line. For FIL1δ in lung, (a) indicates that the PCR product lacks exon 2. The PCR products for FIL1δ, FIL1ε, and FIL1η were especially strong from tonsil RNA, while that for FIL1ζ was strong in placenta and testis.

| Source | FIL1δ | FIL1ε | FIL1ζ | FIL1η |
|---|---|---|---|---|
| **Human tissue** | | | | |
| Spleen | − | a | − | − |
| Lymph node | a | a | a | − |
| Thymus | a | a | a | − |
| Tonsil | a | a | − | a |
| Bone marrow | − | b | a,b | a |
| Fetal liver | − | − | − | − |
| Leukocyte | − | a | − | − |
| Heart | − | − | − | a |
| Brain | a | − | | − |
| Placenta | a,b | − | a | a |
| Lung | (a) | − | a | a |
| Liver | − | − | − | − |
| Skeleton muscle | a | − | − | − |
| Kidney | − | − | − | − |
| Pancreas | − | − | − | − |
| Prostate | a | − | − | − |
| Testis | a | − | a | a |
| Ovary | − | − | − | − |
| Small intestine | − | − | − | − |
| Colon | − | − | − | a |
| Fetal brain | | b | | |
| NK cells | b | | | |
| Parathyroid tumor | c | | | |
| Colon tumor | | | c | |
| Pool | | | c | |
| **Human cell lines** | | | | |
| Mo-T | | b | | |
| HUT-102 | | b | | |
| Raji | | b | | |
| THP-1 | | d | d | |
| U937 | | | d,e | |
| IMTLH | | d | d | |
| HL60 | | d | d | |
| HPT-4 | | b | b | |
| T84 | | b | | |
| **Mouse tissue** | | | | |
| Spleen | d,e | d,e | | |
| Kidney | b | | | |
| Placenta/yolk sac | d | c | | |
| Embryo | c | | | |
| Stomach | c | c | | |
| Tongue | c | c | | |
| Skin | c | | | |
| **Mouse cell lines** | | | | |
| Macrophage (RAW) | d,e | b,d,e | | |

potential splice acceptor site at its 5′ end. PCR primers designed to amplify a hypothetical cDNA formed by splicing of the 5′ portion of the osteoclastoma sequence with this 3′ exon did indeed give a product from human tonsil first strand cDNA, which when sequenced contained the predicted 157-amino acid open reading frame. The open reading frame, and the gene encoding it, were named FIL1η. Like FIL1δ and FIL1ε, FIL1η does not contain an apparent signal peptide or prodomain.

TABLE III

*Sequence identity*

The numbers represent percent sequence identity between the indicated IL-1 superfamily members, as determined by using the program "gap" (Wisconsin Package Version 10.0, Genetics Computer Group (GCG)). For IL-1α, IL-1β, IL-18, and IL-1ra, the mature peptide (lacking signal sequence or prodomain) was used for the comparison. For FIL1ζ, the mature form was assumed to start with Lys27, based on primary sequence alignment and analysis of predicted eight-dimensional structure, and this sequence was used.

| | IL-1α | IL-1β | IL-1ra | IL-18 | FIL1δ | FIL1ε | FIL1ζ | FIL1η |
|---|---|---|---|---|---|---|---|---|
| IL-1α | ... | 24 | 20 | 21 | 20 | 23 | 21 | 26 |
| IL-1β | | ... | 31 | 17 | 32 | 27 | 24 | 32 |
| IL-1ra | | | ... | 22 | 50 | 30 | 29 | 30 |
| IL-18 | | | | ... | 27 | 20 | 21 | 21 |
| FIL1δ | | | | | ... | 31 | 35 | 37 |
| FIL1ε | | | | | | | 36 | 46 |
| FIL1ζ | | | | | | ... | ... | 44 |
| FIL1η | | | | | | | | ... |

FIG. 2. **Dendrogram illustrating the relationship between members of the IL-1 superfamily.** The dendrogram was generated by the program Treeview (40) using the amino acid sequence alignment produced by the program Pileup (Wisconsin Package Version 10.0, Genetics Computer Group (GCG), Madison, WI).

## A Gene Family

*Sequence Comparison*—The novel members of the IL-1 family are approximately as similar to one another in sequence as they are to the classical IL-1s; this level of identity is in turn similar to that shown by the classical IL-1s among themselves. Typically any given pair of family members shows 20–35% sequence identity (Table III). Those that stand out as being more similar to one another than average are FIL1δ/IL-1ra, FIL1ε/FIL1η, and FIL1ζ/FIL1η. These relationships can also be seen in the dendrogram presented in Fig. 2, in which it appears that IL-1α, IL-1β, and IL-18 form one sequence subfamily; FIL1ε, FIL1ζ, and FIL1η form a second subfamily, and IL-1ra and FIL1δ form a third. The novel members can easily
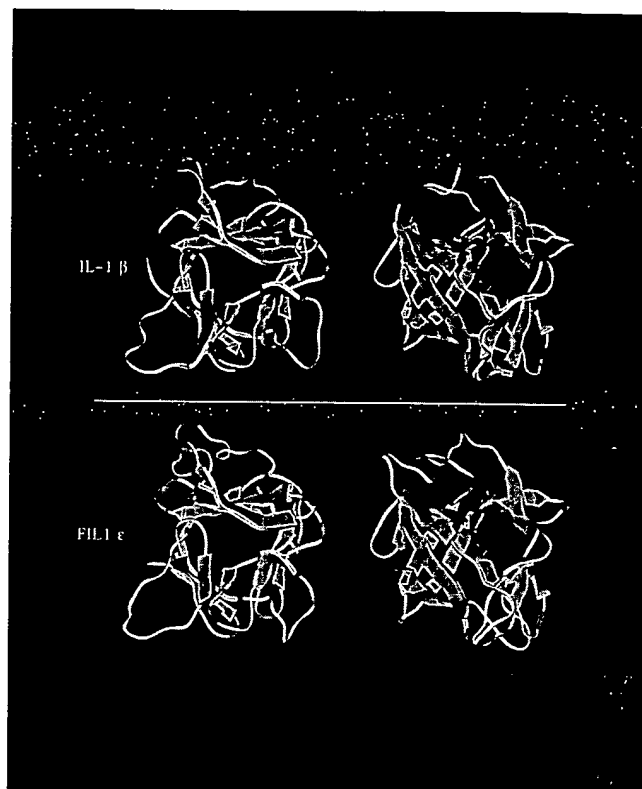


FIG. 3. **Structure models.** Structural models of IL-1β and FIL1ε were generated as described under "Experimental Procedures." The figure shows views looking down the opening of the barrel in the β-trefoil structures, as well as views of the models rotated by 90° along the x axis. *Yellow*, β-strand; *green*, coil; *blue*, β-turn.

be placed onto the structure-based sequence alignment presented by Bazan *et al.* (19) (Fig. 1).

*Three-dimensional Protein Structure Prediction*—The structures of FIL1δ, FIL1ε, and FIL1ζ have been modeled using as templates the experimentally determined structures of IL-1β and IL-1ra. The novel IL-1 superfamily member amino acid sequences could with minimal energy violations be folded into structures which superimpose well onto the IL-1β and IL-1ra crystal structures. In particular, the core 12-stranded, β-trefoil structure appears well conserved (see Fig. 3 for FIL1ε). The major points of difference between the FIL1δ, FIL1ε, and FIL1ζ models, and between them and the experimental structures, lie in the loops connecting the β strands, where IL-1β and IL-1ra also differ most from each other.

*Genomic Structure*—The known genes of the IL-1 family display a conserved pattern of intron placement and intron/exon junctions, clearly indicating their derivation from a common ancestor. The novel IL-1 family members presented here demonstrate the same pattern. The most C-terminal intron in the coding region always falls between codons, and lies immediately after the predicted β-strand 7. By analogy to the structure of the *IL-1α* and *IL-1β* genes, we have called this intron 5, even though the rest of the family has only three introns within the coding sequence (except *IL-18*, which has four). Intron 4 (the intron N-terminal to intron 5) falls between the first and second nucleotides of the codon, and lies just N-terminal to β-strand 4. Intron 3 is more variable in placement. In *IL-1α*, *IL-1β*, *IL-18*, and probably in *FIL1ζ*, it lies within the prodomain, not far upstream of the site of processing. In the other family members, it appears to lie not far downstream of the initiating methionine. It is also more variable in placement within the codon, falling after either the first (*IL-1α*, *IL-1β*, *IL-18*, *FIL1ε*, *FIL1ζ*, *FIL1η*) or second (*IL-1ra*, *FIL1δ*) nucleo-

tide of the codon.

*Chromosomal Location*—The novel IL-1 family members have been mapped using the radiation hybrid method. They cluster on human chromosome 2q, between the framework markers D2S121 and D2S110 (not shown). The *IL-1α/IL-1β/IL-1ra* cluster lies within this same interval. At the level of resolution seen with the Genebridge 4 panel, the novel and classical IL-1 genes appear to be interspersed.

## Expression Pattern

We have analyzed the expression pattern of the novel IL-1 family members in several ways. Using a panel of first strand cDNAs derived from various tissues as templates for PCR, we find that the novel family members are all expressed in lymphoid organs, although the detailed pattern differs somewhat from cytokine to cytokine (Table II). RNA for each is also present in a small number of non-lymphoid tissues. Table II also summarizes expression data obtained from cDNA library screening, from searching EST data bases, and from PCR analysis of individual RNA samples. No easy generalization about expression patterns, either for the individual cytokines or for the family, is obvious.

*Hematopoietic Subsets*—We wanted to look specifically at expression of each of the novel IL-1 family members in individual cell types from peripheral blood. Cells were prepared from human blood and cultured for a short time in various conditions. RNA was made and analyzed by RT-PCR for the presence of FIL1δ, -ε, -ζ, and -η (Table IV). All family members were expressed in activated monocytes and B cells. In most cases, there was some expression present in these cells even without stimulation. FIL1δ was also expressed in activated dendritic

### TABLE IV
*Expression of novel family members in hematopoietic cell subsets*

Expression of IL-1 family members was determined by PCR analysis of RNA isolated from subsets of peripheral blood mononuclear cells, obtained as described under "Experimental Procedures."

| Cell subset | FIL1δ | FIL1ε | FIL1ζ | FIL1η |
|---|---|---|---|---|
| NK cell + IL-12 | ND[a] | ND | + | ND |
| T cell | − | + | − | − |
| Monocyte | + + | + | ND | + |
| Monocyte + LPS | + + | + + | + + | + + |
| B cell | + + | + | − | + |
| B cell stimulated | + + | + | + | + |
| Dendritic cell + LPS | + + | − | ND | ND |

[a] ND, not done.

cells. The only one of the family members expressed by T cells was FIL1ε.

*Receptor Binding*—We asked whether any of the novel IL-1 family members could bind to the known members of the IL-1 receptor family. Conditioned medium from COS cells transfected with each of the different novel ligands and labeled with [$^{35}$S]Cys/Met, as well as from COS cells transfected with IL-18 as a positive control, were incubated with Fc fusions of the characterized IL-1R family members (IL-1R type I, IL-1R AcP, IL-1Rrp1, IL-1Rrp2, AcPL, and T1/ST2), followed by precipitation of the Fc proteins using protein G. The precipitates were electrophoresed on SDS gels, and autoradiographed to see whether any of the ligands were able to bind to any of the receptors. While IL-18 was seen consistently to bind to IL-1Rrp1, no other complexes were observable using this technique (data not shown).

### DISCUSSION

We describe here the discovery of novel genes that double the size of the IL-1 superfamily. Assessment of the *FIL1δ, FIL1ε, FIL1ζ,* and *FIL1η* genes as paralogs of *IL-1α, IL-1β, IL-1ra,* and *IL-18* is based on several factors. First, sequence alignment (Fig. 1) reveals certain conserved amino acid motifs. Not only is there easily recognizable conservation of primary structure, but the amino acid sequences readily allow modeling into a predicted three-dimensional structure that is conserved with the known IL-1s (Fig. 3). In addition, intron placement is highly conserved in these new genes and is similar to that found in the "traditional" IL-1s as well as *IL-18* (Figs. 1, 4). This provides an independent measure of evolution from a common ancestor. Finally, consistent with evolution by gene duplication, the new IL-1 superfamily members are all clustered in the same region of human chromosome 2q that contains *IL-1α, IL-1β,* and *IL-1ra. IL-18* is the only superfamily member that does not map to this location.

The novel IL-1 family members are expressed in a variety of hematopoietic and non-hematopoietic cell types. It is not easy to formulate generalizations about expression patterns, except to say that FIL1ε appears to be the only one of these putative cytokines routinely expressed in T cells, and (not unexpectedly) all of the family members are expressed in activated monocytes and B cells. From the infrequency of ESTs corresponding to these genes in GenBank™, as well as the number of PCR cycles required to detect an amplification product in positive RNA sources, it would appear that they are all expressed at relatively low abundance. Nevertheless, FIL1δ, FIL1ε, and



FIG. 4. **Intron positions.** Intron positions were taken from GenBank™ (*IL-1α,* accession number X03833; *IL-1β,* accession number X04500; *IL-1ra,* accession number X64532; *IL-18,* accession number E17138) or were determined for this paper by sequencing of genomic DNA (either directly cloned, or PCR amplified) and comparison to the cDNA sequences. The "intron 3," "intron 4," "intron 5" designations are by analogy with *IL-1α* and *IL-1β,* and do not imply that there are five introns in each of the other genes. Intron sizes, where known, are indicated. Amino acid numbers are given *below* the lines, and refer to the primary translation product.

FIL1$\zeta$ can be regulated by LPS (and most likely other agents) in monocytes and spleen cells, and FIL1$\delta$ appears to be transcribed from at least two different promoters, indicating that regulation of expression in this family is active.

It might be expected that the new IL-1 superfamily members would bind to members of the IL-1 receptor superfamily. However, we have been unable to demonstrate this in co-precipitation assays using Fc fusions of the known receptors and orphan receptor homologs. It could be that there are as yet undiscovered members of the IL-1R superfamily. Alternatively, unlike the case with the IL-1s and IL-18, high affinity binding detectable by co-precipitation may require two receptor subunits to be present. Finally, of course, it is possible that these cytokines bind to a different type of receptor. IL-18, for example, was recently shown to be capable of binding with high affinity to a soluble protein that has little similarity to other IL-1R family members (39).

The biological activity of the novel IL-1 family members remains to be characterized. IL-1$\alpha$, IL-1$\beta$, and IL-18 are all capable of activating gene expression programs that enhance immune responses and promote inflammation. It is obvious to speculate that FIL1$\delta$, FIL1$\epsilon$, FIL1$\zeta$, and FIL1$\eta$ might have similar actions. On the other hand, IL-1ra acts to block the actions of the agonist IL-1s, and it is possible that one or more of the novel family members might similarly play an antagonist role. In this context, however, it should be noted that none of them binds to either the type I IL-1R or to IL-1Rrp1, and therefore they presumably do not regulate signaling by either IL-1 or IL-18. It is also possible that the resemblance of these molecules to IL-1 says nothing at all about their receptor binding or the type of biological responses they might invoke. These issues will be clarified by further investigation.

## REFERENCES

1. Dinarello, C. A. (1998) *Int. Rev. Immunol.* 16, 457–499
2. O'Neill, L. A., and Greene, C. (1998) *J. Leukocyte Biol.* 63, 650–657
3. Dinarello, C. A. (1996) *Blood* 87, 2095–2147
4. Sims, J. E., March, C. J., Cosman, D., Widmer, M. B., MacDonald, H. R., McMahan, C. J., Grubin, C. E., Wignall, J. M., Call, S. M., Friend, D., Alpert, A. R., Gillis, S. R., Urdal, D. L., and Dower, S. K. (1988) *Science* 241, 585–589
5. Sims, J. E., Acres, R. B., Grubin, C. E., McMahan, C. J., Wignall, J. M., March, C. J., and Dower, S. K. (1989) *Proc. Natl. Acad. Sci. U. S. A.* 86, 8946–8950
6. Greenfeder, S. A., Nunes, P., Kwee, L., Labow, M., Chizzonite, R. A., and Ju, G. (1995) *J. Biol. Chem.* 270, 13757–13765
7. Cullinan, E. B., Kwee, L., Nunes, P., Shuster, D. J., Ju, G., McIntyre, K. W., Chizzonite, R. A., and Labow, M. A. (1998) *J. Immunol.* 161, 5614–5620
8. Hannum, C. H., Wilcox, C. J., Arend, W. P., Joslin, F. G., Dripps, D. J., Heimdal, P. L., Armes, L. G., Sommer, A., Eisenberg, S. P., and Thompson, R. C. (1990) *Nature* 343, 336–340
9. Eisenberg, S. P., Evans, R. J., Arend, W. P., Verderber, E., Brewer, M. T., Hannum, C. H., and Thompson, R. C. (1990) *Nature* 343, 341–346
10. McMahan, C. J., Slack, J. L., Mosley, B., Cosman, D., Lupton, S. D., Brunton, L. L., Grubin, C. E., Wignall, J. M., Jenkins, N. A., Brannan, C. I., Copeland, N. G., Huebner, K., Croce, C. M., Cannizzaro, L. A., Benjamin, D., Dower, S. K., Spriggs, M. K., and Sims, J. E. (1991) *EMBO J.* 10, 2821–2832
11. Colotta, F., Re, F., Muzio, M., Bertini, R., Polentarutti, N., Sironi, M., Giri, J. G., Dower, S. K., Sims, J. E., and Mantovani, A. (1993) *Science* 261, 472–475
12. Colotta, F., Dower, S. K., Sims, J. E., and Mantovani, A. (1994) *Immunol. Today* 15, 562–566
13. Sims, J. E., Gayle, M. A., Slack, J. L., Alderson, M. R., Bird, T. A., Giri, J. G., Colotta, F., Re, F., Mantovani, A., Shanebeck, K., Grabstein, K. H., and Dower, S. K. (1993) *Proc. Natl. Acad. Sci. U. S. A.* 90, 6155–6159
14. March, C. J., Mosley, B., Larsen, A., Cerretti, D. P., Braedt, G., Price, V., Gillis, S., Henney, C. S., Kronheim, S. R., Grabstein, K., Conlon, P. J., Hopp, T. P., and Cosman, D. (1985) *Nature* 315, 641–647
15. Cerretti, D. P., Kozlosky, C. J., Mosley, B., Nelson, N., Van Ness, K., Greenstreet, T. A., March, C. J., Kronheim, S. R., Druck, T., Cannizzaro, L. A., Huebner, K., and Black, R. A. (1992) *Science* 256, 97–100
16. Thornberry, N. A., Bull, H. G., Calaycay, J. R., Chapman, K. T., Howard, A. D., Kostura, M. J., Miller, D. K., Molineaux, S. M., Weidner, J. R., Aunins, J., Elliston, K. O., Ayala, J. M., Casano, F. J., Chin, J., Ding, G. J.-F., Egger, L. A., Gaffney, E. P., Limjuco, G., Palyha, O. C., Raju, S. M., Rolando, A. M., Salley, J. P., Yamin, T.-T., Lee, T. D., Shively, J. E., MacCross, M., Mumford, R. A., Schmidt, J. A., and Tocci, M. J. (1992) *Nature* 356, 768–774
17. Okamura, H., Tsutsi, H., Komatsu, T., Yutsudo, M., Hakura, A., Tanimoto, T., Torigoe, K., Okura, T., Nukada, Y., Hattori, K., Akita, K., Namba, M., Tanabe, F., Konishi, K., Fukuda, S., and Kurimoto, M. (1995) *Nature* 378, 88–91
18. Ushio, S., Namba, M., Okura, T., Hattori, K., Nukada, Y., Akita, K., Tanabe, F., Konishi, K., Micallef, M., Fujii, M., Torigoe, K., Tanimoto, K., Fukuda, S., Ikeda, M., Okamura, H., and Kurimoto, M. (1996) *J. Immunol.* 156, 4274–4279
19. Bazan, J. F., Timans, J. C., and Kastelein, R. A. (1996) *Nature* 379, 591
20. Dinarello, C. A., Novick, D., Puren, A. J., Fantuzzi, G., Shapiro, L., Muhl, H., Yoon, D. Y., Reznikov, L. L., Kim, S. H., and Rubinstein, M. (1998) *J. Leukocyte Biol.* 63, 658–664
21. Ghayur, T., Banerjee, S., Hugunin, M., Butler, D., Herzog, L., Carter, A., Quintal, L., Sekut, L., Talanian, R., Paskind, M., Wong, W., Kamen, R., Tracey, D., and Allen, H. (1997) *Nature* 386, 619–623
22. Gu, Y., Kuida, K., Tsutsui, H., Ku, G., Hsiao, K., Fleming, M. A., Hayashi, N., Higashino, K., Okamura, H., Nakanishi, K., Kurimoto, M., Tanimoto, T., Flavell, R. A., Sato, V., Harding, M. W., Livingston, D. J., and Su, M. S.-S. (1997) *Science* 275, 206–209
23. Torigoe, K., Ushio, S., Okura, T., Kobayashi, S., Taniai, M., Kunikata, T., Murakami, T., Sanou, O., Kojima, H., Fujii, M., Ohta, T., Ikeda, M., Ikegami, H., and Kurimoto, M. (1997) *J. Biol. Chem.* 272, 25737–25742
24. Thomassen, E., Bird, T. A., Renshaw, B. R., Kennedy, M. K., and Sims, J. E. (1998) *J. Interferon Cytokine Res.* 18, 1077–1088
25. Parnet, P., Garka, K. E., Bonnert, T. P., Dower, S. K., and Sims, J. E. (1996) *J. Biol. Chem.* 271, 3967–3970
26. Born, T. L., Thomassen, E., Bird, T. A., and Sims, J. E. (1998) *J. Biol. Chem.* 273, 29445–29450
27. Sims, J. E., Painter, S. L., and Gow, I. R. (1995) *Cytokine* 7, 483–490
28. Bernstein, F. C., Koetzle, T. F., Williams, G. J., Meyer, E. F., Jr., Brice, M. D., Rodgers, J. R., Kennard, O., Shimanouchi, T., and Tasumi, M. (1977) *Eur. J. Biochem.* 80, 319–324
29. Jaroszewski, L., Rychlewski, L., Zhang, B., and Godzik, A. (1998) *Protein Sci.* 7, 1431–1440
30. Sali, A., Potterton, L., Yuan, F., van Vlijmen, H., and Karplus, M. (1995) *Proteins* 23, 318–326
31. Laskowski, R. A., Rullmann, J. A., MacArthur, M. W., Kaptein, R., and Thornton, J. M. (1996) *J. Biomol. NMR* 8, 477–486
32. Gyapay, G., Schmitt, K., Fizames, C., Jones, H., Vega-Czarny, N., Spillett, D., Muselet, D., Prud'Homme, J. F., Dib, C., Auffray, C., Morissette, J., Weissenbach, J., and Goodfellow, P. N. (1996) *Hum. Mol. Genet.* 5, 339–346
33. Kubin, M., Kamoun, M., and Trinchieri, G. (1994) *J. Exp. Med.* 180, 211–222
34. Kubin, M., Chow, J. M., and Trinchieri, G. (1994) *Blood* 83, 1847–1855
35. Cosman, D., Cerretti, D. P., Larsen, A., Park, L., March, C., Dower, S., Gillis, S., and Urdal, D. (1984) *Nature* 312, 768–771
36. Giri, J. G., Ahdieh, M., Eisenman, J., Shanebeck, K., Grabstein, K., Kumaki, S., Namen, A., Park, L. S., Cosman, D., and Anderson, D. (1994) *EMBO J.* 13, 2822–2830
37. Kozlosky, C. J., Maraskovsky, E., McGrew, J. T., VandenBos, T., Teepe, M., Lyman, S. D., Srinivasan, S., Fletcher, F. A., Gayle, R. B., III, Cerretti, D. P., and Beckmann, M. P. (1995) *Oncogene* 10, 299–306
38. Young, P. R., James, I. E., Connor, J. R. (November 25, 1998) European Patent Office publication EP 0 879 889 A2
39. Novick, D., Kim, S. H., Fantuzzi, G., Reznikov, L. L., Dinarello, C. A., and Rubinstein, M. (1999) *Immunity* 10, 127–136
40. Page, R. D. (1996) *Comput. Appl. Biosci.* 12, 357–358
41. Kubin, M. Z., Parshley, D. L., Din, W., Waugh, J. Y., Davis-Smith, T., Smith, C. A., Macduff, B. M., Armitage, R. J., Chin, W., Cassiano, L., Borges, L., Petersen, M., Trinchieri, G., and Goodwin, R. G. (1999) *Eur. J. Immunol.* 29, 3466–3477

# EXHIBIT 3

Smith et al. reference 19:
*Nature* 1996 Feb 15;379(6566):591

Comment on: Nature 1995 Nov 2;378(6552):88-91
**A newly defined interleukin-1?**

**Bazan JF, Timans JC, Kastelein RA**

Smith et al. reference 29:
*Protein Sci* 1998 Jun;7(6):1431-40

**Fold prediction by a hierarchy of sequence, threading, and modeling methods.**

**Jaroszewski L, Rychlewski L, Zhang B, Godzik A.**

Department of Chemistry, University of Warsaw, Warszawa, Poland.

Several fold recognition algorithms are compared to each other in terms of prediction accuracy and significance. It is shown that on standard benchmarks, hybrid methods, which combine scoring based on sequence-sequence and sequence-structure matching, surpass both sequence and threading methods in the number of accurate predictions. However, the sequence similarity contributes most to the prediction accuracy. This strongly argues that most examples of apparently nonhomologous proteins with similar folds are actually related by evolution. While disappointing from the perspective of the fundamental understanding of protein folding, this adds a new significance to fold recognition methods as a possible first step in function prediction. Despite hybrid methods being more accurate at fold prediction than either the sequence or threading methods, each of the methods is correct in some cases where others have failed. This partly reflects a different perspective on sequence/structure relationship embedded in various methods. To combine predictions from different methods, estimates of significance of predictions are made for all methods. With the help of such estimates, it is possible to develop a "jury" method, which has accuracy higher than any of the single methods. Finally, building full three-dimensional models for all top predictions helps to eliminate possible false positives where alignments, which are optimal in the one-dimensional sequences, lead to unsolvable sterical conflicts for the full three-dimensional models.

Smith et al. reference 30:
*J Biomol NMR* 1996 Dec;8(4):477-86

**AQUA and PROCHECK-NMR: programs for checking the quality of protein structures solved by NMR.**

**Laskowski RA, Rullmannn JA, MacArthur MW, Kaptein R, Thornton JM.**

Department of Biochemistry and Molecular Biology, University College London, UK.
roman@bsm.bioc.ucl.ac.uk

The AQUA and PROCHECK-NMR programs provide a means of validating the geometry and restraint violations of an ensemble of protein structures solved by solution NMR. The outputs include a detailed breakdown of the restraint violations, a number of plots in PostScript format and summary statistics. These various analyses indicate both the degree of agreement of the model structures with the experimental dat, and the quality of their geometrical properties. They are intended to be of use both to support ongoing NMR structure determination and in the validation of the final results.

**Evaluation of comparative protein modeling by MODELLER.**

**Sali A, Potterton L, Yuan F, van Vlijmen H, Karplus M.**

Rockefeller University, New York, NY 10021, USA.

We evaluate 3D models of human nucleoside diphosphate kinase, mouse cellular retinoic acid binding protein I, and human eosinophil neurotoxin that were calculated by MODELLER, a program for comparative protein modeling by satisfaction of spatial restraints. The models have good stereochemistry and are at least as similar to the crystallographic structures as the closest template structures. The largest errors occur in the regions that were not aligned correctly or where the template structures are not similar to the correct structure. These regions correspond predominantly to exposed loops, insertions of any length, and non-conserved side chains. When a template structure with more than 40% sequence identity to the target protein is available, the model is likely to have about 90% of the mainchain atoms modeled with an rms deviation from the X-ray structure of approximately 1 A, in large part because the templates are likely to be that similar to the X-ray structure of the target. This rms deviation is comparable to the overall differences between refined NMR and X-ray crystallography structures of the same protein.

# EXHIBIT 4

# Mapping Receptor Binding Sites in Interleukin (IL)-1 Receptor Antagonist and IL-1β by Site-directed Mutagenesis

## IDENTIFICATION OF A SINGLE SITE IN IL-1ra AND TWO SITES IN IL-1β*

Ron J. Evans‡, Jeff Bray§, John D. Childs¶, Guy P. A. Vigers, Barbara J. Brandhuber, Jack J. Skalicky‖**, Robert C. Thompson, and Stephen P. Eisenberg

From Synergen, Inc., Boulder, Colorado 80301 and the ‖Department of Chemistry and Biochemistry, University of Colorado, Boulder, Colorado 80309

Interleukin-1 receptor antagonist (IL-1ra), an IL-1 family member, binds with high affinity to the type I IL-1 receptor (IL-1RI), blocking IL-1 binding but not inducing an IL-1-like response. Extensive site-directed mutagenesis has been used to identify residues in IL-1ra and IL-1β involved in binding to IL-1RI. These analyses have revealed the presence of two discrete receptor binding sites on IL-1β. Only one of these sites is present on IL-1ra, consisting of residues Trp-16, Gln-20, Tyr-34, Gln-36, and Tyr-147. Interestingly, the absent second site is at the location of the major structural difference between IL-1ra and IL-1β, which are otherwise structurally similar. The two receptor binding sites on IL-1β are also present on IL-1α. Thus, it appears that the two IL-1 agonist molecules have two sites for IL-1RI binding, and the homologous antagonist molecule, IL-1ra, has only one. Based on these observations, a hypothesis is presented to account for the difference in activity between the agonist and antagonist proteins. It is proposed that the presence of the two receptor binding sites may be necessary for agonist activity.

The IL-1[1] family of proteins are related by sequence similarity, gene organization, and three-dimensional structure (Eisenberg et al., 1990, 1991; Carter et al., 1990). The three proteins, IL-1α, IL-1β, and IL-1ra, all exhibit a β-trefoil topology characterized by six β-strands forming a tapered β-barrel, which is closed at the wide end by another six β-strands (Murzin et al., 1992; Vigers et al., 1994).

The two agonist proteins, IL-1α and IL-1β, have similar biological activities, mediated through their high affinity interaction with the type 1 IL-1 receptor (IL-1RI) (Sims et al., 1993). These two proteins are believed to play an important role in causing both local and systemic inflammatory responses (Dinarello, 1991).

The third family member, IL-1ra, also binds with high affinity to IL-1RI but does not elicit a biological response (Hannum et al., 1990; Dripps et al., 1991). IL-1ra competitively inhibits the binding of IL-1α and IL-1β and thus acts as a specific inhibitor of IL-1 activity. Exogenously administered human recombinant IL-1ra can significantly reduce the severity of inflammation in many animal models of inflammatory disease, thus implicating IL-1 as an important mediator of inflammation in these models (Dinarello and Thompson, 1991). Endogenous IL-1ra plays an important role in reducing the severity of the inflammatory response by IL-1, since administration of neutralizing antibodies to IL-1ra causes an increase in severity and a prolongation of intestinal inflammation (Ferretti et al., 1994).

Several studies utilizing site-directed mutagenesis have led to the identification of residues in IL-1α and IL-1β that are important for either receptor binding or receptor-mediated biological activity (MacDonald et al., 1986; Gehrke et al., 1990; Yamayoshi et al., 1990; Ju et al., 1991; Labriola-Tompkins et al., 1991, 1993; Grutter et al., 1994; Gayle et al., 1993). An analysis of these results suggests there are two main sites on the surface of the IL-1 agonist molecules that are involved in receptor binding. One site (site A), located on the side of the β-barrel structure, was originally identified by mutagenesis of IL-1β residue histidine 30 (His-30). Additional residues in this region have more recently been identified in both IL-1α and IL-1β. A second site (site B), approximately 20–25 Å from the first site, is located at the open end of the β-barrel and includes several charged residues, e.g. Arg-4, Lys-93, Lys-103, and Glu-105 of IL-1β.

We report here the results of site-directed mutagenesis studies to identify residues on IL-1ra important for IL-1RI binding. Our results indicate that the IL-1ra residues homologous to receptor binding site A of IL-1α and IL-1β also play a role in IL-1RI binding of IL-1ra but that residues of IL-1ra homologous to receptor binding site B on IL-1α and IL-1β do not interact with the receptor. In addition, we believe that site A is the only receptor binding site on IL-1ra because we have mutagenized or deleted almost every residue on the surface of the molecule (a total of 103 residues) and found that only the residues of site A affect receptor binding. We have also performed site-directed mutagenesis of IL-1β and found that site A on IL-1β is larger than previously thought.

## EXPERIMENTAL PROCEDURES

*Mutagenesis and Mutein Expression in Escherichia coli*—Site-directed mutagenesis of IL-1ra and IL-1β genes was performed using a Bio-Rad Mutagene kit. Muteins were expressed in *E. coli* and purified to near homogeneity from the soluble cell lysate as previously described (Eisenberg et al., 1990). Protein concentrations were determined by BCA protein assay (Pierce), absorbance at 280 nm, and relative intensity of bands on a Coomassie-stained polyacrylamide gel.

*Competitive Receptor Binding Assays*—Receptor binding assays were done as described (Hannum *et al.*, 1990). Briefly, a standard amount of ^{35}S-labeled IL-1ra at a concentration approximately equal to its $K_d$ (150 pM) was incubated with mouse EL4 thymoma (ATCC, TIB181, ~5000 receptors per cell) or a Chinese hamster ovary cell line (kindly provided by R. Chizzonite) expressing the human type 1 IL-1 receptor (~30,000 receptors per cell) for 4 h at 4 °C with varying concentrations of cold competitor. The cells were harvested through a Millipore milliliter plate filter system, and radioactivity retained on the filter was counted on an Ambis radioanalytical imaging system. Percent wild type activity was defined as $IC_{50}$ (wild type)/$IC_{50}$ (mutein). The $K_d$ for the wild type IL-1ra (as competitor) was estimated using a simplification of the Cheng-Prusoff relationship ($K_d = IC_{50}/2$, Cheng and Prusoff, 1973) and ranged from 150 to 400 pM, consistent with values previously reported. In each assay, a wild type control was included. All muteins were assayed a minimum of two times with the standard error between assays generally ≤25%.

*NMR Spectroscopy Analysis of IL-1ra and Muteins*—One-dimensional ^{1}H-labeled NMR spectra were collected for IL-1ra and several of its muteins. The spectra were recorded on a VXR500 spectrometer housed at the University of Colorado-Boulder. The 1.5 mM IL-1ra solutions (90% $H_2O$, 10% $D_2O$) were prepared in 10 mM phosphate (pH = 6.0), 100 mM NaCl, and 0.1 mM EDTA. Spectra were recorded at temperatures of 25, 30, and 35 °C. Each spectrum was collected with 8192 complex points over a spectral width of 7000 Hz, and a total of 64 transients were signal averaged for each free induction decay. All data were processed on a Sun 4260 using the NMR processing software FELIX (Hare Research). The spectra of IL-1ra wild type and mutants were plotted to allow for comparison of the backbone (H[n] and Hα) and methyl proton chemical shifts and intensities.

*Structure Modeling of IL-1α*—Since only the C-α coordinates of IL-1α have been deposited in the Brookhaven Data base, we modeled possible side chain positions for comparison to IL-1β and IL-1ra. Initial coordinates were assigned at random for missing atoms and then refined using simulated annealing in X-PLOR (Brunger *et al.*, 1987). Three different starting positions gave similar final conformations in all areas of interest.[2]

## RESULTS

*Mutagenesis of IL-1ra*—Using site-directed mutagenesis, we replaced 93 of the 152 residues of IL-1ra and made two deletion mutants of 3 and 10 amino acids at the amino terminus. Initial single replacements were to glycine or alanine or, in a few instances, to an amino acid of the opposite charge. Muteins were assayed by competition with ^{35}S-labeled IL-1ra for binding to mouse EL4 cells or to Chinese hamster ovary cells expressing recombinant full-length human IL-1RI. From this initial round of mutagenesis, 54 of the muteins were assayed on EL4 cells, 33 were assayed on Chinese hamster ovary cells, and the remaining 6 were assayed on both cell lines.

For the vast majority of muteins, including the two deletion mutants, competition was not significantly different from that of the wild type protein (Fig. 1). The muteins that had less than 35% of wild type activity were investigated further. Five residues in IL-1ra were initially found to be sensitive to alanine or glycine substitution. Four of them, Trp-16, Gln-20, Tyr-34, and Tyr-147, were sensitive to substitution by other residues as well (Table I). At each of these residues, certain changes reduced receptor binding by 100-fold or more. These four residues form a contiguous patch on the IL-1ra surface, and two of them, Trp-16 and Tyr-34, correspond to residues Arg-11 and His-30, which have been previously identified as important in site A of IL-1β. One of the four residues, Tyr-147, exhibited interesting receptor binding properties in that Y147G bound with lower affinity than wild type IL-1ra to human IL-1RI (34%) but with higher affinity to the mouse receptor (252%).

The fifth residue that exhibited ≤35% of wild type activity in the initial screen, D74G, exhibited ~30% of wild type IL-1ra binding to the mouse IL-1RI but ~50% binding to the human receptor. Since muteins D74A, D74F, D74C, and D74W all

exhibit normal IL-1RI binding activity to the human receptor (data not shown), we believe that this residue is not fundamentally important for IL-1ra binding to IL-1RI.

One additional residue, Gln-36, was investigated further (despite the fact that Q36G exhibited normal binding on EL4 cells) due to the importance of the homologous residue on IL-1β, Gln-32 (see below and Discussion). We found Q36F had only 1% of wild type activity (Table I), suggesting that this residue is also important for receptor binding. Gln-36 is adjacent to the four important residues discussed above.

The reduced affinity of muteins with changes at the five residues that make up the important binding site in IL-1ra (Trp-16, Gln-20, Tyr-34, Gln-36, and Tyr-147) suggests these residues contribute to the interaction of IL-1ra with IL-1RI. However, it is also possible that the mutations may disrupt the tertiary structure of the muteins, which causes a reduction in receptor affinity. To address this issue, we performed high resolution one-dimensional NMR on wild type IL-1ra and muteins Y34G, Q20A, and W16G. No significant differences were observed in the spectra of these four molecules, indicating there were no major differences among their structures. In addition, all muteins eluted at approximately the same salt concentration from an ion exchange column, suggesting that these molecules all have a similar conformation and overall charge.

Seven IL-1β residues (Arg-4, Leu-6, Phe-46, Ile-56, Lys-93, Lys-103, and Glu-105) in the vicinity of the open end of the β-barrel have previously been shown to be important for binding to IL-1RI (Labriola-Tompkins *et al.*, 1991). Four of these seven are charged residues. Based on previously published sequence alignments (Stockman *et al.*, 1992), these charges are conserved in IL-1ra and have been suggested to be important for receptor binding. Thus, the homologous region of IL-1ra (Pro-50, Glu-52, His-54, Ser-89, Glu-90, Asn-91, Arg-92, Lys-93, Gln-94, Asp-95, Lys-96, Arg-102, Ser-103, Asp-104, Ser-105) was extensively mutagenized (Figs. 1 and 2, see also Vigers *et al.* (1994)) to investigate whether it had a similar function in the binding of IL-1ra to IL-1RI. Interestingly, none of the changes in this region of IL-1ra affected activity in the competitive receptor binding assay (Fig. 1).

An additional residue near the carboxyl terminus of these proteins, IL-1α Asp-151, IL-1β Asp-145, and IL-1ra Lys-145, has been characterized as important for biological activity but not for IL-1RI affinity. Of particular interest is the human IL-1ra mutein, K145D that has been shown to exhibit partial agonist activity on mouse cells but exhibits normal affinity for both the mouse and human receptors (Yamayoshi *et al.*, 1990; Ju *et al.*, 1991). This is consistent with our observation that replacing Lys-145 of IL-1ra with glycine has no affect on receptor binding activity (Fig. 1).

*Site-directed Mutagenesis of IL-1β*—We performed site-directed mutagenesis on IL-1β to reevaluate the role of the known site A residues and to examine other IL-1β residues in the vicinity of this site. In addition, we wished to analyze residues in or near site B of IL-1β.

We find that three residues in the region of site A appear to be important for binding IL-1β to IL-1RI (Table II). Two residues, Gln-15 and His-30 of IL-1β, align with IL-1ra residues Gln-20 and Tyr-34, which were identified as important from the mutagenesis of that protein. The third residue, Gln-32, corresponds to Gln-36 of IL-1ra, which was not originally identified by the scanning mutagenesis shown in Fig. 1. However, further mutagenesis of this residue in IL-1ra did suggest its importance in receptor binding (Table I).

Two IL-1β residues in the vicinity of site A that interact only slightly or not at all with IL-1RI are Arg-11 and Thr-147.

---

[2] G. Vigers, unpublished data.
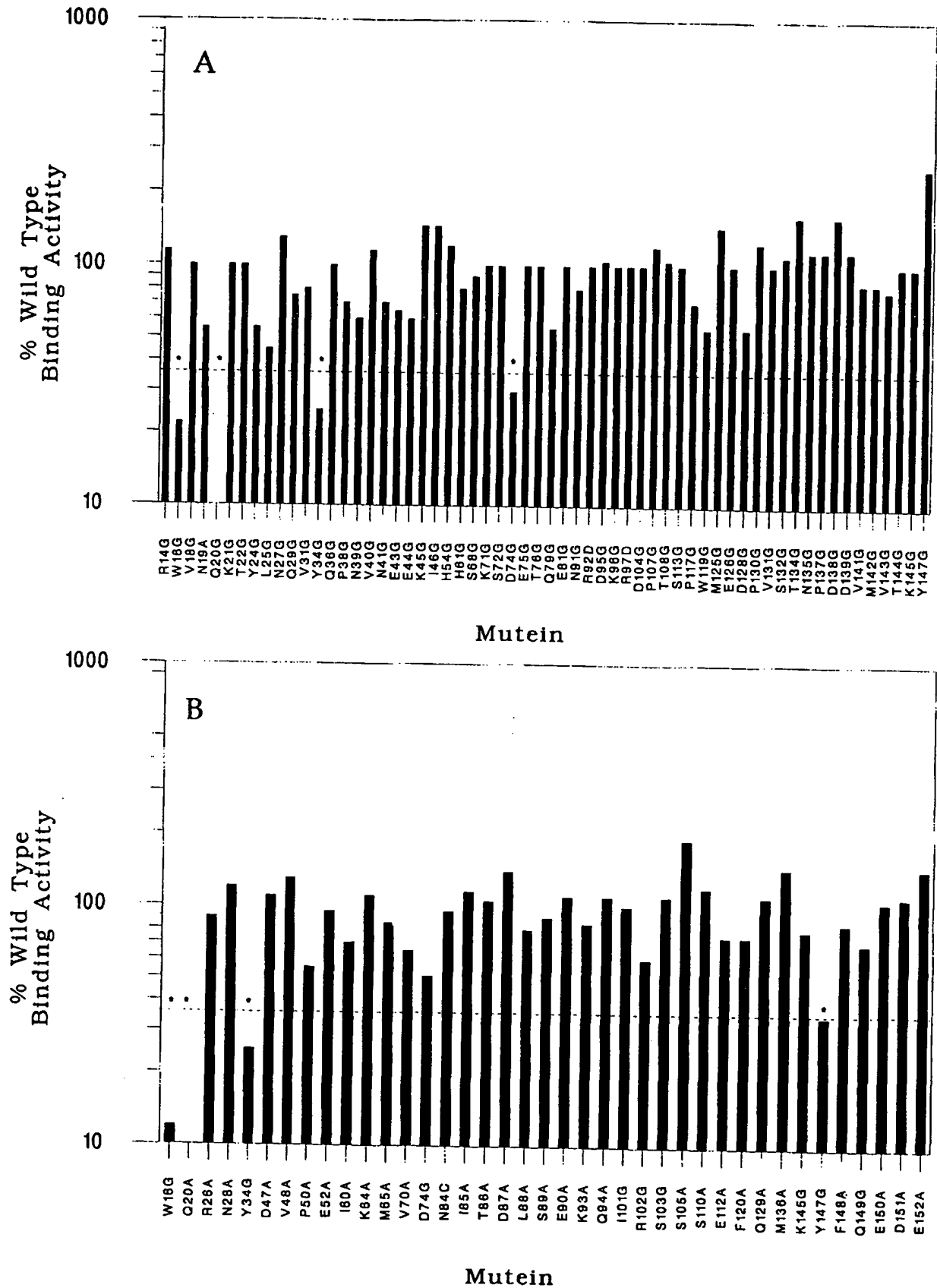
FIG. 1. **Receptor binding activities of muteins of IL-1ra.** Muteins were assayed as described under "Experimental Procedures" on either the mouse receptor (*A*) or the human receptor (*B*). The *horizontal dashed line* indicates 35% of wild type binding activity; muteins with activities below this value are denoted by an *asterisk* and were investigated further (see text). Their activities relative to wild type mouse and human IL-1RI are as follows: W16G, 22% mouse, 6% human; Q20G, 1% mouse; Q20A, 6% human; Y34G, 25% mouse, 25% human; D74G, 30% mouse; and Y147G, 35% human.

Others have previously reported that Arg-11 (which aligns with Trp-16 of IL-1ra) is not critical for receptor binding but is important for biological activity (Gehrke *et al.*, 1990). Our data are consistent with these observations. Thr-147 of IL-1β aligns

### TABLE I
#### Receptor binding activity of IL-1ra muteins

Receptor binding activity of muteins was determined on Chinese hamster ovary cells as described under "Experimental Procedures." Each number represents a single assay except in the case of muteins that were assayed more than twice, where the number is the mean ± S.E. The number of assays performed is shown in parentheses.

| IL-1ra mutein | Wild type activity |
|---|---|
| | % |
| W16G | 12 ± 3 (4) |
| W16K | <1,<1 |
| W16M | 5,7 |
| W16Q | 9,18 |
| W16R | 21 ± 2 (3) |
| W16Y | 53,85 |
| Q20A | 6,8 |
| Q20Y | <1,<1 |
| Q20D | <1,<1,<1 |
| Q20K | <1,<1 |
| Q20M | 18,22 |
| Q20N | 43,46 |
| Y34G | 21,23 |
| Y34K | <1,<1 |
| Y34D | 7,11 |
| Y34H | 80,84 |
| Y34W | 88,98 |
| Y34M | 86,100 |
| Q36F | <1,<1 |
| Y147G | 24,44 |
| Y147K | <1,<1 |
| Y147T | 3,5 |
| Y147H | 41,69 |
| Y147M | 63, 69 |

structurally with the important IL-1ra residue Tyr-147 but is unimportant for IL-1β binding to IL-1RI, possibly due to the distinct chemical nature of the side chains involved.

Site B residues in IL-1β, Ile-56, Lys-93, and Glu-105 were all found to be sensitive to mutagenesis (Table II), consistent with previously reported data (Labriola-Tompkins *et al.*, 1991). An additional important residue in this region of IL-1β is Lys-92 (Table II).

*Location of Important Residues in IL-1ra, IL-1α, and IL-1β*—Fig. 2 shows an alignment of human IL-1α, IL-1β, and IL-1ra, based on their three-dimensional structures. Highlighted on this alignment are the important residues for IL-1RI interaction identified by single-site mutagenesis, either in this work or previously by others. There are a number of key residues present on all three proteins in the equivalent spatial location. One residue that appears to be very important in all three proteins based on our mutagenesis data and the data from Gayle *et al.* (1993) is IL-1ra Gln-20, IL-1β Gln-15, and IL-1α Asn-29. Other residues important for binding IL-1β and IL-1ra to the receptor but not critical for IL-1α binding include IL-1β His-30 and IL-1ra Tyr-34, homologous to IL-1α Ala-44, and IL-1β Gln-32 and IL-1ra Gln-36, which is homologous to IL-1α His-46.

Fig. 3 shows the solvent-accessible surfaces based on the three-dimensional structures of IL-1α, IL-1β, and IL-1ra with the important binding site residues of each protein highlighted on the structure. There is a remarkable correspondence in the spatial location of site A on all three molecules and an interesting difference between the two agonist proteins and the antagonist protein at site B, in that this site is present in IL-1α and IL-1β but absent in IL-1ra.

For the three molecules, the total solvent-accessible areas of the binding site residues as indicated in Fig. 2 are approximately 650, 1440, and 330 Å² for IL-1α, IL-1β, and IL-1ra, respectively. The total solvent-accessible area of each molecule is approximately 7500 Å². Since all three molecules have the
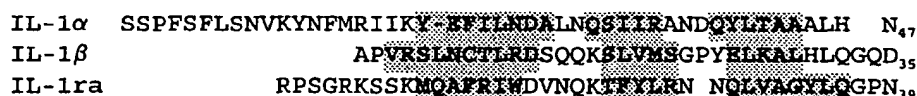
FIG. 2. **Residues in IL-1α, IL-1β, and IL-1ra identified by single-site mutagenesis as important for receptor interaction.** Sequences are aligned as in Vigers *et al.* (1994), based on x-ray structures. Important residues are indicated by the following symbols: ◆, IL-1α (Yamayoshi *et al.*, 1990; Kawashima *et al.*, 1991; Gayle *et al.*, 1993; Labriola-Tompkins *et al.*, 1993); ■, IL-1β (Mac-Donald *et al.* (1986), Gehrke *et al.* (1990), Labriola-Tompkins *et al.* (1991), Grutter *et al.* (1994), Ju *et al.* (1991), and this work); ●, IL-1ra (Ju *et al.* (1991) and this work). Shaded residues are in β-strands according to Graves *et al.* (1990) for IL-1α, Priestle *et al.* (1989) for IL-1β, and Vigers *et al.* (1994) for IL-1ra.
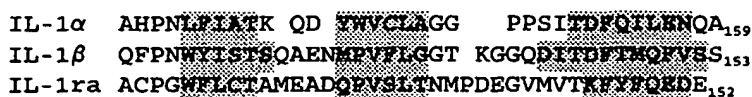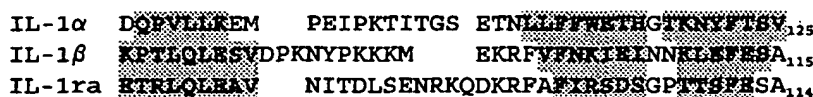
same affinity for the IL-1RI, one can conclude that IL-1ra generates more binding energy from site A than do IL-1α or IL-1β. To check whether the single site A of IL-1ra could account for the observed binding affinity, we applied the equations $\Delta G = -RT \, ln(K)$ and $\Delta\Delta G = -RT \, ln(K_1/K_2)$ to the observed binding equilibria. We find that the wild type IL-1ra has a change in free energy upon binding of approximately 52 kJ/mol. Considering only the neutral mutations of Trp-16, Gln-20, Tyr-34, and Tyr-147 to glycine (Table I), the four residues at the center of site A in IL-1ra account for at least 18.3 kJ/mol binding energy. If we consider the more extreme mutations to these four residues, e.g. W16K, and include Q36F, we can account for >53 kJ/mol. Thus there is reasonably close agreement between these numbers, considering the broad assumptions made in the calculations.

## DISCUSSION

A simple way of defining the regions of a protein important for receptor binding is through the use of *in vitro* site-directed

TABLE II
*Receptor binding activity of IL-1β muteins*

Receptor binding activity of muteins was determined on Chinese hamster ovary cells as described under "Experimental Procedures." Numbers represent the mean of at least two assays.

| IL-1β mutein | Wild type activity |
|---|---|
| | % |
| R11G[a] | 45 |
| R11A[a] | 55 |
| Q15G[a] | <1 |
| Q15H[a] | 130 |
| H30G[a] | <1 |
| H30E[a] | 2 |
| H30A[a] | 10 |
| H30S[a] | 10 |
| Q32G[a] | <1 |
| I56G[b] | 10 |
| K92G[b] | 8 |
| K93G[b] | <1 |
| K93M[b] | <1 |
| K93Q[b] | 5 |
| E105G[b] | 30 |
| T147G[a] | 70 |

[a] Site A residues.
[b] Site B residues.

mutagenesis. This method has been used over the past few years by several groups to identify residues involved in the high affinity binding of IL-1α and IL-1β to IL-1RI. These studies have led to the conclusion that two distinct receptor binding regions (site A and site B) are present on both IL-1α and IL-1β. Site A, located on the side of the β-barrel structure, was originally identified by the mutagenesis of IL-1β residues His-30 (MacDonald et al., 1986) and Arg-11 (Gehrke et al., 1990). Recently, additional residues in this region have been identified on IL-1α (Gayle et al., 1993) and on IL-1β (Grutter et al., 1994). We have extensively mutagenized IL-1ra and identified only five residues, Trp-16, Gln-20, Tyr-34, Gln-36, and Tyr-147, that are important for binding to the IL-1RI. These five residues, when changed to glycine, were also found to be important for binding to recombinant soluble human IL-1RI using surface plasmon resonance technology on a BIAcore instrument. Glycine substitutions at other positions had no significant affect on binding to human IL-1RI either on the surface of cells or to the purified receptor on the BIAcore.[3] All of these important amino acids map to site A, which is conformationally conserved among the IL-1 family members.

The chemical nature of the IL-1ra site A side chains is critical for high affinity binding to IL-1RI, as shown by the effect of amino acid substitution on binding. In addition to identifying substitutions that lead to a significant loss in binding, we have found some substitutions that have little or no affect on binding. In this regard, we show that replacing the aromatic amino acids Trp-16 and Tyr-34 in IL-1ra with other aromatic amino acids has no significant affect on binding. It is also interesting to note that Tyr-34 of IL-1ra can be replaced with histidine, which is the corresponding residue in IL-1β, with no loss in binding, and Gln-20 of IL-1ra can be replaced with asparagine, which is the corresponding IL-1α residue, with only a moderate loss in binding. In addition, Gln-20 and Gln-36 of IL-1ra correspond to Gln-15 and Gln-32 of IL-1β, based on the three-dimensional structures of these molecules. In light of the chemical similarity of site A among these proteins and the effect of mutagenesis of residues comprising this site, it appears that this region is both structurally and functionally homologous among the three IL-1 family members.

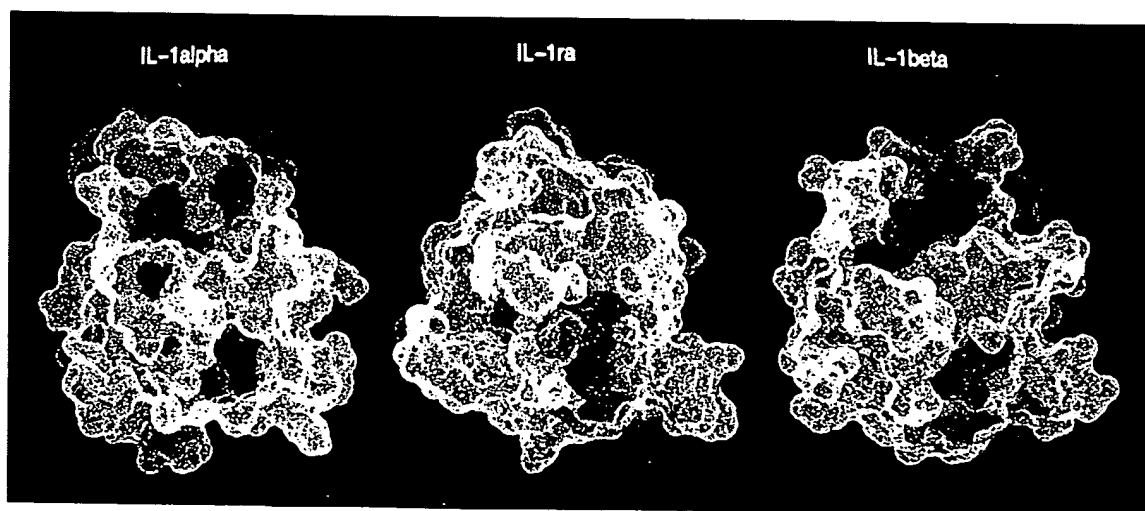FIG. 3. **Receptor binding sites in the IL-1 family.** Comparison of the three-dimensional structure solvent-accessible surface of IL-1α, IL-1β, and IL-1ra showing the residues important for receptor interaction in red. Site A (common to all three proteins) is on the *top* of the molecules, and site B (found in IL-1α and IL-1β only) is near the *bottom*. Residues colored are the same as those marked in Fig. 2.

IL-1 alpha or beta                          IL-1ra

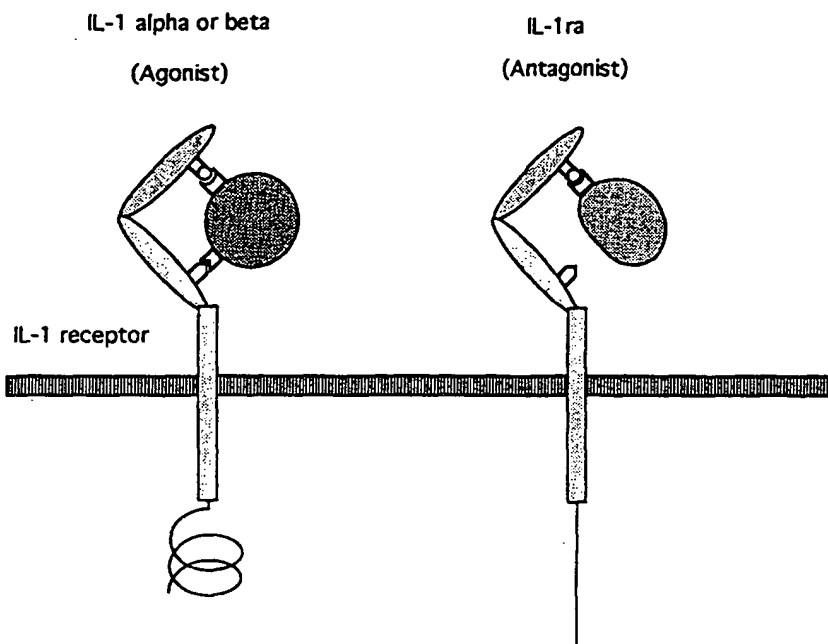(Agonist)                                   (Antagonist)



IL-1 receptor

FIG. 4. A model of receptor binding and activation. The agonists, IL-1α and IL-1β, contact two sites on the receptor causing activation (indicated by the *spiral*), whereas IL-1ra contacts only one site and does not activate (indicated by the *straight line*).

The second receptor binding region (site B) is located at the open end of the β-barrel and includes IL-1β residues Arg-4, Lys-6, Phe-46, Ile-56, Lys-92, Lys-93, Lys-103, and Glu-105 and IL-1α residues Arg-16, Ile-18, Asp-64, Asp-65, Ile-68, Lys-100, Asn-108, Trp-113, Gly-17, and Gln-136 (Labriola-Tompkins et al., 1991, 1993). The area in IL-1ra that is structurally analogous to site B of IL-1β is *not* involved in binding to IL-1RI. A careful comparison of IL-1β and IL-1ra in this region revealed very significant structural differences between the two molecules (Vigers et al., 1994). Thus, the difference in function in this region between the agonists and the antagonist is consistent with this being the region exhibiting the greatest difference in structure between these two classes of protein.

Through the extensive use of site-directed mutagenesis, we have demonstrated that the IL-1 antagonist is missing one of the two receptor binding regions identified on the two IL-1 agonists. This finding suggests a model for receptor activation in which IL-1α and IL-1β, by contacting two sites on IL-1RI, causes activation, but IL-1ra, in making contacts with the receptor at only one of the two receptor binding sites, is unable to induce an IL-1-like signal (Fig. 4). An alternative model, in which the IL-1 agonists act by dimerizing two IL-1 receptors molecules, as in the case of human growth hormone (Wells et al., 1993), or by forming a heterodimer of IL-1R1 and the recently identified IL-1 receptor accessory protein (Greenfeder et al., 1994) is also possible and is consistent with the observation that IL-1ra binds with a substantially higher affinity to the soluble form of IL-1RI than either IL-1α or IL-1β (Swenson et al., 1993). However, dimerizing two IL-1RI molecules seems unlikely because attempts to demonstrate the involvement of aggregation of IL-1RI by either IL-1α or IL-1β in receptor activation have been unsuccessful (Slack et al., 1993). In addition, binding experiments with IL-1β muteins and soluble IL-1RI on the BIAcore indicate that site A and site B residues both interact with the purified IL-1RI.[4]

IL-1ra binds to IL-1RI with the same affinity as the IL-1 agonists but uses only one binding site instead of two. Since site A of IL-1ra is compact and generates high affinity binding with the IL-1RI, it may act as a template for rational design for a small molecule IL-1 antagonist. Such a small molecule is

likely to contain pharmacophoric elements that match side-chain atoms of the site A residues. Additional structure-function studies are being done to further discern how these side chain atoms of IL-1ra contact residues in IL-1RI.

REFERENCES

Brünger, A., Kuriyan, J., and Karplus, M. (1987) *Science* 235, 458–460
Carter, D. B., Deibel, M. R., Jr., Dunn, C. J., Tomich, C-S. C., Laborde, A. L., Slightom, J. L., Berger, A. E., Bienkowski, M. J., Sun, F. F., McEwan, R. N., Harris, P. K. W., Yem, A. W., Waszak, G. A., Chosay, J. G., Sieu, L. C., Hardee, M. M., Zurcher-Neely, H. A., Reardon, I. M., Heinrickson, R. L., Truesdell, S. E., Shelly, J. A., Eessalu, T. E., Taylor, B. M., and Tracey, D. E. (1990) *Nature* 344, 633–638
Cheng, Y., and Prusoff, W. H. (1973) *Biochem. Pharmacol.* 22, 3099–3108
Dinarello, C. A. (1991) *Blood* 77, 1627–1652
Dinarello, C. A., and Thompson, R. C. (1991) *Immunol. Today* 12, 404–410
Dripps, D. J., Brandhuber, B. J., Thompson, R. C., and Eisenberg, S. P. (1991) *J. Biol. Chem.* 266, 10331–10336
Eisenberg, S. P., Evans, R. J., Arend, W. P., Verderber, E., Brewer, M. T., Hannum, C. H., and Thompson, R. C. (1990) *Nature* 343, 341–346
Eisenberg, S. P., Brewer, M. T., Verderber, E., Heimdal, P., Brandhuber, B. J., and Thompson, R. C. (1991) *Proc. Natl. Acad. Sci. U. S. A.* 88, 5232–5236
Ferretti, M., Casini-Raggi, V., Pizarro, T. T., Eisenberg, S. P., Nast, C. C., and Cominelli, F. (1994) *J. Clin. Invest.* 94, 449–453
Gayle, R. B., III, Poindexter, K., Cosman, D., Dower, S. K., Gillis, S., Hopp, T., Jerzy, R., Kronheim, S., Lum, V., Lewis, A., Goodgame, M. M., March, C. J., Smith, D. L., and Srinivasan, S. (1993) *J. Biol. Chem.* 268, 22105–22111
Gehrke, L., Jobling, S. A., Paik, L. S. K., McDonald, B., Rosenwasser, L. J., and Auron, P. E. (1990) *J. Biol. Chem.* 265, 5922–5925
Graves, B. J., Hatada, M. H., Hendrickson, W. A., Miller, J. K., Madison, V. S., and Satow, Y. (1990) *Biochemistry* 29, 2679–2684
Greenfeder, S., Chizzonite, R., Ju, G. (1994) *J. Cell. Biochem.* 18, (suppl.) 217
Grütter, M. G., van Oostrum, J., Priestle, J. P., Edelmann, E., Joss, U., Feige, U., Vosbeck, K., and Schmitz, A. (1994) *Protein Eng.* 7, 663–671
Hannum, C. H., Wilcox, C. J., Arend, W. P., Joslin, F. G., Dripps, D. J., Heimdal, P. L., Armes, L. G., Sommer, A., Eisenberg, S. P., and Thompson, R. C. (1990) *Nature* 343, 336–340
Ju, G., Labriola-Tompkins, E., Campen, C. A., Benjamin, W. R., Karas, J., Plocinski, J. Biondi, D., Kaffka, K. L., Kilian, P. L., Eisenberg, S. P., and Evans, R. J. (1991) *Proc. Natl. Acad. Sci. U. S. A.* 88, 2658–2662
Kawashima, H., Yamagishi, J., Yamayoshi, M., Ohue, M., Fukui, T., Kotani, H., and Yamada, M. (1991) *Protein Eng.* 5, 171–172
Labriola-Tompkins, E., Chandran, C., Kaffka, K. L., Biondi, D., Graves, B. J., Hatada, M., Madison, V. S., Karas, J., Kilian, P. L., and Ju, G. (1991) *Proc. Natl. Acad. Sci. U. S. A.* 88, 11182–11186
Labriola-Tompkins, E., Chandran, C., Varnell, T. A., Madison, V. S., and Ju, G. (1993) *Protein Eng.* 6, 535–539
MacDonald, H. R., Wingfield, P., Schmeissner, U., Shaw, A., Clore, G. M., and Gronenborn, A. M. (1986) *FEBS Lett.* 209, 295–298
Murzin, A. G., Lesk, A. M., and Chothia, C. (1992) *J. Mol. Biol.* 223, 531–543
Priestle, J. P., Schär, H. P., and Grütter, M. G. (1989) *Proc. Natl. Acad. Sci. U. S. A.*

[4] P. Caffes and R. J. Evans, unpublished data.

86, 9667–9671

Sims, J. E., Gayle, M. A., Slack, J. L., Alderson, M. R., Bird, T. A., Giri, J. G., Colotta, F., Re, F., Mantovani, A., Shanebeck, K., Grabstein, K. H., and Dower, S. K. (1993) *Proc. Natl. Acad. Sci. U. S. A.* **90**, 6155–6159

Slack, J., McMahan, C. J., Waugh, S., Schooley, K., Spriggs, M. K., Sims, J. E., and Dower, S. K. (1993) *J. Biol. Chem.* **268**, 2513–2524

Stockman, B. J., Scahill, T. A., Roy, M., Ulrich, E. L., Strakalaitis, N. A., Brunner, D. P., Yem, A. W., and Deibel, M. R., Jr. (1992) *Biochemistry* **31**, 5237–5244

Svenson, M., Hansen, M. B., Heegaard, P., Abell, K., and Bendtzen, K. (1993) *Cytokine* **5**, 427–435

Vigers, G. P. A., Caffes, P., Evans, R. J., Thompson, R. C., Eisenberg, S. P., and Brandhuber, B. J. (1994) *J. Biol. Chem.* **269**, 12874–12879

Wells, J. A., Cunningham, B. C., Fuh, G., Lowman, H. B., Bass, S. H., Mulkerrin, M. G., Ultsch, M., and deVos, A. M. (1993) *Recent Prog. Horm. Res.* **48**, 253–275

Yamayoshi, M., Ohue, M., Kawashima, H., Kotani, H., Iida, M., Kawata, S., and Yamada, M. (1990) *Lymphokine Res.* **9**, 405–413

# EXHIBIT 5



0 min

2 min

4 min
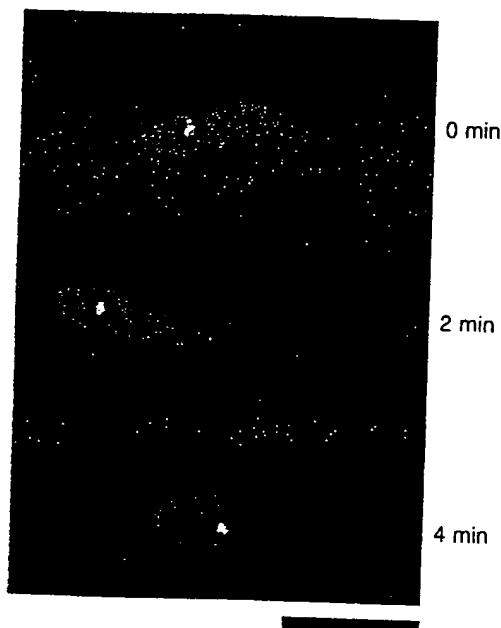
**Figure 4** Live video observation of the Mei2-GFP dot in meiotic phrophase. A diploid cell generated by conjugation was monitored. Three images taken at 2-min intervals are shown. Red regions, nuclear DNA; yellow spots, fluorescence of Mei2-GFP. The whole-cell body is faintly visible in red. Scale bar, 5 μm.

**Expression vectors.** pREP1 carries the authentic thiamine-repressible *nmt1* promoter, whereas pREP41 and pREP81 carry its modified versions, the expression of which is respectively 10-fold and 100-fold lower than that of pREP1 (ref. 22). To express full-length *mei2* from the *nmt1* promoter, an *Nde*I site was created at the initiation codon of the *mei2* open reading frame (ORF) and a 2.6-kb *Nde*I–*Bgl*II fragment was cloned into pREP vectors. Integration of *nmt1-mei2+* or *nmt1-mei2-SATA* on pREP41 into the chromosomal *leu1* locus was done, as described[23]. We used minimal medium SD with 1% glucose, which contains thiamine (1.2 μM), to repress the *nmt1* promoter, and minimal medium MM with 1% glucose to derepress it. Cell growth and sporulation were monitored on synthetic agar plates SSA with or without 2 μM thiamine (see ref. 12 for more details of the media).

*In vitro* **kinase assay and tryptic phosphopeptide mapping.** Full-length Pat1[24] and full-length Mei3[4], each fused to GST, were used in the *in vitro* phosphorylation assay. The assay was carried out as follows: 3 pmol of GST–Mei2 was mixed with 0.2 pmol GST–Pat1 and 2 μg BSA in K buffer (150 mM Tris-HCl, pH 7.5, 20 mM MgCl₂, 10 mM MnCl₂, 15 mM 2-mercaptoethanol). The reaction was initiated by adding 20 μM[γ-³²P]ATP and terminated by adding SDS–PAGE buffer after 30 min incubation at 30 °C. To label Mei2 protein *in vivo*, we transformed *mei2Δpat1+* and *mei2Δpat1Δ* haploid strains with pREP41-*mei2-FA*, carrying the inactive F644A allele[12] (Fig. 1a). *mei2-FA*, rather than *mei2+*, was used here because viable transformants could be obtained from a *pat1Δ* strain. Transformed cells were labelled with ortho-[³²P]-phosphate for 18 h in MM liquid, collected by centrifugation, and broken in 10% TCA with glass beads. After washing with acetone, the pellet was dissolved in S buffer (50 mM Tris-HCl, pH 7.5, 1 mM EDTA, 1 mM 2-mercaptoethanol, 0.5 mM PMSF, 1% SDS). An aliquot of the supernatant was immunopreciptiated with anti-Mei2 antibodies[12]. The immunocomplex was resolved by SDS–PAGE and the Mei2 band eluted from the gel and digested with trypsin as described[25]. GST-Mei2C phosphorylated *in vitro* was processed similarly. Tryptic samples were applied to thin-layer cellulose plates and separated by high-voltage electrophoresis (at 1,000 V) at pH 1.9 for 30 min, followed by ascending chromatography.

**Screening for *mei2* alleles encoding constitutively active gene products.** We randomly mutagenized the C-terminal half of *mei2* encoding residues 429–750 by polymerase chain reaction (PCR) and expressed their full-length versions from pREP41 in wild-type haploid cells. Three relatively weak

'activated' *mei2* alleles, which could induce haploid meiosis upon induction of transcription, were isolated and sequenced.

**Fluorescence microscopy of GFP-tagged Mei2 protein.** We cloned a mutant version (Ser65 → Thr) of GFP[26] into pREP81, and inserted an *Nde*I–*Sal*I fragment carrying the exact *mei2* ORF before the GFP ORF. The fusion protein Mei2–GFP was expressed in *mei2Δ* cells to eliminate the competitive effects of endogenous Mei2 protein. Living cells were counter-stained with Hoechst 33342 and video-recorded by a Peltier-cooled CCD camera (Photometrics) attached to an Olympus inverted microscope IMT-2, as described[18,27].

1. Iino, Y. & Yamamoto, M. *Mol. Gen. Genet.* 198, 416–421 (1985).
2. Nurse, P. *Mol. Gen. Genet.* 198, 497–502 (1985).
3. Beach, D., Rodgers, L. & Gould, J. *Curr. Genet.* 10, 297–311 (1985).
4. McLeod, M., Stein, M. & Beach, D. *EMBO J.* 6, 729–736 (1987).
5. McLeod, M. & Beach, D. *Nature* 332, 509–514 (1988).
6. Yamamoto, M. *Trends Biochem. Sci.* 21, 18–22 (1996).
7. Eberhart, C. G., Maines, J. Z. & Wasserman, S. A. *Nature* 381, 783–785 (1996).
8. Egel, R. in *Molecular Biology of the Fission Yeast* (eds Nasim, A. *et al.*) 31–73 (Academic, San Diego, 1989).
9. Iino, Y. & Yamamoto, M. *Proc. Natl Acad. Sci. USA* 82, 2447–2451 (1985).
10. Watanabe, Y., Iino, Y., Furuhata, K., Shimoda, C. & Yamamoto, M. *EMBO J.* 7, 761–767 (1988).
11. Birney, E., Kumar, S. & Krainer, A. R. *Nucleic Acids Res.* 12, 5803–5816 (1993).
12. Watanabe, Y. & Yamamoto, M. *Cell* 78, 487–498 (1994).
13. Robinow, S., Campos, A., Yao, K. & White, K. *Science* 242, 1570–1572 (1988).
14. Nakashima, N., Tanaka, K., Sturm, S. & Okayama, H. *EMBO J.* 14, 4794–4802 (1995).
15. Fernandez-Sarabia, M. J., McInerny, C., Harris, P., Gordon, C. & Fantes, P. *Mol. Gen. Genet.* 238, 241–251 (1993).
16. Sugiyama, A., Tanaka, K., Okazaki, K., Nojima, H. & Okayama, H. *EMBO J.* 13, 1881–1887 (1994).
17. Chalfie, M., Tu, Y., Euskirchen, G., Ward, W. W. & Prasher, D. C. *Science* 263, 802–805 (1994).
18. Chikashige, Y. *et al. Science* 264, 270–273 (1994).
19. Bohmann, K., Fereira, J., Santama, N., Weis, K. & Lamond, A. I. *J. Cell Sci.* (suppl.) 19, 107–113 (1995).
20. Li, P. & McLeod, M. *Cell* 87, 869–880 (1996).
21. Sugimoto, A., Iino, Y., Maeda, T., Watanabe, Y. & Yamamoto, M. *Genes Dev.* 5, 1990–1999 (1991).
22. Basi, G., Schmidt, E. & Maundrell, K. *Gene* 123, 131–136 (1993).
23. Mochizuki, N. & Yamamoto, M. *Mol. Gen. Genet.* 233, 17–24 (1992).
24. McLeod, M. & Beach, D. *EMBO J.* 5, 3665–3671 (1986).
25. Boyle, W. J., Geer, P. V. d. & Hunter, T. *Meth. Enzymol.* 201, 110–149 (1991).
26. Heim, R., Cubitt, A. B. & Tsien, R. Y. *Nature* 373, 663–664 (1995).
27. Hiraoka, Y., Swedlow, J. R., Paddy, M. R., Agard, D. A. & Sedat, J. W. *Semin. Cell Biol.* 2, 153–165 (1991).
28. Shimoda, C. *et al. J. Bacteriol.* 169, 93–96 (1987).
29. Takeda, T. & Yamamoto, M. *Proc. Natl Acad. Sci. USA* 84, 3580–3584 (1987).

# Crystal structure of the type-I interleukin-1 receptor complexed with interleukin-1β

**Guy P. A. Vigers, Lana J. Anderson, Patricia Caffes & Barbara J. Brandhuber**

*Amgen Inc., 3200 Walnut Street, Boulder, Colorado 80301, USA*

Interleukin-1 (IL-1) is an important mediator of inflammatory disease. The IL-1 family currently consists of two agonists, IL-1α and IL-1β, and one antagonist, IL-1ra. Each of these molecules binds to the type I IL-1 receptor (IL1R)[1]. The binding of IL-1α or IL-1β to IL1R is an early step in IL-1 signal transduction and blocking this interaction may therefore be a useful target for the development of new drugs. Here we report the three-dimensional structure of IL-1β bound to the extracellular domain of IL1R (s-IL1R) at 2.5 Å resolution. IL-1β binds to s-IL1R with a 1:1 stoichiometry. The crystal structure shows that s-IL1R consists of three immunoglobulin-like domains which wrap around IL-1β in a manner distinct from the structures of previously described cytokine–receptor complexes. The two receptor-binding regions

on IL-1β identified by site-directed mutagenesis[2,3] both contact the receptor: one binds to the first two domains of the receptor, while the other binds exclusively to the third domain.

Human IL1R was first cloned from T cells[4] and its sequence predicted a mature receptor consisting of a 552 amino-acid protein containing an extracellular ligand-binding domain of 319 amino acids having three immunoglobulin-like (Ig-like) domains, a single transmembrane segment, and a 213 amino-acid cytoplasmic domain. IL-1α, IL-1β and IL1RA (IL-1 receptor antagonist) all bind to IL1R and although they share only about 25% amino-acid sequence identity, these molecules all have the same β-trefoil, 12-stranded β-barrel structure[5]. In order to further our understanding of IL-1–IL1R interactions we have solved the crystal structure of recombinant human IL-1β bound to recombinant human s-IL1R. The current structure has an R-factor of 23.2% at 2.5 Å resolution.

The IL-1β–s-IL1R complex structure (Fig. 1) was solved using a combination of molecular replacement and multiple isomorphous replacement (MIR) phasing methods (Table 1). The complex has rough dimensions of 97 Å × 52 Å × 35 Å with one s-IL1R molecule wrapping around the IL-1β molecule to contact both the receptor binding sites previously identified by structure : function studies[2,3]. As predicted by its sequence, s-IL1R has three Ig-like domains (see Fig. 1). All three Ig-like domains contain a conserved pair of cysteines and a tryptophan residue about 14 residues after the first conserved cysteine of each domain. Domain 3 is of the c-type, seven-stranded variety[6], similar to the immunoglobulin (Ig) constant domain whereas domains 1 and 2 are more unusual topologically. In both of these domains, strand a is strand-switched to the 'front' face of the barrel, as seen in some v-type Igs, but the c' strand is very short (as in constant domains) and the c" strand is not detectable. Strands d and e are also extremely short, and are comparable in length to those seen in the cell-adhesion molecule N-cadherin[7] (Protein Database (PDB) entry 1NCG). Furthermore, strands c, d and e are on the distal side of domains 1 and 2 from the IL-1β molecule, and are not involved in IL-1 binding. Thus, all three domains of the IL1RI are most simply classified as c-type. Domains 1 and 2 are closely juxtaposed, with a disulphide bond (C104–

C147) holding them together, whereas domain 3 is connected by a 5-residue linker (L201–K205). Domain 3 provides a 'lid' which covers most of the top of the IL-1β β-barrel, whereas domains 1 and 2 form a groove which binds to the lower rim of the barrel.

The structure of IL-1β does not change substantially upon binding. The r.m.s. deviation in position for all non-hydrogen atoms is 1.76 Å between the starting structure of IL-1β[8] and the refined complex structure. Maximum differences are seen at Q32 (r.m.s.d. = 5.6 Å), K88 (r.m.s.d. = 5.5 Å), Q141 (r.m.s.d. = 4.3 Å) and the C-terminal S153 (r.m.s.d. = 9.6 Å). Of these residues, Q32 is involved in receptor binding, whereas the other three are in flexible loops of the molecule. Minimum differences are seen in residues such as A59, L60, F112 and F133 (all about 0.2 Å r.m.s.d.) which are involved in the packing of the hydrophobic core of the IL-1β[5].

Extensive site-directed mutagenesis work has delineated two receptor-binding sites on IL-1α and IL-1β and one on IL1RA. Figure 2 shows that on IL-1β the two binding sites correspond extremely well with residues buried in the receptor : ligand interface. For example, Gln 15 (shown in blue in the middle of Fig. 2) lost 100% of its IL1R binding activity when mutated to glycine, and 116 Å[2] of its solvent-accessible surface is buried upon binding s-IL1R. In addition, numerous residues, which showed a loss of 30–50% of their receptor binding activity upon conservative mutation, are located on the edges of the binding sites and show corresponding changes in computed solvent accessibility upon receptor binding. These results demonstrate the utility of mutagenesis studies for mapping ligand : receptor contacts.

The binding site common to all three IL-1 family members, on the 'side' of the IL-1β β-barrel (site A), makes contacts with β-strands a1, a2, b2 and the b2–c2 loop in domains 1 and 2 of the receptor (Fig. 1) and consists of residues 11, 13–15, 20–22, 27, 29–36, 38, 126–131, 147 and 149. The critical binding residues Arg 11 and Gln 15 contact domain 2 whereas His 30 and Gln 32 bind in the domain 1–2 junction. The surface of the receptor at this binding site has a number of pockets that will accept side chains of IL-1β. Thus a significant component of the binding energy at this site probably
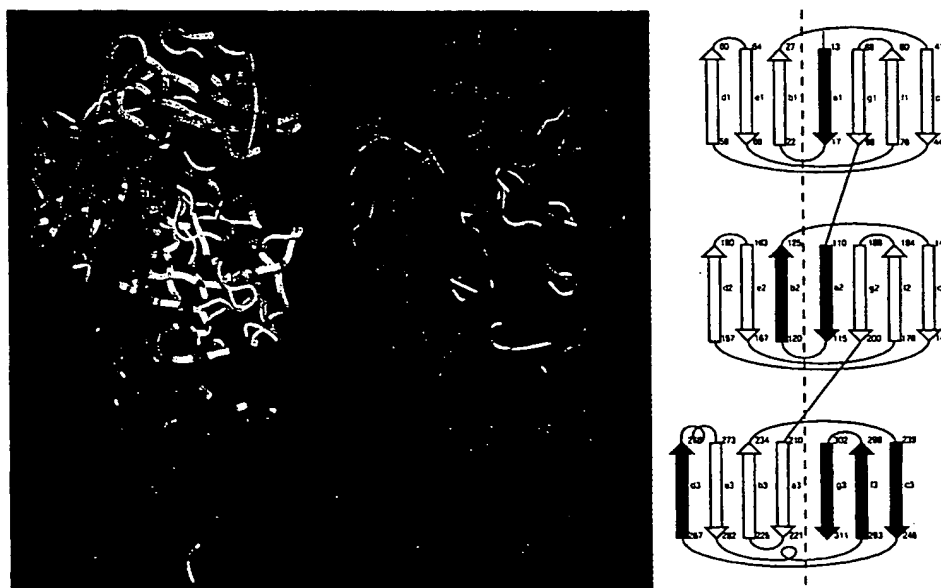


**Figure 1** Left, Ribbon diagram of s-IL1R complexed to IL-1β. Domains 1, 2 and 3 of s-IL1R are coloured light, medium and dark blue, respectively. IL-1β is yellow, with site A residues in green and site B residues in red. Middle, Ribbon diagram of the structure of IL-1β bound to s-IL1R. The β-strands are shown as arrowed ribbons in green, α-helices are red, and the connecting loops are purple. The structure is oriented so that the carboxy terminus of s-IL1R and the cell membrane, if present, are at the bottom of the picture. Right, Topology diagram of s-IL1R. The IL-1β-binding elements in site A and site B are coloured green and red, respectively. Secondary structural elements are not to scale.

comes from van der Waals contacts between IL-1β and s-IL1R. Interestingly, the position of Gln 32 has moved by more than 5 Å from its position in the unliganded X-ray structure, and now fits in a deep pocket on the s-IL1R (Fig. 3).

Site B, the second binding site identified on IL-1α and IL-1β but not IL1RA, is on the top of the β-barrel and is formed by residues 1–4, 6, 46, 48, 51, 53–54, 56, 92–94, 103, 105–106, 108, 109, 150 and 152. Site B makes contacts only with domain 3 of s-IL1R. Previous work from our group[5] suggested that site B of IL-1β was composed of a 'horseshoe' of hydrophilic residues surrounding several hydrophobic residues. As shown in Fig. 3, both the hydrophilic residues (Arg 4, Gln 48, Glu 51, Asn 53, Lys 93, Glu 105 and Asn 108) and the hydrophobic residues (Leu 6, Phe 46, Ile 56 and Phe 150) do indeed contact IL1R over a large and relatively flat surface (formed by β-strands c3, d3, f3, g3 and the b3–c3, c3–d3, f3–g3 and g2–a3 loops), which is complementary to IL-1β in hydrophobicity. Thus, the binding energy of site B appears to be more dependent upon hydrophobic and hydrophilic interactions than in site A. Because IL1RA lacks the distinctive 'horseshoe' feature of IL-1β, formation

of the IL1RI-IL1RA complex will presumably not make the same energetically favourable site B contacts seen in this structure.

Calculating the changes in solvent-accessible area of the IL-1β on binding s-IL1R, 1,087 Å[2] are buried in site A over 25 residues and 1,001 Å[2] in site B over 21 residues, for a total of 2,088 Å[2] overall. In addition to the hydrophilic–hydrophobic interactions described above (which are particularly apparent for site B), both binding sites also make extensive use of salt bridges and hydrogen bonds. Site A and site B have 10 and 13 salt bridges, respectively, and both sites also contain seven intramolecular hydrogen bonds (as deduced from the X-ray structure). It is interesting to note that in this complex, the ligand-binding interactions are with the β-strands in the faces of the Ig-like domains, not with the 'elbow' formed by the loops between the domains, as seen in the structures of interferon-γ–interferon-γ receptor[9], human growth hormone–human growth hormone-binding protein[10] (PDB entry 3HHR) and the erythropoietin mimetic peptide–erythropoietin-binding protein[11] (PDB entry 1EBP). Also, in previously determined cytokine–receptor structures, whereas the cytokine might exist as a monomer



**Figure 2** Surface representations of IL-1β. Left, Structure of unbound IL-1β[8]; spectral colouring based on site-directed mutagenesis experiments. Blue residues lost 100% of IL1R binding activity, red residues lost no activity, and grey residues were not done. Right, Structure of IL-1β from the complex coloured to show the change in solvent-accessible area upon complex formation[18]. Blue residues bury 100 Å[2] or greater, and red residues bury 2 Å[2]. Grey residues bury less than 2 Å[2]. Site B is at the top and site A faces the viewer.

**Table 1 MIR data**

| Data set | Resolution (Å) | $R_{sym}$ (last shell) | Completeness (last shell) | $\langle I/s(I)\rangle$ (last shell) | Sites ($n$) | $R_{cullis\_a}$ | $R_{cullis\_c}$ | $R_{cullis\_ano}$ | Phasing power_a | Phasing power_c |
|---|---|---|---|---|---|---|---|---|---|---|
| Native* | 2.5 | 6.6 (10.4) | 96.2 (94.9) | 28.03 (10.94) | – | – | – | – | – | – |
| HgCl2_1 | 3.0 | 7.5 (27.2) | 79.3 (29.5) | 15.11 (5.46) | 2 | 50.0 | 48.0 | 70.0 | 2.0 | 1.7 |
| HgCl2_2 | 2.8 | 8.1 (31.4) | 97.4 (98.5) | 13.74 (4.51) | 2 | 64.0 | 62.0 | 70.0 | 1.5 | 1.2 |
| PtCl_ | 3.0 | 6.1 (27.6) | 84.4 (91.6) | 15.31 (4.55) | 5 | 76.0 | 66.0 | 60.0 | 1.1 | 1.0 |
| PtCl_2 | 3.0 | 7.8 (30.7) | 76.5 (80.4) | 15.07 (5.33) | 5 | 75.0 | 68.0 | 80.0 | 1.2 | 1.1 |
| C71S_1† | 3.0 | 7.2 (19.8) | 74.7 (80.3) | 14.15 (6.23) | 1 | 63.0 | 62.0 | 80.0 | 1.6 | 1.2 |
| C71S_2† | 2.5 | 6.6 (19.6) | 93.0 (95.2) | 16.66 (5.79) | 1 | 72.0 | 71.0 | 80.0 | 1.4 | 1.1 |
| Q126C_1‡ | 3.0 | 7.3 (23.7) | 78.7 (85.8) | 15.93 (5.95) | 2 | 74.0 | 63.0 | 80.0 | 1.1 | 1.0 |
| Q126C_2‡ | 2.5 | 4.9 (18.3) | 94.3 (97.2) | 17.90 (6.85) | 2 | 86.0 | 78.0 | 80.0 | 0.9 | 0.8 |

* Data merged from two data sets.
† IL-1β mutated so that cysteine 71 is serine.
‡ IL-1β mutated so that cysteine 71 is serine and glutamine 126 is cysteine.
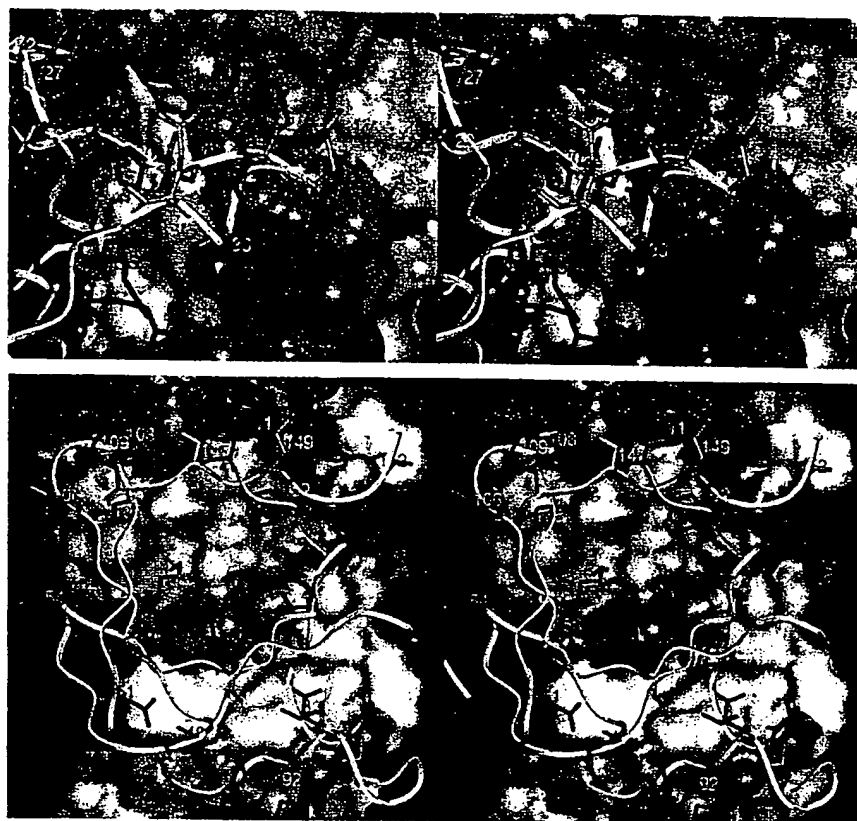
**Figure 3** Stereoscopic surface representations of s-IL1R and ribbon diagrams of IL-1β. Top, Site A. Bottom, Site B. Side chains in IL-1β and the surface of s-IL1R are coloured red for hydrophobic residues and purple for hydrophilic residues. The IL-1β backbone ribbon is yellow.

(hGH), dimer (IFN-γ) or trimer (TNFβ)[12], in every case two or more receptors bound to the cytokine and each receptor made a single contiguous surface contact with the cytokine. The s-IL1R binding motif thus provides a new model for receptor–cytokine interactions.

IL-1 signalling is believed to result from the formation of a ternary complex consisting of an IL-1 agonist, IL1R and IL1R accessory protein (IL1RAcP)[13]. When IL1RA binds IL1R, the ternary complex is not formed and signalling does not occur. Formation of the ternary complex therefore presumably requires an epitope that is created when IL1RI binds IL-1β but not IL1RA. Whether the epitope is created by formation of the receptor–ligand interface, or by conformational changes of IL1RI on complex formation, has yet to be determined. Site-directed mutagenesis of additional surface residues in IL-1 and IL1R, and solving the structure of the ternary complex, will further advance our understanding of the IL-1 family members' activities. □

## Methods

**Purification and crystallization.** Recombinant human s-IL1R (residues 1–315, GenBank numbering) was expressed in *Escherichia coli*, refolded and purified using an IL1RA affinity column, MonoQ ion-exchange column and gel filtration column (B.J.B. *et al.*, manuscript in preparation). Wild-type and mutants of IL-1β used for heavy-atom phasing were generated and purified as described previously[3]. the mercury chloride derivative was found to derivatize the cysteines only in IL-1β, therefore cysteine mutants of IL-1β were made to augment the phase information available. All mutants that were crystallized and derivatized were isomorphous with native, wild-type complex crystals. The s-IL1R was incubated overnight in a fivefold molar excess of IL-1β, purified over a Superdex 75 column and concentrated to 5 mg ml⁻¹. Crystals were grown by hanging-drop diffusion against 1.8 M ammonium sulphate, 100 mM MES pH 6.0 at 0–4 °C. The crystals grew to about 0.4 × 0.4 × 3 mm in 1–2 weeks.

**Data collection and phasing.** Initial characterization of the crystals and searches for heavy-atom derivatives were performed on room-temperature crystals in an artificial mother liquor containing 2.8 M ammonium sulphate, 100 mM MES pH 6.0. However, the crystals proved to be very radiation sensitive at room temperature and all data sets for MIR phasing and refinement were therefore collected on cryo-cooled crystals. Crystals were cryoprotected with 25% glucose, 1.3 M ammonium sulphate, 100 mM MES pH 6.0 and diffracted to 2.5 Å resolution. The crystals were of space group C2 with unit cell dimensions $a = 146.95$ Å, $b = 68.45$ Å, $c = 65.87$ Å, $\alpha = \gamma = 90.0°$, $\beta = 108.95°$. X-ray data were collected on an R-axisII area detector, reduced using Denzo and Scalepack[14] and processed using the CCP4 suite of programs including MLPHARE and DM[15]. The position of the IL-1β molecule in the complex was determined by molecular replacement with X-plor 3.1 from the PDB coordinates pdb2i1b.ent[3].

**Structure refinement.** The s-IL1R structure was traced and rebuilt using program O[16]. Refinement by conjugant gradient and simulated annealing was performed in X-PLOR 3.1[17] for all reflections with $F > 2\sigma(F)$ from 15.0 to 2.5 Å ($n = 20,723$). All solvent-accessibility calculations were performed in X-PLOR using the method of Lee and Richards[18], using a 1.4 Å radius probe and assuming that the ligand and receptor structures do not change significantly upon binding. Potential hydrogen bonds were determined using the 'Hbonds_all' facility in O. Salt bridges were assigned in X-PLOR by picking all intermolecular oxygen–nitrogen pairs separated by 3.4 Å or less. Secondary structure assignments were made with the YASSPA algorithm in O and pictures were generated using Setor[19]. The current structure contains 31 ordered water molecules and a bulk solvent correction (sol density = 0.40, sol rad = 0.25) was used for the glucose cryoprotectant. The R-factor of the current structure is $R = 23.2\%$ with a free R-factor of 33.1%. In the MIR maps, part of the amino terminus of the first Ig-like domain showed only weak density. For this reason residues 1–8 and 30–41 are not modelled, and the 40–54 loop is poorly defined. Fortunately, this region is distal to the IL-1 binding site, and so does not significantly affect the conclusions of the study. The r.m.s. deviations from ideality are 0.012 Å for bond lengths and 1.98° for bond angles. Running

Procheck on the refined structure showed that four residues are in disallowed regions of the Ramachandran plot. Two of these residues (E11 and Q53) are in the poorly defined region of the molecule whereas the other two (L186 and N246) are at the apex of very tight loops.

1. Dinarello, C. A. Biologic basis for interleukin-1 in disease. *Blood* 87, 2095–2147 (1996).
2. Labriola-Thompkins, E. *et al.* Identification of the discontinuous binding site in human interleukin 1β for the type I interleukin 1 receptor. *Proc. Natl Acad. Sci. USA* 88, 11182–11186 (1991).
3. Evans, R. J. *et al.* Mapping receptor binding sites in interleukin (IL)-1 receptor antagonist and IL-1β by site-directed mutagenesis. *J. Biol. Chem.* 270, 11477–11483 (1995).
4. Sims, J. E. *et al.* Cloning the interleukin 1 receptor from human T cells. *Proc. Natl Acad. Sci. USA* 86, 8346–8950 (1989).
5. Vigers, G. P. A. *et al.* X-ray structure of interleukin-1 receptor antagonist at 2.0 Å resolution. *J. Biol. Chem.* 269, 12874–12879 (1994).
6. Bork, P., Holm, L. & Sander, C. The immunoglobulin fold. Structural classification, sequence patterns and common core. *J. Mol. Biol.* 242, 309–320 (1994).
7. Shapiro, L. *et al.* Structural basis of cell-cell adhesion by cadherins. *Nature* 374, 327–337 (1995).
8. Priestle, J. P., Schaer, H. P. & Gruetter, M. G. Crystallographic refinement of interleukin 1 beta at 2.0 Å resolution. *Proc. Natl Acad. Sci. USA* 86, 9667–9671 (1989).
9. Walter, M. R. *et al.* Crystal structure of a complex between interferon-γ and its soluble high-affinity receptor. *Nature* 376, 230–235 (1995).
10. de Vos, A. M., Ultsch, M. & Kossiakoff, A. A. Human growth hormone and extracellular domain of its receptor: crystal structure of the complex. *Science* 255, 306–312 (1992).
11. Livnah, O. *et al.* Functional mimicry of a protein hormone by a peptide agonist: the EPO receptor complex at 2.8 Å. *Science* 273, 464–471 (1996).
12. Banner, D. W. *et al.* Crystal structure of the soluble human 55 kd TNF receptor-human TNF beta complex: implications for TNF receptor activation. *Cell* 73, 431–445 (1993).
13. Greenfeder, S. A. *et al.* Molecular cloning and characterization of a second subunit of the interleukin 1 receptor complex. *J. Biol. Chem.* 270, 1357–13765 (1995).
14. Otwinowski, Z. in *Data Collection and Processing* (eds Sawyer, L., Isaacs, N. & Bailey, S.) (SERC Daresbury Laboratory, Warrington, UK, 1993).
15. CCP4: Collaborative Computational Project No 4, Daresbury UK. *Acta Crystallogr. D* 50, 760 (1994).
16. Jones, T. A., Zou, J. Y., Cowan, S. W. & Kjeldgaard, M. Improved methods for binding protein models in electron density maps and the location of errors in these models. *Acta Crystallogr. A* 47, 110–119 (1991).
17. Brunger, A. T., Kuriyan, J. & Karplus, M. Crystallographic R factor refinement by molecular dynamics. *Science* 235, 458–460 (1987).
18. Lee, B. & Richards, F. M. The interpretation of protein structures: estimation of static accessibility. *J. Mol. Biol.* 55, 379–400 (1971).
19. Evans, S. V. SETOR: hardware-lighted three-dimensional solid model representations of macromolecules. *J. Mol. Graphics* 11, 134–138 (1993).

# A new cytokine-receptor binding mode revealed by the crystal structure of the IL-1 receptor with an antagonist

**Herman Schreuder**[*][†], **Chantal Tardif**[*][†],
**Susanne Trump-Kallmeyer**[*], **Adolfo Soffientini**[‡],
**Edoardo Sarubbi**[‡], **Ann Akeson**[§], **Terry Bowlin**[‡][§],
**Stephen Yanofsky**[||] & **Ronald W. Barrett**[||]

[*] *Marion Merrell Dow Research Institute, 67080 Strasbourg Cedex, France*
[‡] *Lepetit Research Centre, 21040 Gerenzano, Italy*
[§] *Hoechst Marion Roussel Inc., Cincinnati, Ohio 45215-6300, USA*
[||] *Affymax, Palo Alto, California 94304, USA*

......................................................................................................................

Inflammation, regardless of whether it is provoked by infection or by tissue damage, starts with the activation of macrophages which initiate a cascade of inflammatory responses by producing the cytokines interleukin-1 (IL-1) and tumour necrosis factor-α (ref. 1). Three naturally occurring ligands for the IL-1 receptor (IL1R) exist: the agonists IL-1α and IL-1β and the IL-1-receptor antago-

† Present addresses: Hoechst AG, Building G865A, 65926 Frankfurt, Germany (H.S.); Synthelabo Biomoleculaire, 67080 Strasbourg Cedex, France (C.T.); Parke Davis Pharmaceutical Research, Ann Arbor, MI 48105, USA (S.T.-K.); Biochem Therapeutice, Laval, Quebec H7V4A7, Canada (T.B.).

nist IL1RA (ref. 2). IL-1 is the only cytokine for which a naturally occurring antagonist is known. Here we describe the crystal structure at 2.7 Å resolution of the soluble extracellular part of type-I IL1R complexed with IL1RA. The receptor consists of three immunoglobulin-like domains. Domains 1 and 2 are tightly linked, but domain three is completely separate and connected by a flexible linker. Residues of all three domains contact the antagonist and include the five critical IL1RA residues which were identified by site-directed mutagenesis[3]. A region that is important for biological function in IL-1β, the 'receptor trigger site', is not in direct contact with the receptor in the IL1RA complex. Modelling studies suggest that this IL-1β trigger site might induce a movement of domain 3.

A soluble form of the IL-1 receptor, comprising residues 1–311, was expressed in insect cells and purified by affinity chromatography[4]. The soluble receptor was mixed with recombinant IL1RA at a ratio of 1:1 and was crystallized from 30% PEG3350 at pH 7.0–7.5[4]. The structure has been solved by a combination of molecular replacement and heavy-atom derivatives and has been refined at 2.7 Å resolution to an $R$ factor of 21.1% ($R_{free} = 31.4\%$) with excellent geometry (see Methods and Table 1). A representative sample of the original squashed multiple isomorphous replacement (MIR) electron density map is given in Fig. 1.

The IL1R molecule resembles a question mark which curls round the IL1RA molecule held in its centre (Fig. 2a). The IL1RA consists of a six-stranded β-barrel closed at one side by three β-hairpin loops and is similar to the structure of the free molecule we solved previously[5]. The root-mean-square (r.m.s.) differences in alpha carbon (Cα) positions between bound and free IL1RA are 0.7 Å and 0.8 Å, respectively for the two independent IL1RA molecules present in the crystals of the free IL1RA. The largest differences in the antagonist occur in the loop comprising residues 51–54. This loop interacts with the third IL1R domain but is partially disordered in the free antagonist. Upon binding to IL1R, there is a rotation of the side chain of Glu 52 away from the receptor, a rotation of the side chain of His 54 towards the receptor, and a change in conformation from *cis* to *trans* for Pro 53. Other differences in atomic position greater than 5.0 Å involve solvent-exposed, flexible side chains, namely those of Lys 64, Glu 75, Arg 77, Lys 93, Lys 96, Asp 138, Glu 139 and Lys 145.

As predicted[6], the folding of the three IL1R domains, consisting of a sandwich of two β-sheets, resembles the folding of immunoglobulin domains. The topology of domains 1 and 2 (residues 1–94 and 106–198) is distantly related to the telokin I-set[7] topology, although it diverges significantly from the canonical I-set structures. A β-bulge is present between residues 8 and 11 in strand a of domain 1. The bed sheets in domains 1 and 2 are very short, with strand lengths of only 3–4 residues. Strands g and f in domain 2 are long and have extensive contacts with domain 1. Residues involved are Glu 18, Gln 50, His 55 and Val 64 of domain 1, and Tyr 182, Leu 183, Tyr 187, Pro 188 and Thr 190 of domain 2. Domains 1 and 2 are linked through a well-defined β-turn between Pro 98 and Asn 99 which lies on top of the agfcc' sheet (Fig. 2b). Domains 2 and 3 are connected through an extended, flexible linker.

The electron density maps clearly indicated four carbohydrate-binding sites at Asn 173, 213, 229 and 243. The electron density quickly disappears after the first N-acetylglucosamine unit, indicating that most sugar units are disordered. The first attachment site, Asn 173, is at the surface of the second domain and its sugar chain is facing the solvent. The other three attachment sites (Asn 213, 229 and 243) are at the surface of domain 3, and in the natural situation their sugar chains will be close to the cell membrane. Interactions of these sugar chains with the membrane could help to stabilize the orientation of the IL1R with respect to the membrane.

Alignment of the sequence of the extracellular part of the type-1 IL1R with homologous proteins (Fig. 3) reveals a number of conserved sequence motifs: the conserved disulphide link and

Procheck on the refined structure showed that four residues are in disallowed regions of the Ramachandran plot. Two of these residues (E11 and Q53) are in the poorly defined region of the molecule whereas the other two (L186 and N245) are at the apex of very tight loops.

1. Dinarello, C. A. Biologic basis for interleukin-1 in disease. Blood 87, 2095–2147 (1996).
2. Labriola-Thompkins, E. et al. Identification of the discontinuous binding site in human interleukin 1β for the type I interleukin 1 receptor. Proc. Natl Acad. Sci. USA 88, 11182–11186 (1991).
3. Evans, R. J. et al. Mapping receptor binding sites in interleukin (IL)-1 receptor antagonist and IL-1β by site-directed mutagenesis. J. Biol. Chem. 270, 11477–11483 (1995).
4. Sims, J. E. et al. Cloning the interleukin 1 receptor from human T cells. Proc. Natl Acad. Sci. USA 86, 8946–8950 (1989).
5. Vigers, G. P. A. et al. X-ray structure of interleukin-1 receptor antagonist at 2.0 Å resolution. J. Biol. Chem. 269, 12874–12879 (1994).
6. Bork, P., Holm, L. & Sander, C. The immunoglobulin fold. Structural classification, sequence patterns and common core. J. Mol. Biol. 242, 309–320 (1994).
7. Shapiro, L. et al. Structural basis of cell-cell adhesion by cadherins. Nature 374, 327–337 (1995).
8. Priestle, J. P., Schaer, H. P. & Gruetter, M. G. Crystallographic refinement of interleukin 1 beta at 2.0 Å resolution. Proc. Natl Acad. Sci. USA 86, 9667–9671 (1989).
9. Walter, M. R. et al. Crystal structure of a complex between interferon-γ and its soluble high-affinity receptor. Nature 376, 230–235 (1995).
10. de Vos, A. M., Ultsch, M. & Kossiakoff, A. A. Human growth hormone and extracellular domain of its receptor: crystal structure of the complex. Science 255, 306–312 (1992).
11. Livnah, O. et al. Functional mimicry of a protein hormone by a peptide agonist: the EPO receptor complex at 2.8 Å. Science 273, 464–471 (1996).
12. Banner, D. W. et al. Crystal structure of the soluble human 55 kd TNF receptor-human TNF beta complex: implications for TNF receptor activation. Cell 73, 431–445 (1993).
13. Greenfeder, S. A. et al. Molecular cloning and characterization of a second subunit of the interleukin 1 receptor complex. J. Biol. Chem. 270, 13757–13765 (1995).
14. Otwinowski, Z. in Data Collection and Processing (eds Sawyer, L., Isaacs, N. & Bailey, S.) (SERC Daresbury Laboratory, Warrington, UK, 1993).
15. CCP4: Collaborative Computational Project No 4, Daresbury UK. Acta Crystallogr. D 50, 760 (1994).
16. Jones, T. A., Zou, J. Y., Cowan, S. W. & Kjeldgaard, M. Improved methods for binding protein models in electron density maps and the location of errors in these models. Acta Crystallogr. A 47, 110–119 (1991).
17. Brunger, A. T., Kuriyan, J. & Karplus, M. Crystallographic R factor refinement by molecular dynamics. Science 235, 458–460 (1987).
18. Lee, B. & Richards, F. M. The interpretation of protein structures: estimation of static accessibility. J. Mol. Biol. 55, 379–400 (1971).
19. Evans, S. V. SETOR: hardware-lighted three-dimensional solid model representations of macromolecules. J. Mol. Graphics 11, 134–138 (1993).

# A new cytokine-receptor binding mode revealed by the crystal structure of the IL-1 receptor with an antagonist

Herman Schreuder*†, Chantal Tardif*†,
Susanne Trump-Kallmeyer*, Adolfo Soffientini‡,
Edoardo Sarubbi‡, Ann Akeson§, Terry Bowlin‡§,
Stephen Yanofsky‖ & Ronald W. Barrett‖

* Marion Merrell Dow Research Institute, 67080 Strasbourg Cedex, France
‡ Lepetit Research Centre, 21040 Gerenzano, Italy
§ Hoechst Marion Roussel Inc., Cincinnati, Ohio 45215-6300, USA
‖ Affymax, Palo Alto, California 94304, USA

Inflammation, regardless of whether it is provoked by infection or by tissue damage, starts with the activation of macrophages which initiate a cascade of inflammatory responses by producing the cytokines interleukin-1 (IL-1) and tumour necrosis factor-α (ref. 1). Three naturally occurring ligands for the IL-1 receptor (IL1R) exist: the agonists IL-1α and IL-1β and the IL-1-receptor antago-

† Present addresses: Hoechst AG. Building G865A. 65926 Frankfurt. Germany (H.S.); Synthelabo Biomoleculaire, 67080 Strasbourg Cedex. France (C.T.); Parke Davis Pharmaceutical Research, Ann Arbor, MI 48105. USA (S.T.-K.); Biochem Therapeutic. Laval. Quebec H7V4A7. Canada (T.B.).

nist IL1RA (ref. 2). IL-1 is the only cytokine for which a naturally occurring antagonist is known. Here we describe the crystal structure at 2.7 Å resolution of the soluble extracellular part of type-I IL1R complexed with IL1RA. The receptor consists of three immunoglobulin-like domains. Domains 1 and 2 are tightly linked, but domain three is completely separate and connected by a flexible linker. Residues of all three domains contact the antagonist and include the five critical IL1RA residues which were identified by site-directed mutagenesis[3]. A region that is important for biological function in IL-1β, the 'receptor trigger site', is not in direct contact with the receptor in the IL1RA complex. Modelling studies suggest that this IL-1β trigger site might induce a movement of domain 3.

A soluble form of the IL-1 receptor, comprising residues 1–311, was expressed in insect cells and purified by affinity chromatography[4]. The soluble receptor was mixed with recombinant IL1RA at a ratio of 1:1 and was crystallized from 30% PEG3350 at pH 7.0–7.5[4]. The structure has been solved by a combination of molecular replacement and heavy-atom derivatives and has been refined at 2.7 Å resolution to an R factor of 21.1% ($R_{\text{free}} = 31.4\%$) with excellent geometry (see Methods and Table 1). A representative sample of the original squashed multiple isomorphous replacement (MIR) electron density map is given in Fig. 1.

The IL1R molecule resembles a question mark which curls round the IL1RA molecule held in its centre (Fig. 2a). The IL1RA consists of a six-stranded β-barrel closed at one side by three β-hairpin loops and is similar to the structure of the free molecule we solved previously[5]. The root-mean-square (r.m.s.) differences in alpha carbon (Cα) positions between bound and free IL1RA are 0.7 Å and 0.8 Å, respectively for the two independent IL1RA molecules present in the crystals of the free IL1RA. The largest differences in the antagonist occur in the loop comprising residues 51–54. This loop interacts with the third IL1R domain but is partially disordered in the free antagonist. Upon binding to IL1R, there is a rotation of the side chain of Glu 52 away from the receptor, a rotation of the side chain of His 54 towards the receptor, and a change in conformation from cis to trans for Pro 53. Other differences in atomic position greater than 5.0 Å involve solvent-exposed, flexible side chains, namely those of Lys 64, Glu 75, Arg 77, Lys 93, Lys 96, Asp 138, Glu 139 and Lys 145.

As predicted[6], the folding of the three IL1R domains, consisting of a sandwich of two β-sheets, resembles the folding of immunoglobulin domains. The topology of domains 1 and 2 (residues 1–94 and 106–198) is distantly related to the telokin I-set[7] topology, although it diverges significantly from the canonical I-set structures. A β-bulge is present between residues 8 and 11 in strand a of domain 1. The bed sheets in domains 1 and 2 are very short, with strand lengths of only 3–4 residues. Strands g and f in domain 2 are long and have extensive contacts with domain 1. Residues involved are Glu 18, Gln 50, His 55 and Val 64 of domain 1, and Tyr 182, Leu 183, Tyr 187, Pro 188 and Thr 190 of domain 2. Domains 1 and 2 are linked through a well-defined β-turn between Pro 98 and Asn 99 which lies on top of the agfcc' sheet (Fig. 2b). Domains 2 and 3 are connected through an extended, flexible linker.

The electron density maps clearly indicated four carbohydrate-binding sites at Asn 173, 213, 229 and 243. The electron density quickly disappears after the first N-acetylglucosamine unit, indicating that most sugar units are disordered. The first attachment site, Asn 173, is at the surface of the second domain and its sugar chain is facing the solvent. The other three attachment sites (Asn 213, 229 and 243) are at the surface of domain 3, and in the natural situation their sugar chains will be close to the cell membrane. Interactions of these sugar chains with the membrane could help to stabilize the orientation of the IL1R with respect to the membrane.

Alignment of the sequence of the extracellular part of the type-I IL1R with homologous proteins (Fig. 3) reveals a number of conserved sequence motifs: the conserved disulphide link and

tryptophan, present in the core of many immunoglobulin domains, are absolutely conserved with the exception of IL1R-related protein (IL1RR). A motif that appears to be specific for the IL1R family domains 1 and 2 is a proline immediately after the first cysteine of the conserved core disulphide link. This proline disrupts strand b and is responsible for the very short bed sheets observed in domains 1 and 2 of the IL1R. The presence of Asp 20 and Arg 22 on strand b1 at positions usually occupied by highly conserved hydrophobic residues is unusual. The two residues form, together with Ser 14, a hydrophilic cluster in what would otherwise be the hydrophobic core. Almost perfectly conserved is a DxGxYxC motif at the beginning of strands f1 and f2. This motif indicates the presence of a D4 tyrosine corner and is found in many immunoglobulin variable domains[8]. The cysteine of the motif (76 and 176 in IL1R) is part of the core disulphide link. The hydroxyl of the tyrosine makes a hydrogen bond with the carbonyl oxygen of residue $n - 4$, usually Asp. In domain 1, this Asp makes a salt link with a conserved Arg at the beginning of strand d. The conserved Gly residue in the motif allows the main chain to curve around the tyrosine side chain. Although a D4 tyrosine corner is not present in IL1R domain 3 (the Tyr has been replaced by a Phe and there is a one-residue insertion), the overall conformation of the main chain is similar. Glu 18, at the beginning of strand b1, and Thr 190, halfway along strand g2, make a hydrogen bond in IL1R. These residues are conserved in all sequences, except FGR4, suggesting that the hydrogen bond between them is conserved as well. This would mean that the orientation of domain 1 with respect to domain 2 is similar in these proteins. We conclude from the presence of these common sequence motifs that the proteins listed in Fig. 3 are all similarly folded.
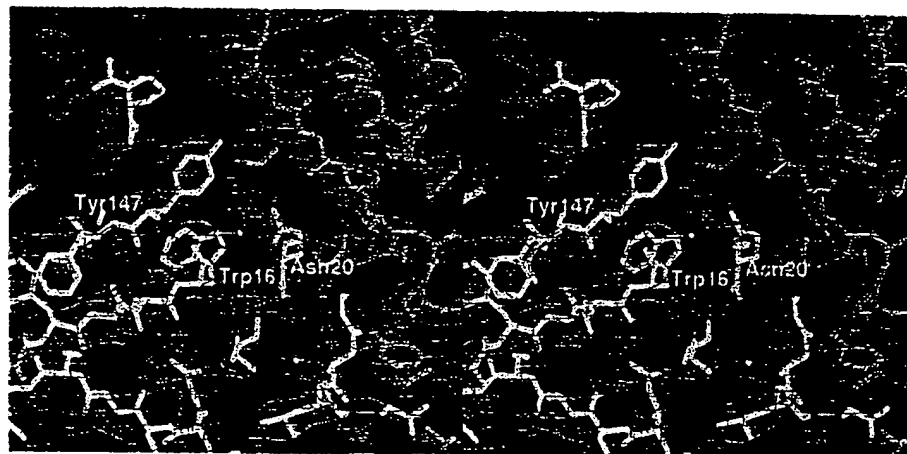


**Figure 1** Stereo view of the squashed MIR map contoured at $1\sigma$. Shown is the receptor–antagonist interface in the region around Trp 16 of the antagonist. The refined model of the IL1RA is shown in yellow; IL1R is in green.

**Table 1 Crystallographic data**

Data collection and phasing statistics

| Data set | Native | Hg(CN)$_2$ | K$_2$PtCl$_4$ | Hg(CN)$_2$ + K$_2$PtCl$_4$ |
|---|---|---|---|---|
| Measured reflections | 73,407 | 71,530 | 66,081 | 43,056 |
| Unique reflections | 15,631 | 15,725 | 14,086 | 10,835 |
| Resolution (Å) | 2.7 | 2.7 | 2.8 | 3.0 |
| Completeness (%) | 97.2 | 98.2 | 98.5 | 92.4 |
| $R_{merge}$(%)* | 6.0 | 6.0 | 6.8 | 7.5 |
| $R_{iso}$(%)† | | 22.3 | 14.8 | 39.7 |
| Binding sites | | 1 | 2 | 3 |
| Phasing power‡ | | 1.29 | 0.91 | 0.68 |
| $R_{cullis}$§ | | 0.58 | 0.63 | 0.69 |
| Mean figure of merit | 0.47 | | | |

Refinement statistics

| | |
|---|---|
| Number of protein atoms | 3,638 |
| Number of sugar atoms (NAG) | 56 |
| Number of water moelcules added | 86 |
| Resolution range | 8.0–2.7 Å |
| Data cutoff | None |
| R factor (number of reflections) | 21.1% (13,487) |
| $R_{free}$ (number of reflections) | 31.4% (1,525) |
| $R_{total}$ (number of reflections) | 22.2% (15,012) |
| Average temperature factor | 45.2 Å$^2$ |

R.m.s. deviations with respect to ideal (target) values

| | |
|---|---|
| Bond lengths | 0.004 Å |
| Bond angles | 1.2° |
| Dihedrals | 26.5° |
| Impropers | 1.0° |

NAG, N-acetylglucosamine.
* $R_{merge} = \Sigma_{hkl}\,|I_{hkl} - \langle I_{hkl}\rangle|\,/\,\Sigma_{hkl}\langle I_{hkl}\rangle$.
† $R_{iso} = \Sigma_{hkl}\,|F_{der} - F_{nat}|\,/\,\Sigma_{hkl}\,|F_{nat}|$.
‡ Phasing power = $\Sigma_{hkl}\,|F_{h}|\,/\,\Sigma_{hkl}\,|$ lack of closure$|$.
§ $R_{cullis}$ = (lack of closure)/(isomorphous differences) for centric reflections, as calculated by HEAVY[9].

⬤          ⬤

A large area of 1,774 Å$^2$ of the IL1RA surface and 1,767 Å$^2$ of the receptor surface (calculated by using DSSP[9]) gets buried upon receptor binding (Fig. 4). This area corresponds to about 20% of the total surface of IL1RA and may explain the tight binding ($\sim 10^{-9}$ M)[6] of the antagonist to the receptor.

The IL1RA molecule interacts with all three receptor domains. Leu 25, Arg 26, Asn 27, Glu 29, Leu 42 and Pro 130 contact strand a and loop bc in the N-terminal half of receptor domain 1. The loop comprising residues 34–39, which is fully exposed in the crystal structure of free IL1RA[5], fits in the cleft between domains 1 and 2. Arg 14, Trp 16, Val 18, Asn 19, Gln 20, Ala 127, Asp 128, Tyr 147 and Gln 149 contact strands of both sheets of the β-sandwich of domain 2. Finally, Ser 8, Lys 9, Pro 50, Ile 51, Pro 53, His 54, Leu 56, Glu 150 and Asp 151 contact loops bc and fg at the top of domain 3 (Fig. 2).

The interactions between the IL1R and the antagonist are mainly polar in character. We observe only three hydrophobic contacts (Table 2). Surprisingly, despite the many charged residues on the IL1R and the antagonist, we find only two direct and one indirect

**Table 2 Selected interactions ($d \leq 3.5$ Å) between the IL1R and IL1RA**

| Side-chain–side-chain interactions | | Interactions involving the main chain | |
|---|---|---|---|
| Receptor | Antagonist | Receptor | Antagonist |
| Salt links | | Receptor side chain to antagonist main chain | |
| Glu 8 | Arg 26 | Lys 9 | Leu 25 |
| Arg 268 | Glu 150 | Glu 126 | Ala 127 |
| Hydrogen bonds | | Tyr 124 | Tyr 34 |
| Tyr 124 OH | Asp 128 oδ2 | Arg 160 | Val 18 |
| Ser 235 Oγ | Gln 11 Oε1 | Receptor main chain antagonist side chain | |
| Hydrophobic contacts | | Ile 11 | Asn 39* |
| Ile 10 | Leu 42 | Val 13 | Gln 36* |
| Leu 198 | Trp 16 | Ala 106 | Gln 36 |
| Pro 113 | Tyr 147 | Lys 111 | Trp 16 |
| | | Lys 111 | Gln 20* |
| | | Gly 119 | Gln 20 |
| | | Receptor main chain to antagonist main chain | |
| | | Ile 107 | Gly 37 |
| | | Asn 296 | Pro 53 |
| | | Thr 297 | His 54 |

* These residues make two hydrogen bonds: one from the side-chain amide to the main-chain carbonyl, and one from the side-chain carbonyl to the main-chain amide.
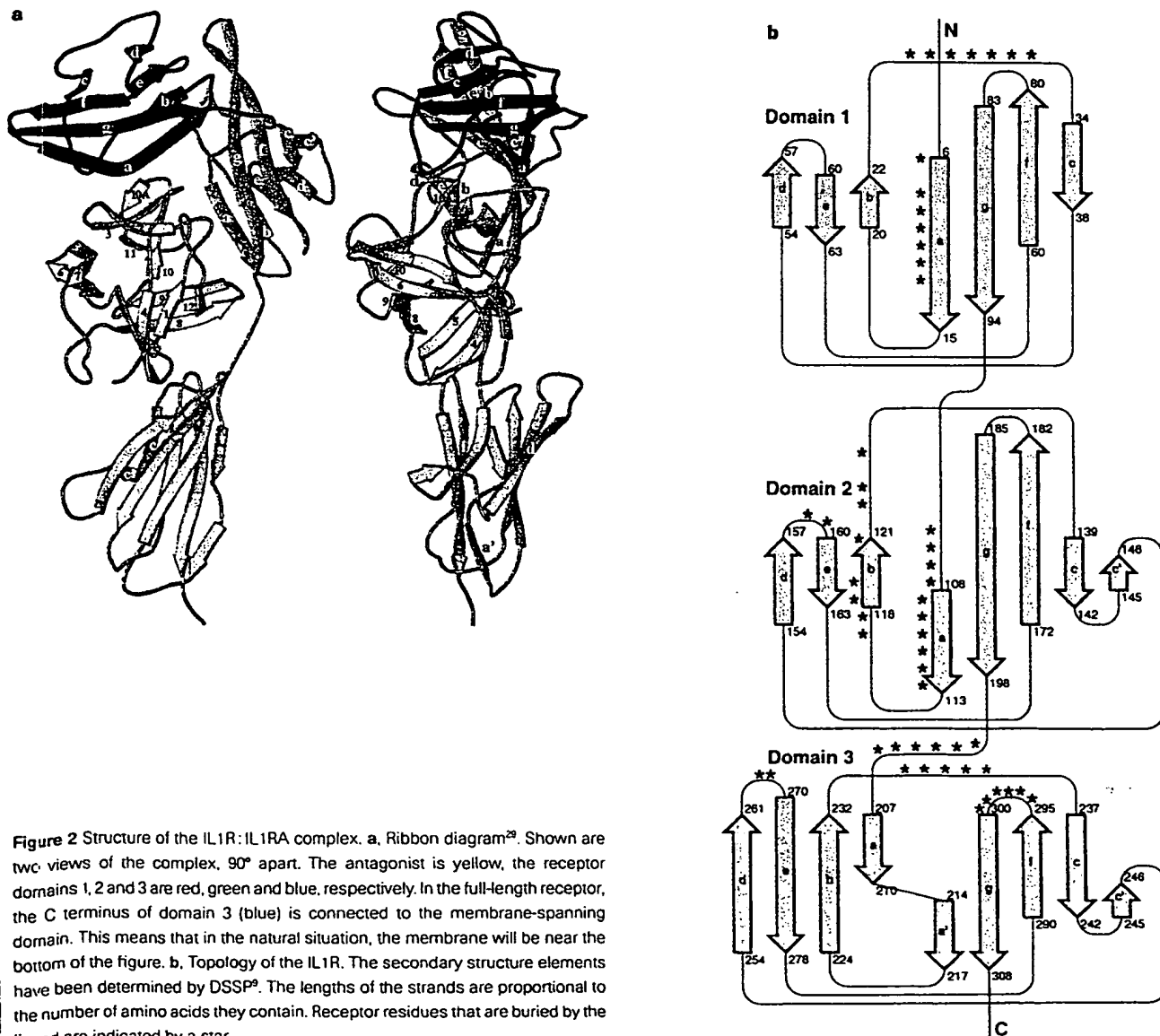




Figure 2 Structure of the IL1R:IL1RA complex. a, Ribbon diagram[29]. Shown are two views of the complex, 90° apart. The antagonist is yellow, the receptor domains 1, 2 and 3 are red, green and blue, respectively. In the full-length receptor, the C terminus of domain 3 (blue) is connected to the membrane-spanning domain. This means that in the natural situation, the membrane will be near the bottom of the figure. b, Topology of the IL1R. The secondary structure elements have been determined by DSSP[9]. The lengths of the strands are proportional to the number of amino acids they contain. Receptor residues that are buried by the ligand are indicated by a star.

Sequence alignment figure (row labels, left to right):

```
                    a1            b1                              c1
IL1R_human    .......... ...dkckere eKIILVSSAN B OVRP  LN PNEHK-----  ......g  T  DDSkt pvs teqss......  52
IL1S_human    itiqpashtg aarscrirgr hYKREFALEG B VALR  OV PYWLW----a avpri nIT HKNDSartvp geest......  71
IL1RR_human   ........ ......escl sRPHITVVEG B FYLKHCSC SLAHE-----  ..lett  kS  SSGsqebv elnprsss--  55
AcP_murine    .......sha sercddwgid t MRCI QVFED B PARI K  F EHFLKynysi absagl  I  WTROdrdI e eplnlrlpen  73
ST2_human     .......... ..... - SKOSWGLEN B ALIVR  RO GKPSY-----  .......vD  YSQTnksI p tqern-----  43
FGR4_human    ....seevsI epclapsieq qEOELTVALG OBVRLC  GRA ERGG------  ........H  KEGSrIapa g---------  53
```

```
                d1    e1            f1              g1                                     a2
IL1R_human    B HQHKEK  W FVI AKVE  S HIY  VV  ss  ycIrikisak Iven------ ............ ......-EPNL  YNAQAI FKQ 110
IL1S_human    AWAQDGAI W LLI ALQE  S TIV TT  ss  ycdkmslelr vf-------- ............ ......-ENTO AFLPFI SYPQ 127
IL1RR_human   B ALHDCV I E FW VELN  T SI FQM  yt  qkwsInvIrr -------- ............ ......-NKHS TEROVTSK 109
AcP_murine    B SKEKDV  E FR TLLN  T N T ML  it  ycskvalple vv-------- ............ ......-QKDS NSAMRFPV 129
ST2_human     GVFASGQL  X ELG AEVA  S I T  V  pt  fartgyaavt Iyk------- ............ ......-KQSD NVPDYLMYS 100
FGR4_human    VRGWRGR  E IASFLPE  AG RI L A  sm  ivIqnItiit gdsItssndd edpksbrdps nrbsypQOAP YWTHPQRMEK 133
```

```
                      b2               c2   c2'          d2      e2                  f2
IL1R_human    KLpva---gd gGLV  ymet fknenMELPK LO   OKPE LLDRI HFSgv kdrIIvmmva e-----KHR   HASYTYL 183
IL1S_human    ILtIs---ts gVLV  dIse ftrd-KTDVK IO  DSLLL DKDMEKFLsv rgtthII vhd val--E A  R VLTFAHE 201
IL1RR_human   I Vsvk---kf I QIT  ssyy q----TLVHS TSL  KKL LLE NKNPtI kknsel---- -----EDO  Y VHFLHHM 173
AcP_murine    HKmyl-sbgl hKIT  nvdg yIps-SVKPS VT  GTEI VDFHNVLPeg mnlsIfIpIv -----SHN N VTYPEM 202
ST2_human     TVsgs--skn sKIY  IdI y-----NWTAP LE  QAE QGSRYRAHks fIvIdnvm - -----E A  D KFI HNEM 168
FGR4_human    KLhavpagnl vKFR  sag- -----NPTPT IR  DGQAF HGE RI GGIr IrhqhwsIvm ssvvpSOR T VENAVG 207
```

```
                 g2            a3    a3'          b3          c3  c3'             d3
IL1R_human    XQ  PI RVI eIItieenkp trpvIvspsn et ms--VDL SOI Q I  WT GOt----sdi AY KW gavI deddpvIgsd 257
IL1S_human    OO  NI RSI sIrIkkkkee tiqvIspik tfs----ASL SRLTIP KF LGTGTPLTTM LW TAMOTHI sssypggrvt 278
IL1RR_human   KL  NI KTf nIt IvsdrsO IvgvIgpki nhva--VEL KNVRN SAL LNs----sdv I Y FGsang sdpnIhsske 247
AcP_murine    RL  HL RTv tvkvvgspkd sIfpqIyspn drvvysKEP KNAN T SAC FSfImdsbnE VW TI Dgtkp ddvtvdItI n 282
ST2_human     AN  SV ATr sItvkdsqgl sIfpvIgsps qneIksVEI KNANCT SAC FGKGTQFLAA VL OLMGTKI tdf geprIqq 248
FGR4_human    SI R  NYLLDv IsrsphrpiI qsgIpanit- ------AVV SOVE L  KY SOs--qphiq --I khIvIn gssIgsdgip 276
```

```
                  e3                          f3              g3
IL1R_human    yysvenpaak rrsIIItvEN SSEIESRFYK HP  I F  K  H R daayI q  IypvtnIqk-  316
IL1S_human    egprqsysen nsnyIevpII FDPVTREDI H MD K  VH E LSI qt Ir I Iv keasstIsw-  337
IL1RR_human   srIsIpsg-- -kwhaskvIR EENI GESNIN VL S  TVAS G dtkslI vrkadmsdip  304
AcP_murine    ssvsyssI-- sdetrtqILS IXKKVTPEDIR RN    AR H K ssqsskv kqkvIppryt  340
ST2_human     sogqnqsIsn gIacIdmvI R EADVKEEDI L LO  Q L AL L H rrhtvr  srkapskecf  308
FGR4_human    yvqvikIa-- dimsssvsVL YLRNVSAEDA GE  T L AG S I syqssw I tvIpsedptw  334
```

**Figure 3** Sequence alignment of the extracellular portion of the IL1R with the extracellular portions of 5 homologous proteins. IL1R, type-I IL-1 receptor; IL1S, type-II IL-1 receptor; IL1RR, IL-1-receptor-related protein; AcP, IL-1-receptor accessory protein; ST2, ST2 protein; FGR4, fibroblast growth factor receptor 4. The cysteines and tryptophans that are conserved in most immunoglobulin folds are indicated in dark blue. Also highlighted are the prolines immediately following conserved cysteins, which appear to be conserved in the particular immunoglobulin fold of IL-1 domains 1 and 2. Highlighted in green are 5 conserved cysteine pairs which, based on the IL1R structure, are likely to form disulphide bonds. Other highly conserved residues are indicated in blue. Conserved glutamic acids and threonines, which are probably involved in a hydrogen bond between domains 1 and 2, are indicated in red.
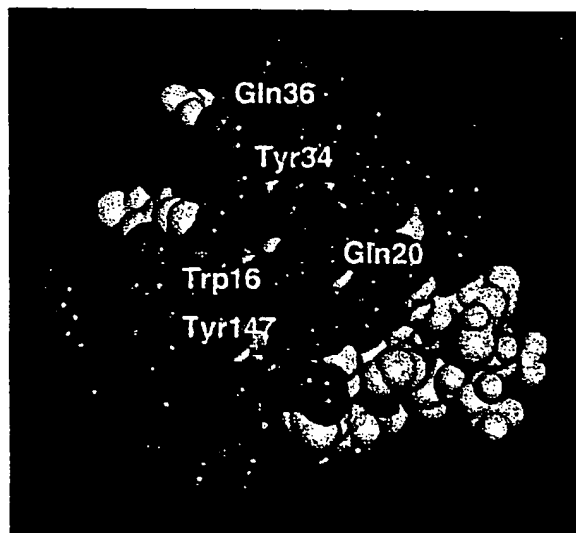


**Figure 4** Space-filling model of bound IL1RA. Residues shown by mutagenesis to be important for receptor interaction[3] are in red, other residues that are buried by the receptor are in blue, and those that do not interact with the receptor are in yellow. The five residues defined by site-directed mutagenesis are right in the centre of the area that is buried by the receptor in the crystal structure. However, the contact area defined by the mutagenesis studies is only 29% of the area defined by the crystal structure, suggesting that many of the contacting residues contribute less significantly to the overall binding energy.



**Figure 5** Comparison of the IL1R (left) and HGHR (right) complexes. IL1RA is shown in yellow, IL1R in green, HGH in red and the two HGHR molecules in blue and magenta. The two receptors use opposite faces of the immunoglobulin domains to bind their ligands.

salt link (Lys 11R and Glu 43A are linked through a water molecule). Some oppositely charged side chains (Lys 129R–Glu 126A, Lys 295R–Glu 52A, Lys 295R–Glu 90A) are less than about 8 Å apart, but do not seem to make any direct interactions. It may be that for these residue pairs, the gain in electrostatic energy is offset by a loss of entropy. This idea is supported by a mutagenesis study that shows that one of the salt links in the crystal structure of human growth hormone complexed to its receptor[10] contributes little, if anything, to the overall binding energy, an effect the authors ascribe to entropy loss.

We observe only two side-chain–side-chain hydrogen bonds between the receptor and the antagonist. Most of the hydrogen bonds between antagonist and receptor involve main-chain carbonyl or nitrogen atoms (Table 2). Of special interest are the double hydrogen bonds made by Gln 20, Gln 36 and Asn 39 of the antagonist with the backbone of the receptor, which suggests that these residues may contribute significantly to the overall binding. The potential advantages of using main-chain atoms for receptor–ligand interactions are twofold: the main chain is usually more rigid than the side chains so that the entropy loss for the main chain will be less than for side chains; and interactions involving main-chain atoms depend less on the sequence and more on the overall folding than interactions between side chains, which may explain how the IL1R is able to bind its three natural ligands, IL-1α, IL-1β and IL1RA with high affinity, despite the low sequence identity (20–25%) between them.

The crystal structure of the receptor complex fully explains the published mutagenesis studies. IL1RA residues Trp 16, Gln 20, Tyr 34, Gln 36 and Tyr 147, identified as critical for antagonist binding[9], are all in direct contact with the receptor (Table 2; Fig. 4). The same residues (Tyr, Trp, Gln) are present in the YWQPWA consesus sequence, identified by affinity screening using phage

display peptide libraries[11]. The indole side chain of Trp 16 is completely buried by the receptor and makes a hydrogen bond with the carbonyl oxygen of Lys 111. The side chain of Gln 20 makes two hydrogen bonds with the receptor backbone. The side chain of Tyr 34 makes no direct contacts of less than 3.5 Å with the receptor. It does face a hydrophobic region on the receptor surface, consisting of the side chains of Phe 108, Val 121, Pro 123 and Tyr 124. The side chain of Tyr 34 is tightly fixed in position by a hydrogen bond with the carbonyl oxygen of Asn 19 and its carbonyl oxygen makes a hydrogen bond with the hydroxyl group of Tyr 124. The Gln 36 side chain is found in a pocket between receptor domains 1 and 2 and makes three hydrogen bonds with the receptor backbone. These hydrogen bonds and the restricted pocket clearly explain the large loss of binding affinity associated with the Gln 36 → Phe mutation. Finally, the hydroxyl of the critical Tyr 147 binds to a network of two fixed water molecules on top of loop bc of receptor domain 2.

The binding of IL1RA in the IL1R complex is fundamentally different from the binding of ligands in the cytokine–receptor complexes whose three-dimensional structures are known. In the tumour necrosis factor-β (TNF-β) complex[12], three elongated receptor molecules are bound to the ligand and the receptor domains do not possess an immunoglobulin fold. In the receptor complexes with human growth hormone (HGHR[13]), interferon-γ (IFNγR[14]) and erythropoietin peptide (EPOR[15]), the ligand binds to the outside of the elbow between two immunoglobulin-like domains of the fibronectin type and is sandwiched between two receptor molecules (Fig. 5). In the IL1RA complex, the receptor has three immunoglobulin-like domains and the ligand binds to the inside of the elbow formed by domains 1 and 2.

Another way in which the IL1R differs from HGHR, IFNγR and many other proteins with immunoglobulin-like domains is in the interactions between its domains. Most immunoglobulin-like
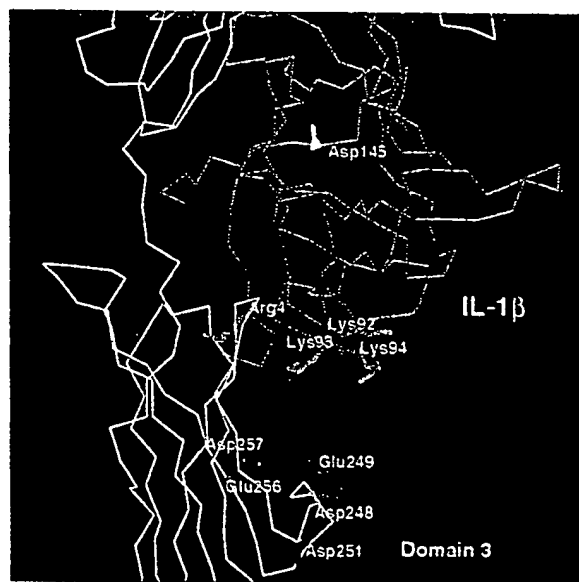


Figure 6 Model obtained after superimposing IL-1β onto IL1RA in the complex. IL-1β is indicated in magenta and the receptor in green. After this superposition, a region of positively charged residues (Arg 4, Lys 92, Lys 93 and Lys 94) in IL-1β is at a distance of ~15 Å from a region of negatively charged residues (Asp 248, Glu 249, Asp 251, Glu 256 and Asp 257) in domain 3 of IL1R but do not directly interact with them. Modelling studies (not shown) suggest that upon movement of IL1R domain 3, these two regions interact directly. A definitive answer must come from the crystal structure of the IL1R–IL1β complex.
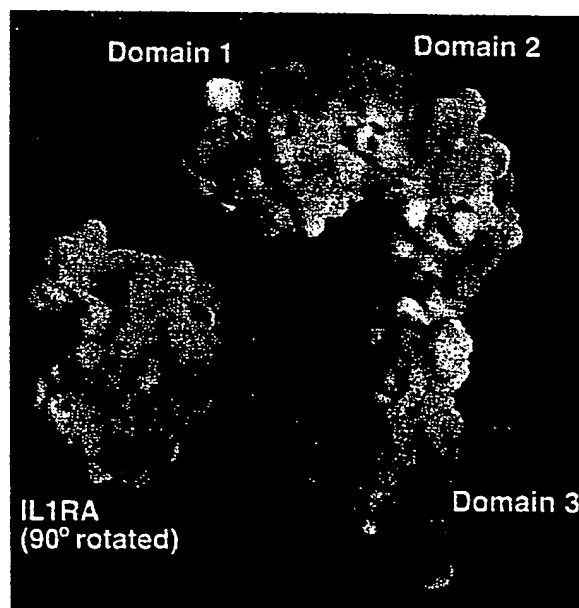


Figure 7 Solvent-accessible surface of the IL1R, coloured according to the electrostatic potential using GRASP[30]. The contours run form $-5K_BT$ (red) to $+5K_BT$ (blue), where $K_B$ is the Boltzmann constant and $T$ the absolute temperature. The IL1RA molecule is peeled off and rotated by 90° to show the receptor-binding region.

domains are connected by relatively short linkers which allow flexibility while maintaining contact between the domains. Domains 1 and 2 of IL1R are close together and have tight and extensive contacts. The upper halves of strands f2 and g2 (Fig. 2) in particular have more contacts with domain 1 than with domain 2 to which they belong. The centres of mass of domains 1 and 2 are ~8 Å closer in IL1R than they are in HGHR. Judging from the crystal structure, it seems unlikely that domains 1 and 2 are able to move with respect to each other, suggesting that domains 1 and 2 could behave as a single module. The connection between domains 2 and 3, on the other hand, is a long and flexible linker with no direct contacts between the domains. We would therefore expect that domain 3 is able to move with respect to domains 1 and 2 when no ligand is present.

An IL-1-receptor-like protein, the IL1R accessory protein, may be involved in the IL-1 response[16]. Association of this accessory protein with the complex of the IL1R with the agonists IL-1α or IL-1β is believed to trigger the receptor response. The accessory protein might need binding sites both on the IL1R and on the agonists IL-1α or IL-1β, or alternatively, the agonists may induce a conformational change in the receptor which allows binding of the accessory protein.

We investigated these possibilities by constructing a preliminary model of IL-1β bound to the receptor, in which the structure of IL-1β[17] was superimposed onto IL1RA in the complex by means of a procedure described before[5]. We compared this model of the complex with the extensive mutagenesis data available for IL-1β[5]. Some IL-1β residues that are important for binding (Arg 11, His 30, Asn 108 and Glu 128) are all close to the receptor after superimposition and face receptor domains 1 and 2, indicating that similar regions on the surface of IL-1β and IL1RA may interact with receptor domains 1 and 2.

The situation is quite different for residues facing domain 3. Whereas Lys 92 and Lys 94 are part of the proposed receptor trigger site[2], after superimposition they are facing the solvent and do not interact with the receptor. They are part of a highly positively charged region on IL-1β involving Arg 4, Lys 92, Lys 93 and Lys 94, about 15 Å away from a region rich in negative charged on the receptor, involving Asp 248, Glu 249, Asp 251, Glu 256 and Asp 257 (Fig. 6). Electrostatic calculations (Fig. 7) indicate that this negative patch, together with a negative patch on top of domain 1, are the strongest features on the relatively featureless electrostatic surface. The close complementarity of the positive and negative sites suggests that they might interact directly with each other. A rotation of domain 3 of ~20° would bring the two sites together. The flexible linker between domains 2 and 3 allows such a rotation, which would make the conformation of the IL1β–receptor complex more closed than that of the IL1RA–receptor complex, inducing binding of the accessory protein and hence activation of the receptor. Without a crystal structure of the IL1β–receptor complex, however, we cannot exclude the possibility that the accessory protein will simply bind between the two charged regions.

To test the importance of domain 3 for agonist and antagonist binding, we prepared a truncated receptor consisting only of domains 1 and 2. This truncated receptor binds IL-1α and IL-1β with low affinity (dissociation constant ($K_d$) values of 7 μM and >10 μM, respectively) whereas it binds IL1RA with high affinity ($K_d$ 28 nM). This shows that agonists, but not antagonists, need domain 3 for high-affinity binding and suggests that domain 3 strongly interacts with IL-1 agonists.

Residue 145 (Asp in IL-1β, Lys in IL1RA), which is crucial in determining agonist or antagonist activity[18], does not interact directly with the receptor, either in the IL1RA complex or in our model of the IL-1β complex (Fig. 6), suggesting that this residue might be important for interaction with the accessory protein.

The structure presented here illustrates in detail a new binding mode for cytokine receptors and provides insight into the possible differences between agonist and antagonist interaction. □

## Methods

**Equipment and crystals.** The IL1R–antagonist complex was crystallized as described[4]. Native and heavy-atom data were recorded with a Siemens X1000 area detector, mounted on a Siemens rotating-anode generator equipped with a copper anode and graphite monochromator, operating at 50 kV and 90 mA. The crystals had dimensions of ~0.2 × 0.3 × 0.5 mm³ and one crystal was used per data set. Data were processed using XDS software[19]. The space group was $P2_12_12_1$, with $a = 47.2$ Å, $b = 84.6$ Å and $c = 140.2$ Å.

**Structure solution.** The structure was solved with a combination of molecular replacement and heavy-atom derivatives. For molecular replacement, we used the AMoRe package[20] and data between 15.0 and 4.0 Å. The structure of the free IL1RA as solved by us[5] gave clear solution with a correlation of 25.8% (R factor = 51.3%). We tried structures of various protein domains with immunoglobulin folds but most of them did not produce any clear signal, probably because these models were too different from the receptor domains and because one receptor domain represents only a small fraction of the total contents of the asymmetric unit of the crystals. A truncated model of the first CD4 domain[21], however, gave a correlation of 29.2% in combination with the IL1RA model (R factor 50.3%). The maps, based on this partial model, were not readily interpretable and it was therefore decided to search for heavy-atom derivatives. We obtained two independent heavy-atom derivatives and one double derivative. Scaling of heavy-atom derivative data, calculation of Pattersons and refinement of heavy-atom parameters were done by using programs from the CCP4 suite[22]. Heavy-atom positions were located in difference Patterson maps and the parameters were refined with HEAVY[23]. Phases were calculated with MLPHARE[24]. Cross-difference Fouriers were used to define a common origin and to confirm the sites. Difference fouriers using phases from the partial model, obtained by molecular replacement, did not reproduce the sites, indicating that the model phases were rather poor. This is most probably caused by the large fraction of the diffracting matter (two receptor domains), which is missing in the partial model. However, phased translation functions[25] using phases from the partial model and single iso-morphous replacement (SIR) phases calculated with the Hg(CN)₂ and K₂PtCl₄ derivatives, defined a common origin and indicated the correct hand for the heavy-atom solution. The MIR map, calculated with three derivatives, was improved by solvent flattening and histogram matching using SQUASH[26]. Map interpretation and model building were done using the program O[27]. The model of IL1RA needed only minor rebuilding, but the model of the truncated CD4 domain needed major rebuilding to become an IL1R domain; two additional receptor domains had to be built from scratch. The structure was refined by simulated annealing and energy minimization using X-PLOR[28]. The final model contains residues 7–151 of the IL1RA and residues 1–311 of the IL1R.

**Binding studies.** Truncated receptors were expressed on the surface of CHO cells and radiolabelled peptides were used for competitive binding[11].

1. Baumann, H. & Gauldie. J. The acute phase response. Immunol. Today 15, 74–80 (1994).
2. Dinarello, C. A. The interleukin-1 family: 10 years of discovery. FASEB J. 8, 1314–1325 (1994).
3. Evans, R. J. et al. Mapping receptor binding sites in interleukin (IL)-1 receptor antagonist and IL-1β by site-directed mutagenesis. Identificaiton of a single site in IL-1ra and two sites in IL-1β. J. Biol. Chem. 270, 11477–11483 (1995).
4. Schreuder, H. A. et al. Crystals of soluble interleukin-1 receptor complexed with its natural antagonist reveal a 1:1 receptor–ligand complex. FEBS Lett. 373, 39–40 (1995).
5. Schreuder, H. A. et al. Refined crystal structure of the interleukin-1 receptor antagonist. Presence of a disulfide link and a cis proline. Eur. J. Biochem. 227, 838–847 (1995).
6. Sims, J. E. et al. cDNA expression cloning of the IL-1 receptor, a member of the immunoglobulin superfamily. Science 241, 585–589 (1988).
7. Harpaz, Y. & Chothia, C. Many of the immunoglobulin superfamily domains in cell adhesion molecules and surface receptors belong to a new structural set which is close to that containing variable domains. J. Mol. Biol. 238, 528–539 (1994).
8. Hemmingsen, J. M., Gernert, K. M., Richardson, J. S. & Richardson, D. C. The tyrosine corner: A feature of most greek key β-barrel proteins. Prot. Sci. 3, 1927–1937 (1994).
9. Kabsch, W. & Sander, C. Dictionary of protein secondary structure: Pattern recognition of hydrogen-bonded and geometrical features. Biopolymers 22, 2577–2637 (1983).
10. Clackson, T. & Wells, J. A. A hot spot of binding energy in a hormone–receptor interface. Science 267, 383–386 (1995).
11. Yanofsky, S. D. et al. High affinity type 1 interleukin 1 receptor antagonists discovered by screening recombinant peptide libraries. Proc. Natl Acad. Sci. USA 93, 7381–7386 (1996).
12. Banner, D. W. et al. Crystal structure of the soluble human 55 kd TNF receptor–human TNFβ complex: Implications for TNF receptor activation. Cell 73, 431–445 (1993).

13. Vos, A. M., Ultsch, M. & Kossiakoff, A. A. Human growth hormone and extracellular domain of its receptor: Crystal structure of the complex. *Science* 255, 306–312 (1992).
14. Walter, M. R. *et al.* Crystal structure of a complex between interferon-γ and its soluble high-affinity receptor. *Nature* 376, 230–235 (1995).
15. Livnah, O. *et al.* Functional mimicry of a protein hormone by a peptide agonist: The EPO receptor complex at 2.8 Å. *Science* 273, 464–471 (1996).
16. Greenfeder, S. A. *et al.* Molecular cloning and characterization of a second subunit of the interleukin 1 receptor complex. *J. Biol. Chem.* 270, 13757–13765 (1995).
17. Priestle, J. P., Schär, H.-P. & Grutter, M. G. Crystal structure of the cytokine interleukin-1β. *EMBO J.* 7, 339–343 (1988).
18. Ju, G. *et al.* Conversion of the interleukin 1 receptor antagonist into an agonist by site-specific mutagenesis. *Proc. Natl Acad. Sci. USA* 88, 2658–2662 (1991).
19. Kabsch, W. Automatic processing of rotation diffraction data from crystals of initially unknown symmetry and cell constants. *J. Appl. Crystallogr.* 26, 795–800 (1993).
20. Navaza, J. AMoRe: an automated package for molecular replacement. *Acta Crystallogr. A* 50, 157–163 (1994).
21. Wang, J. *et al.* Atomic structure of a fragment of human CD4 containing two immunoglobulin-like domains. *Nature* 348, 411–418 (1990).
22. Collaborative Computational Project Number 4. The CCP4 suite: Programs for protein crystallography. *Acta Crystallogr. D* 50, 760–763 (1994).
23. Terwilliger, T. C. & Eisenberg, D. Unbiased three-dimensional refinement of heavy-atom parameters by correlation of origin-removed Patterson functions. *Acta Crystallogr. A* 39, 813–817 (1983).
24. Otwinowsky, W. Maximum likelihood refinement of heavy atom parameters. In *Isomorphous Replacement and Anomalous Scattering* Proc. CCP4 Study Weekend, 25–26 January 1991 (compiled by Wolf, W., Evans, P. R. & Lesly, A. G. W.) 80–86 (1991).
25. Read, R. J. & Schierbeck, A. J. A phased translation function. *J. Appl. Crystallogr.* 13, 490–495 (1988).
26. Zhang, K. Y. J. SQUASH–combining constraints for macromolecular phase refinement and extension. *Acta Crystallogr. D* 49, 213–222 (1993).
27. Jones, T. A., Zou, J.-Y., Cowan, S. W. & Kjeldgaard, M. Improved methods for building protein models in electron density maps and the location of errors in these models. *Acta Crystallogr. A* 47, 110–119 (1991).
28. Brünger, A. X-PLOR, version 3.1. A system for X-ray crystallography and NMR. (Yale University Press, New Haven, Connecticut, 1992).
29. Kraulis, P. MOLSCRIPT: A program to produce both detailed and schematic plots of protein structures. *J. Appl. Crystallogr.* 24, 946–950 (1991).
30. Nicholls, A., Sharp, K. A. & Honig, B. Protein folding and association: Insights from the interfacial and thermodynamic properties of hydrocarbons. *Proteins* 11, 281–296 (1991).
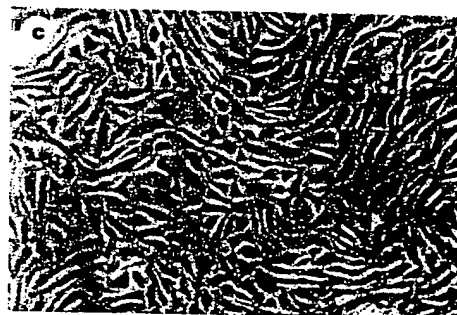
# ERRATUM

# Viable offspring derived from fetal and adult mammalian cells

I. Wilmut, A. E. Schnieke, J. McWhir, A. J. Kind & K. H. S. Campbell

In this Letter in the 27 February issue, a production error led to the image for part b of Fig. 1 (fetal fibroblasts) being used twice, as parts b and c. The correct image for Fig. 1c (mammary-derived cells) is shown below, and is also on the *Nature* web site and in reprints.